1 Chapter 1: Introduction

1.1 Background

Water is one of the planet's most vital resources. Water is essential for humanity in conducting daily household, industrial, and agricultural activities that enable the functioning of society. Despite covering 70% of the planet's surface, only 0.5 % of this resource is considered freshwater, which is safe for drinking. Approximately one-sixth of the world's population is impacted by freshwater scarcity. To sustainably satisfy water needs, it is crucial to effectively manage the available water resources (Elimelech, 2006).

Most water sources are contaminated thus, the water needs to be treated before it can be used. Contaminants in water are categorized into physical, chemical, and microbial agents. Physical contaminants include suspended and dissolved particles, making water appear murky and aesthetically unappealing. Chemical contaminants include nitrogen, salts, pesticides, metals, and toxins produced by bacteria. Bacteria, viruses, and protozoa are some of the microbiological pollutants in water that pose one of the biggest threats to global health. One of the main causes of disease and mortality, particularly in underdeveloped countries, is contaminated water. A staggering 828 million people worldwide lack access to safe drinking water, with 37% residing in developing nations (Dos Santos et al., 2017)

Conventional water treatment systems, typically centralized in nature, are primarily used in larger urban or suburban areas with higher population densities to provide water treatment services. The centralized water treatment approach combines the processes of sedimentation, filtration, flocculation, coagulation, and disinfection to effectively remove contaminants. After treating the water in one place, it is distributed over a special distribution network (Roefs et al., 2017). However, the maintenance and operation of these systems relies on trained professionals to maintain consistent water quality and meet regulatory standards. Additionally, centralized systems require significant investments in infrastructure, including pipelines, treatment plants, and distribution networks, which makes them impractical for deployment in peri-urban and rural areas (Mintz et al., 2001).

Alternatively, point-of-use (POU) water treatment technology has emerged as a strategy that enables individuals in rural communities to access safe water by treating it at home (Sobsey et al., 2008). The inexpensiveness, easy installation, and irrelevance of qualified personnel make Point-of-Use water treatment technologies viable for developing communities. The most common POU water treatment technologies are solar disinfection, chlorination, ceramic filters, biosand water filters, and membrane

nitrogen and hydrogen atoms with relatively low reactivity. Introducing KOH to remove a hydrogen atom generates a nitrogen anion, increasing nucleophilicity and molecule reactivity. This reactivity, in turn, facilitates more effective bonding of the hydantoin functional group with the polymeric resin (Mąkosza, 2020).

3.2.1.1 Nucleophilic substitution reaction

A nucleophilic substitution reaction is a chemical reaction in which a nucleophile (an electron-rich species) reacts with a substrate molecule, substituting one group or atom in the substrate with the nucleophile. The nucleophilic hydroxide ion (OH^-) from KOH abstracts a hydrogen proton from one of the NH groups in 5,5-dimethylhydantoin, forming water as a byproduct. This deprotonation step generates a negatively charged nitrogen species on the hydantoin. The potassium cation (K^+) interacts with the negatively charged nitrogen in DMH, stabilising the resulting compound. The resulting compound is the potassium salt of hydantoin that has been activated to react with the resin. Figure 3-1 shows the complete reaction.

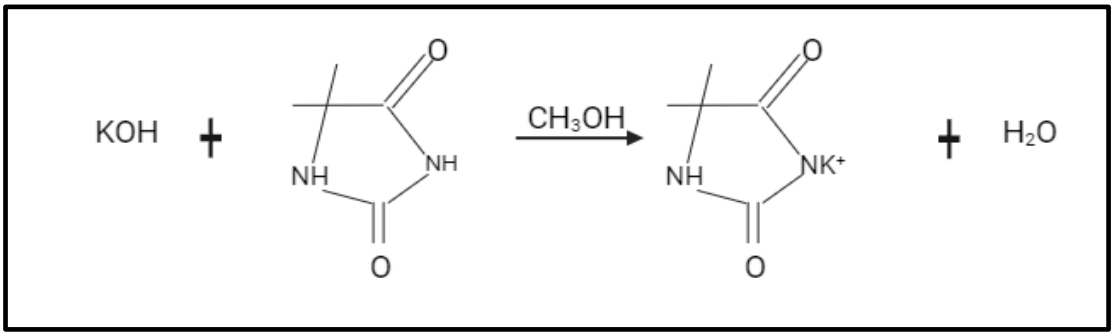

Figure 3-1: The nucleophilic substitution reaction of KOH and DMH

3.2.1.2 Optimization of the nucleophilic substitution reaction

Results from preliminary experiments and literature survey by Chylińska et al., (2014) were used to identify the factors influencing the nucleophilic reaction. The factors included the molar ratio of dimethylhydantoin (DMH) and potassium hydroxide (KOH), the solvent volume, the reaction temperature, and the reaction time.

The factors that were selected for optimization were temperature and reaction time. The dimethylhydantoin (DMH) and potassium hydroxide (KOH) molar ratio was kept constant. Equal molar amounts of DMH and KOH are required because the reaction stoichiometry demands that one mole of each reactant is consumed in the reaction. The reaction would not be complete if there were an excess of either DMH or KOH. The reaction between DMH and KOH is a neutralisation reaction where

time also significantly affected the response variable. All the coefficients of the main effects were integrated into the model Equation 3-4.

Table 3-4: ANOVA of the nucleophilic substitution reaction performed with a 95% confidence level

Parameters	P-value	Test of significance (α=0.05)	Significance
Temperature (Linear)	0.000013	p< α	Significant
Temperature (Quadratic)	0.000128	p< α	Significant
Reaction Time (linear)	0.000045	p< α	Significant
Reaction Time (Quadratic)	0.066351	p> α	insignificant
Temperature(L) *Reaction Time(L)	0.021077	p< α	Significant

An evaluation was conducted to see how well the model predicted the response variable. The projected integral values of the N-H peak are shown graphically in Figure 3-9 in comparison to the actual experimental data. The graph indicates a perfect match between the predicted outcomes from the model and the actual observed experimental values. This alignment signifies that the model's predictions are accurate. Hence, the mathematical model Equation 3-4 is desirable, and it can be applied to predict the response variable (integral of the NH signal/number of hydrogen protons in the signal) of the nucleophilic substitution reaction of DMH and potassium.

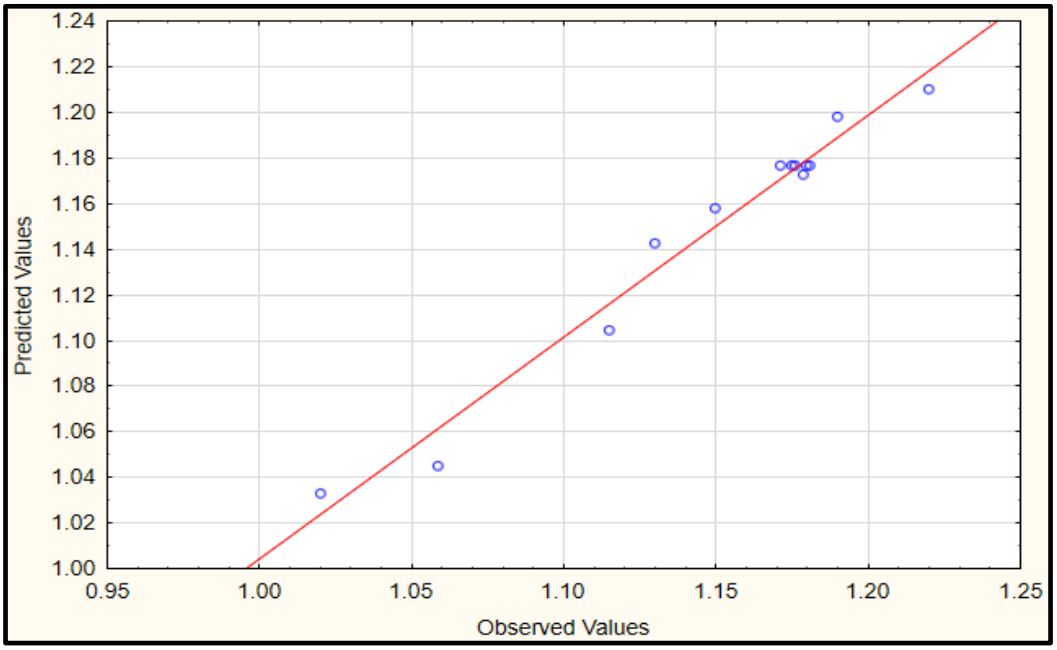

Figure 3-9: The predicted number of hydrogen protons in the N-H signal VS the experimental number of hydrogen protons in the N-H signal

This study yielded an R^2 value of 0.974 and this concludes that the model fits the data very well and that the predictions nearly match the experimental values. It suggests a significant linear relationship between the model's variables. The desirability profile conducted at a desirability of 0.0, as shown in Figure 3-10, was also used to find optimal conditions. Based on the model and desirability profile, the preparation of a hydantoin salt was optimized at a temperature of 44°C and a reaction time of 29 minutes. Under these conditions, the predicted integral was 1.02, (mass balance yield of 95.9%) indicating that one hydrogen proton remained after the substitution reaction, thus confirming the introduction of potassium into the DMH compound. These specific conditions were established as the ideal parameters for synthesizing the potassium salt of hydantoin. More salts of hydantoin were produced to be used in the grafting procedure.

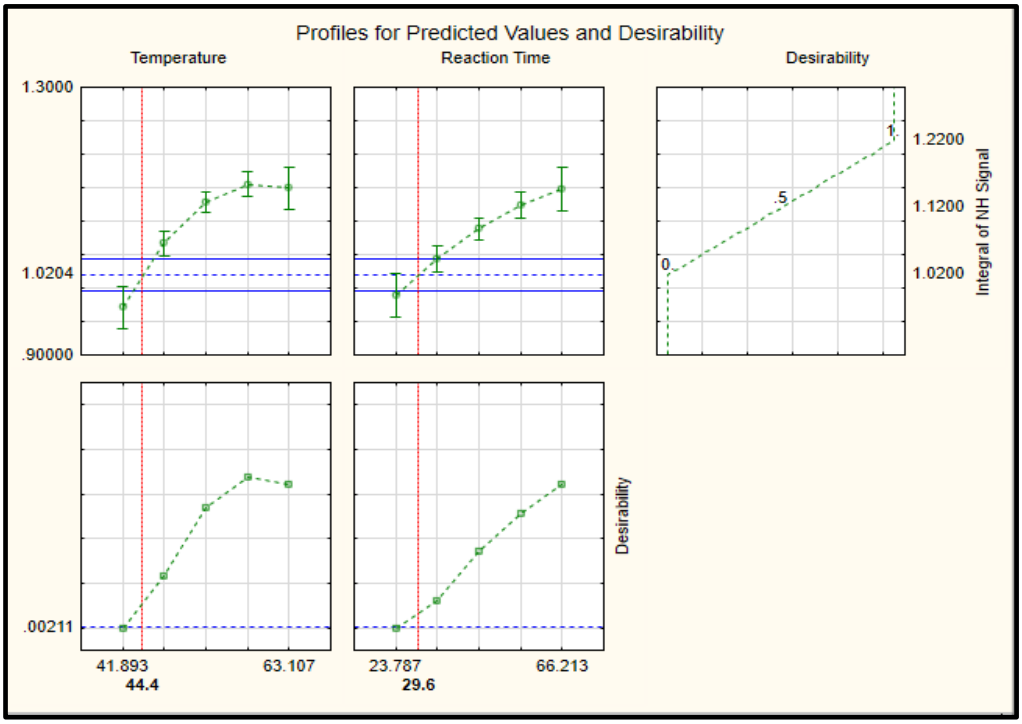

Figure 3-10: Profiles for the predicted response variable

3.4.1.3 Effects of the substitution reaction factors on the yield

The ANOVA analysis showed that reaction time and temperature influenced the response variable. This section discusses the effects of the parameters of the nucleophilic substitution reaction on the response variable (integral under the NH signal). The integral equals the number of hydrogen atoms substituted. An integral value of 1 represents 100% yield. Figure 3-11 shows how substitution reaction factors affect the response variable (yield).

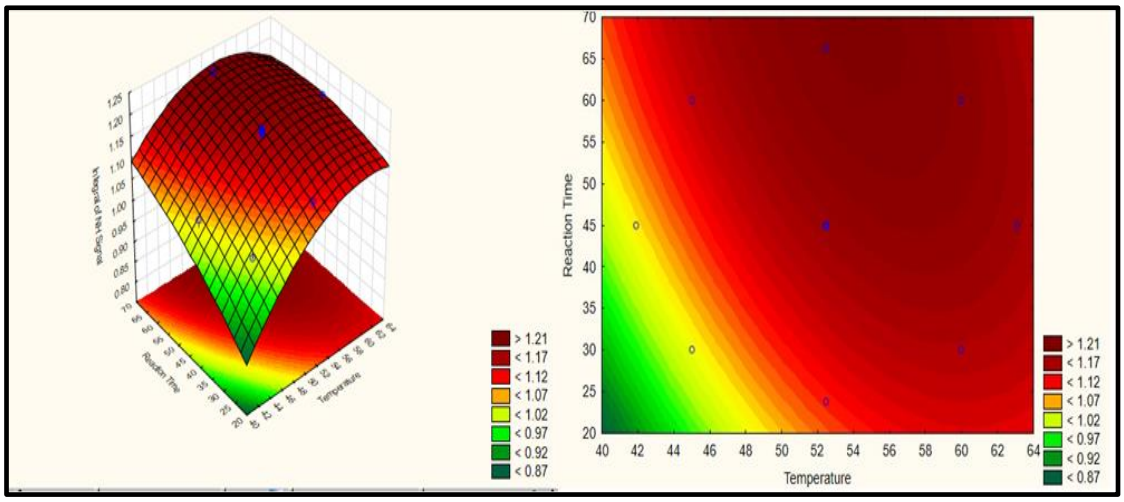

Figure 3-11: Effects of temperature and reaction time on the integral of the NH signal

From the Figure 3-11, an increase in temperature caused the integral of the NH signal to deviate from a value greater than 1 and decreasing the temperature to a certain level caused the NH signal integral to approach 1 again; however, further temperature decrease caused the integral to deviate to an integral of lesser than 1. As stated in section 3.2.1.2, the integral of the NH peak is directly proportional to the number of hydrogen protons in a compound, and for this reaction, an optimum of 1.02 was achieved.

In a nucleophilic substitution reaction, an existing group on the substrate is eliminated, and a new molecule takes place. At high temperatures, the activation energy of elimination reactions is lower than that of substitution reactions. The lower the activation energy, the higher the rate of the reaction. As a result, more elimination products are obtained than substitution products (Estopiñá-Durán et al., 2021). In substituting the hydrogen in the hydantoin with potassium, an integral greater than 1 was obtained at higher temperatures. This means the hydrogen was not fully substituted with the potassium, contributing to more hydrogen protons (less substitution product), thus an integral greater than 1 on the NH peak. The substitution reaction's activation energy is lower than the elimination reaction's at low temperatures. As a result, a reduction in temperature to a certain level yielded an integral of 1. However, a further decrease in temperature favoured more substitution, leading to an integral of less than 1. This indicates that substitution reaction is not energy intensive and occurs at low temperatures, but to avoid over-substitution, an optimum low temperature of 41°C is enough for this reaction (Liu et al., 2017).

Furthermore, from Figure 3-11, it can be observed that an increase in reaction time caused the integral of the NH signal to approach 1 from 0.87; a further increase in time caused the integral to deviate from 1 to 1.2. According to Zhang et al., (2016), the early phases of the nucleophilic substitution reaction involve the nucleophile, commonly a potent base like KOH, initiating an attack on the

hydantoin substrate. This attack prompts the removal of hydrogen from hydantoin through deprotonation, leading to the creation of an intermediate that is highly susceptible to nucleophilic substitution. Prolonged reaction times lead to multiple nucleophilic attacks; the proton is lost to competing reaction pathways such as elimination. Hence, the degree of substitution is minimal. During a short reaction time, the deprotonation of hydantoin is more likely to be a dominant step. The reaction favours the desired substitution pathway over competing pathways in this scenario. The effect of reaction time on nucleophilic substitution reaction was previously reported by Monteiro et al., (2016); based on the reported results, short reaction times minimise the existence of competing reaction pathways.

An interactive effect of reaction time and temperature on the response variable was also observed. A short reaction time caused the integral of the NH signal to approach 1 depending on the temperature during the reaction. A decrease in temperature to a certain level led to the substitution reaction being complete in a short period. Low temperatures favour the reaction to a substitution pathway and not elimination, causing the reaction to complete faster. This brings out a positive interactive effect of reaction time and temperature.

3.4.2 Grafting of hydantoin onto resin results

3.4.2.1 Characterisation results

I. Fourier transform infrared (FTIR)

Figure 3-12 represents the FTIR spectra for the resin before the grafting reaction with DMH-K and after the grafting reaction. The response variable was the low transmittance of the C=O band at 1650 cm^{-1}. In FTIR, a low transmittance of a functional group implies that it is absorbing a significant amount of the incident infrared radiation at the specific wavenumber associated with its vibrational mode. This absorption indicates the presence of that functional group in the sample.

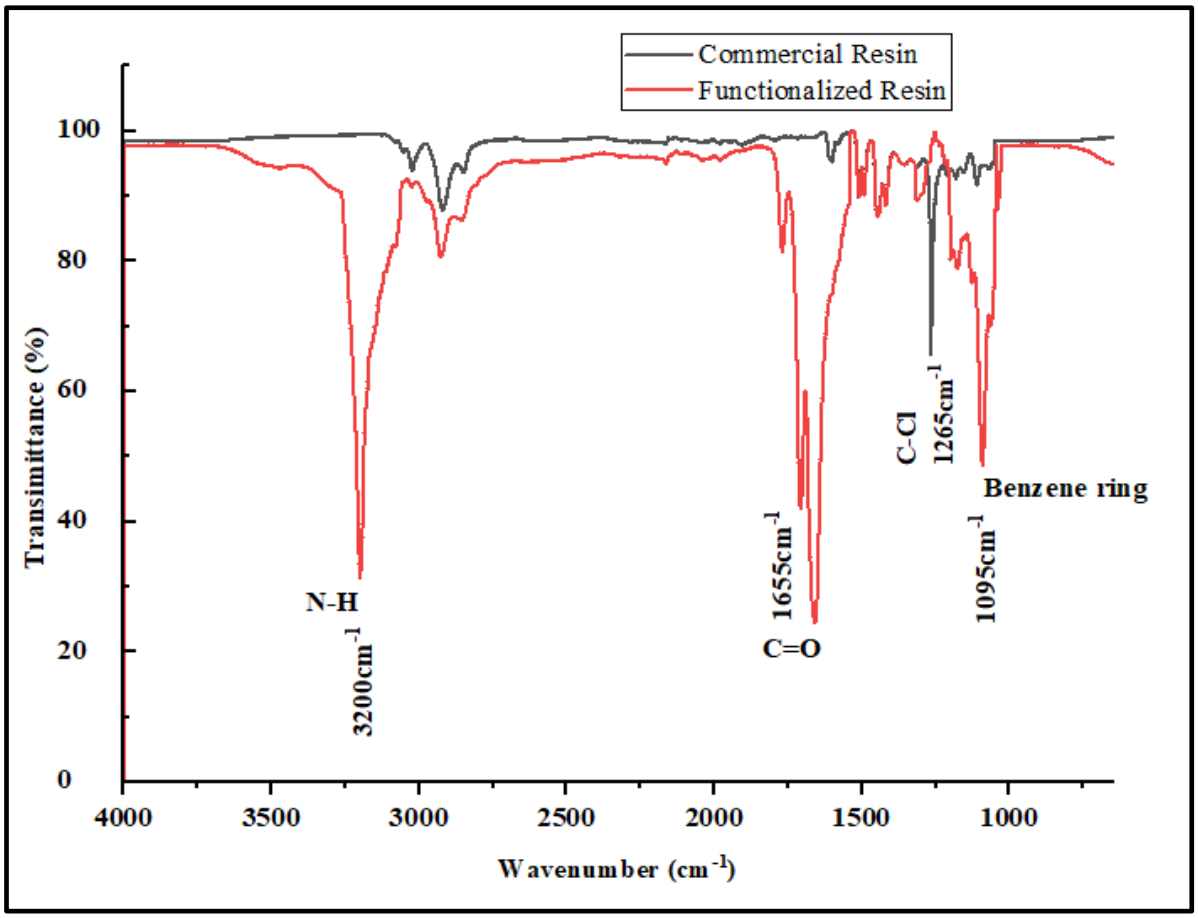

Figure 3-12: FTIR spectra of the functionalized resin indicating the presence of the amide functional group

FTIR spectra of the commercial resin and the resin containing the hydantoin compound are depicted in Figure 3-12. Each peak corresponds to a functional group present in the resin. The original peak at 1265 cm^{-1}, attributed to the C–Cl bond in the first commercial Merrifield resin, was replaced by a new peak at 1655 cm^{-1}, corresponding to the C=O group. The new characteristic bands at 1655 cm^{-1} are assigned to the carbonyl group (C=O) (amide I), which indicates the introduction of an amide group of the hydantoin ring in the resin. A characteristic band at 1095 cm^{-1} indicated the aromatic ring belonging to the hydantoin group grafted on the resin. The characteristic bands at 3200 cm^{-1} were attributed to the N-H (amide II) stretching vibrations of the hydantoin rings, indicating a successful covalent bonding of the amide functional group onto the resin. These bands were confirmed by referencing the IR Spectrum table provided by the supplier of the components used in the research. The table lists IR spectroscopy frequency ranges, the appearance of the vibration, and absorptions for functional groups, and it is shown in the appendix Figure D 3. Similar findings have been documented in a previous study (Papadopoulos et al., 2020), where they synthesized a bio-based unsaturated poly (ester amide) using itaconic acid, and the material exhibited thixotropic behaviour. The FTIR spectra of this newly synthesized compound displayed a prominent peak at 1640 cm^{-1}, representing the

double bond characteristic of itaconic acid. These spectra also showed overlapping signals associated with C=O (Amide I) stretching vibrations of the amido diol. Furthermore, a novel absorption peak was detected at 3300 cm^{-1}, corresponding to hydrogen-bonded N-H groups. In conclusion, the hydantoin, N-halamine precursor, was successfully grafted on the resin.

II. Scanning electron microscopy (SEM)

Following the grafting process of Merrifield resin with the hydantoin functional group in two different solvents (DMSO and DMF), SEM images were captured for both samples, along with an image of the unreacted raw resin. This step was undertaken to validate and confirm the successful incorporation of the NH group into the resin. Figure *3-13* shows the SEM images of the unreacted resin, the resin reacted in DMSO, and the resin reacted in DMF.

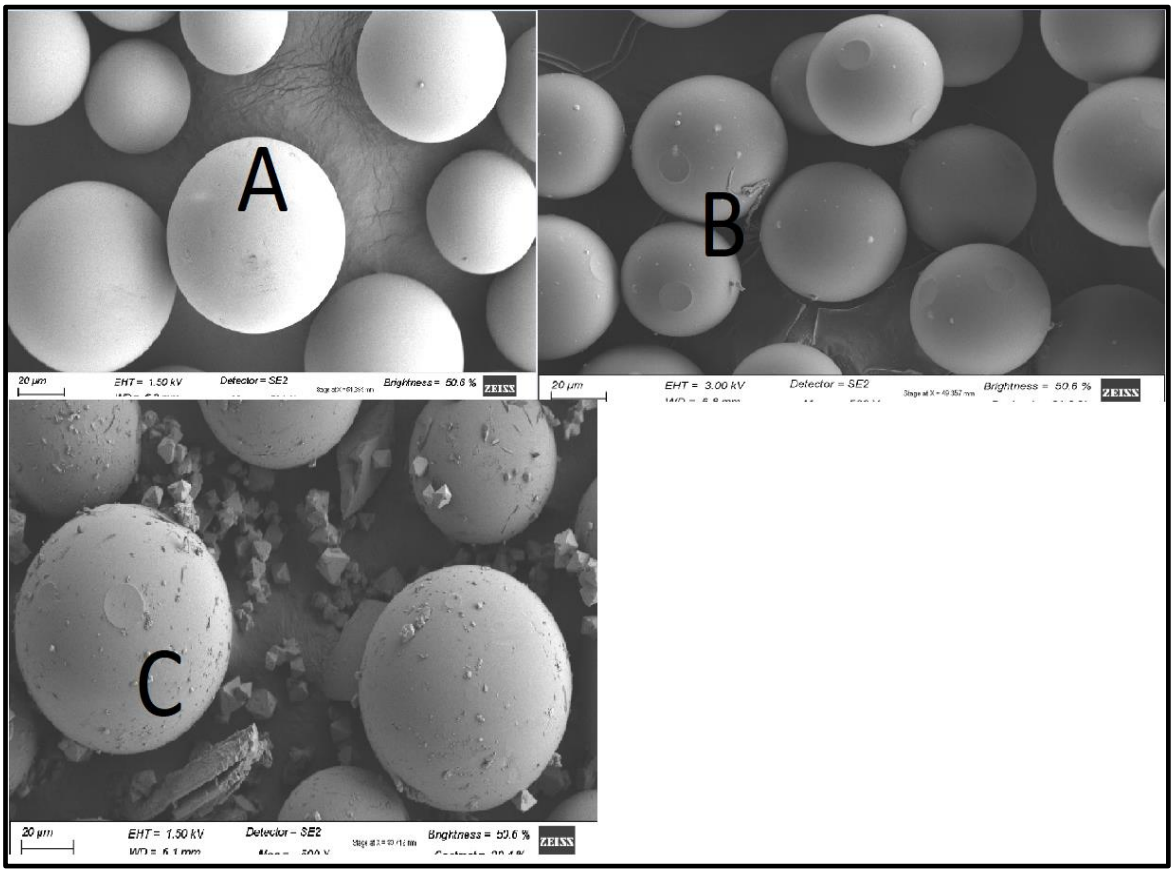

Figure 3-13 SEM Images of (A) unreacted resin, (B) modified resin in DMSO, (C) modified resin in DMF

From Figure 3-13, it was observed that the SEM image of the unreacted resin was brighter, attributing to a lower contrast, and the SEM images of the reacted resin in the different solvents were darker, attributing to a higher contrast even when the scanning was done at the same settings.

According to Suemori et al., (2020), several characteristics, including the sample's material composition, have been linked to contrast fluctuations in SEM images. The elements that make up different materials have different atomic numbers, which affects how those materials interact with the incident electron beam. Heavier elements have higher atomic numbers, which makes them contrast more than light elements during SEM image analysis. The main elements of the unreacted Merrifield resin are carbon and hydrogen, both of which have a lower atomic number than nitrogen. Nitrogen from the amide group in the modified resin increased the backscattered electron signal, resulting in higher contrast.

The effect of nitrogen on the contrast of SEM images was also observed by Kovács et al., (2013), who characterised Fe-N nanocrystals and nitrogen-containing (Ga,Fe)N thin films. Their results showed a dark field in the SEM images of the films.

An important observation from the SEM images is that the resin in DMF showed degradation. The degradation was due to the instability of DMF. DMF is less stable at elevated temperatures and undergoes hydrolysis, causing resin DMF degradation. DMSO is known for its high stability in elevated temperatures. It is less prone to decomposition or degradation compared to some other solvents. DMSO is more resistant to hydrolysis compared to DMF. Hence, more functionalized resins for the chlorination reaction were synthesized using DMSO.

3.4.2.2 Optimization results

Results from the optimization of the grafting reaction are discussed below. The results of the experimental runs are displayed in the appendix, Table A-3, where the transmittance of the C=O bond in FTIR was used as the outcome.

3.4.2.2.1 Validation of the experimental runs

The validation of the experimental results was done using five centre-point repetitions during optimization. These repetitions were carried out under constant conditions, with a temperature of 90 °C and a reaction time of 15 hours. Figure *3-14* illustrates the transmittance of the C=O bond analysed during these five runs.

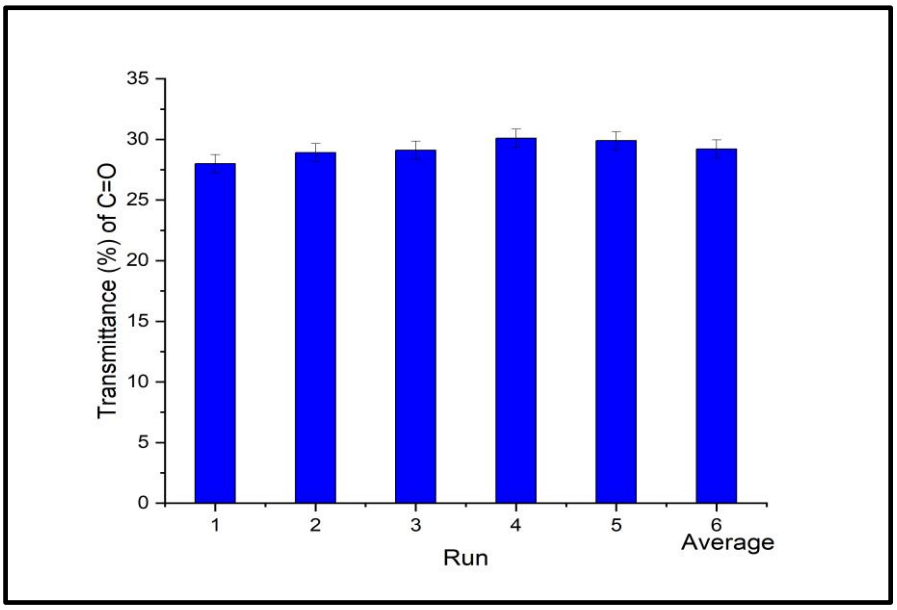

Figure 3-14: Five experimental centre point runs of the grafting reaction

Figure 3-14 above shows that the average transmittance of the C=O bond for the five repeat runs was 29.2, with a standard deviation of +/- 0.753658. This data shows the validity of the experimental runs in the optimization process, as the small standard deviation suggests minimal variation among the repeated runs.

3.4.2.2.2 Optimization

A two-factor central composite design (CCD) was applied to establish a relationship relating the reaction's response variable, the transmittance (%) of the carbonyl group (C=O) denoted as (Y) with the two variables: temperature (X_1) and reaction time (X_2). Both X_1 and X_2 served as independent variables, while Y was the dependent variable. A mathematical model from Equation 3-5 was derived from regression coefficients.

$$\boldsymbol{Y = -397.49 + 8.746X_1 - 0.0465X_1^2 + 0.929X_2} \qquad \textbf{(Eq. 3-5)}$$

ANOVA analysis assessed the linear and quadratic effects of the reaction factors. A summary of these results is presented in Table 3-5. Factors with p-values less than 0.05 significantly impacted the response variable, while those with higher p-values were regarded as having little influence. Looking at Table 3-5, temperature had significant linear and quadratic effects on the response variable. Additionally, the analysis indicated that the linear term of reaction time impacted the response variables. However, the analysis revealed that the interactions between linear temperature and reaction time had no significant influence on the response variable. All

regression coefficients of the main effects were incorporated into the mathematic equation, as shown in Equation 3-5.

Table 3-5 ANOVA analysis of the grafting procedure performed with a 95% confidence level

Parameters	P-value	Test of significance (α=0.05)	Significance
Temperature (Linear)	0.00024	p< α	Significant
Temperature (Quadratic)	0.00208	p< α	Significant
Reaction Time (linear)	0.00059	p< α	Significant
Reaction Time (Quadratic)	0.19855	p> α	insignificant
Temperature(L) *Reaction Time(L)	0.07907	p> α	insignificant

An evaluation was conducted to see how well the model predicted the response variable. The projected transmittance of the C=O bond is shown graphically in Figure 3-15 in comparison to the actual experimental data. The graph indicates a perfect match between the predicted outcomes from the model and the actual observed experimental values. This alignment confirms the accuracy of the model's predictions. Hence, the mathematical model Equation 3-5 is desirable, and it can be used to predict the response variable, the transmittance of the C=O for the covalent grafting reaction.

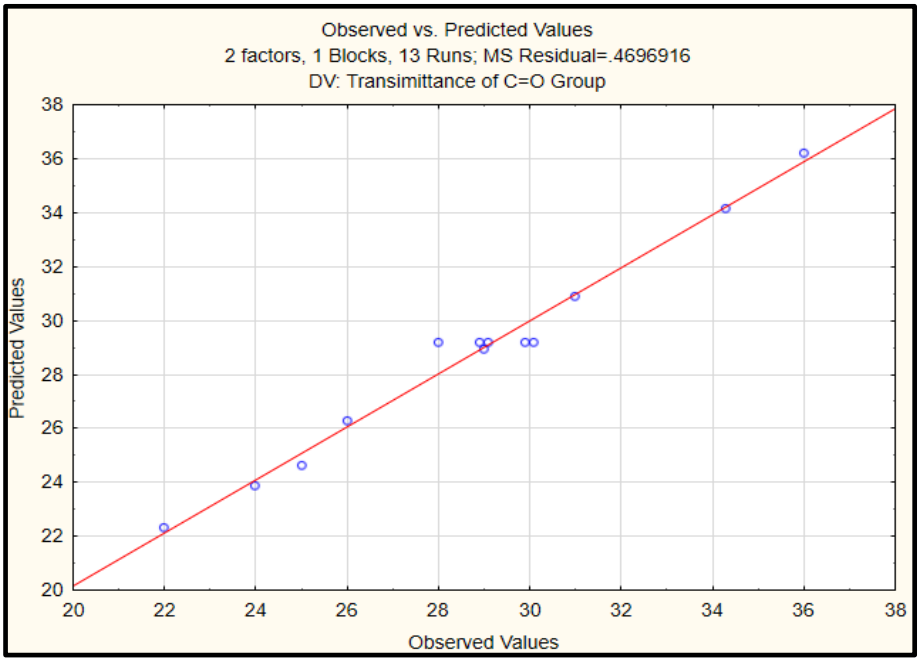

Figure 3-15: Profile of the predicted transmittance of C=O bond vs. observed transmittance of C=O

The R^2 value of 0.937 provides additional evidence for the model's validity. Given the strong R^2 value, it can be concluded that the model fits the data very well and that the predictions nearly match the experimental values. It suggests a significant linear relationship between the model's variables. The model was solved using the experimental data from appendix Table A 5, revealing that the optimal conditions were as follows: a temperature of 83 °C and reaction time of 11 hours, resulting in a predicted transmittance (%) of 22 (mass balance yield of 93.5%). The desirability profile also confirmed these optimal conditions set, as Figure 3-16 depicts. Therefore, these conditions were ideal for grafting the hydantoin salt onto the resin.

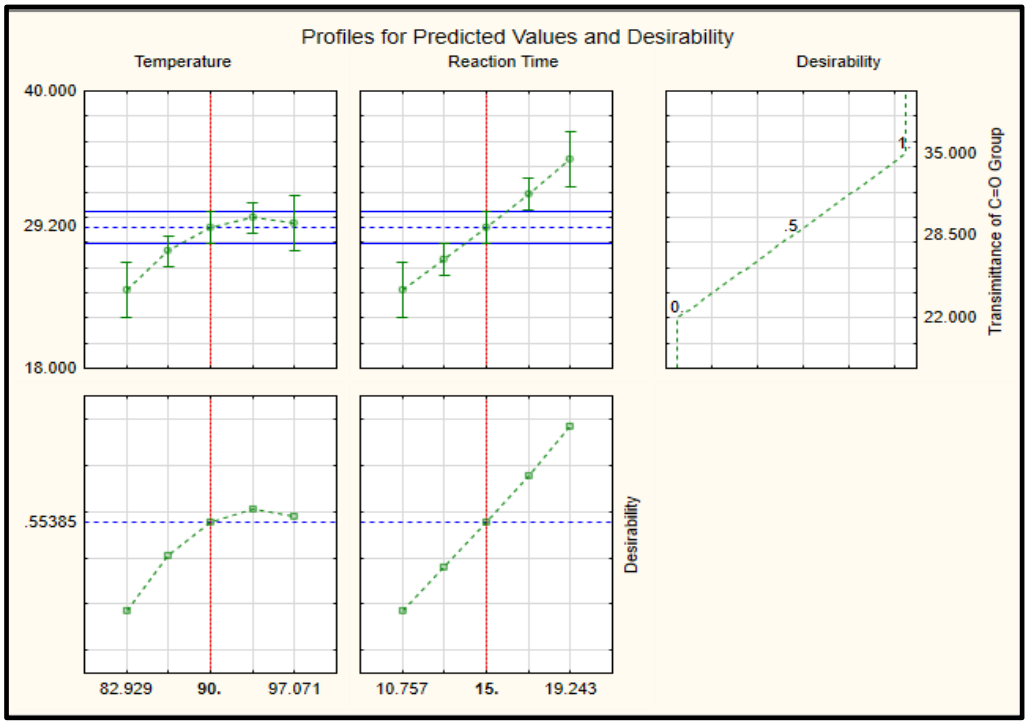

Figure 3-16: Profile of the predicted optimum values of the grafting reaction based on the experimental results

3.4.2.3 Effects of the grafting process parameters on the response variable

From the ANOVA analysis, both the reaction time and temperature influenced the response variable. This section discusses the effects of the covalent grafting reaction factors on the response variable (the transmittance of the C=O band). A low transmittance (high yield) of a functional group in an FTIR spectrum implies that the functional group absorbs a significant amount of incident infrared radiation. This absorption indicates the presence of the functional group in the sample.

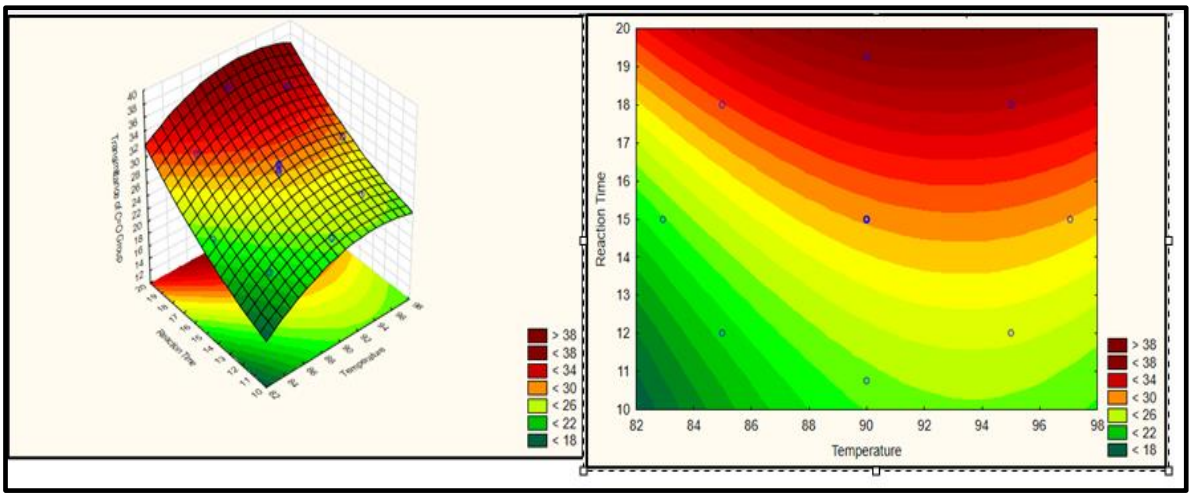

Figure 3-17: Effect of the grafting reaction parameters

From the plots in Figure 3-17, an increase in temperature caused the transmittance of the C=O peak to increase. A decrease in temperature resulted in a low transmittance. An increase in temperature from 82°C to 96°C increased the transmittance from 18% to 22%. The covalent grafting of a hydantoin functional group to a Merrifield resin highly depends on temperature. Elevated temperatures result in the degradation of the polymer backbone within the resin, leading to elimination reactions and the cleavage of the two bonds required to connect the resin and the hydantoin. This degradation compromises the resin, reducing its capacity to support the covalent grafting of the hydantoin group on the resin (Kluczyk et al., 2010). Therefore, a decrease in temperature promotes the cleavage of only one bond, thus promoting the occurrence of the covalent graft reaction of the hydantoin group to the resin. As a result, the transmittance of C=O on FTIR spectra is reduced, indicating a higher yield (incorporation of the amide functional group onto the resin).

Furthermore, increased transmittance was observed with increased reaction time and vice versa. The transmittance increased from 18% to 34 % when the reaction time increased from 10 to 20 hours. The solvent's potential for hydrolysis is the reason for the yield decline. Prolonged exposure of the hydantoin to a polar solvent (DMSO) causes hydrolysis of the amide functional groups in the hydantoin. When amides undergo hydrolysis, they produce carboxylic acids. This reduces the success of covalent grafting with the resin as the reactants (hydantoin) are lost to the solvent, decreasing the overall yield. Komarov et al., (2019) state that while many functional groups can undergo hydrolysis, esters and amides are more vulnerable to this process when subjected to polar solvents for prolonged periods during chemical reactions. A decrease in reaction time reduces the chances of hydrolysis of the amide groups, leading to a successful covalent grafting reaction of the hydantoin and the resin; thus, a low transmittance of the C=O peak is obtained.

3.4.3 Chlorination results

3.4.3.1 Characterisation results

Figure 3-18 represents the FTIR spectra for the resin before the grafting reaction with DMH-K, after the grafting reaction and the spectra of the chlorinated resin. The presence of the N-Cl band indicates the effective chlorination of the resin, thus the synthesis of a chlorinated resin.

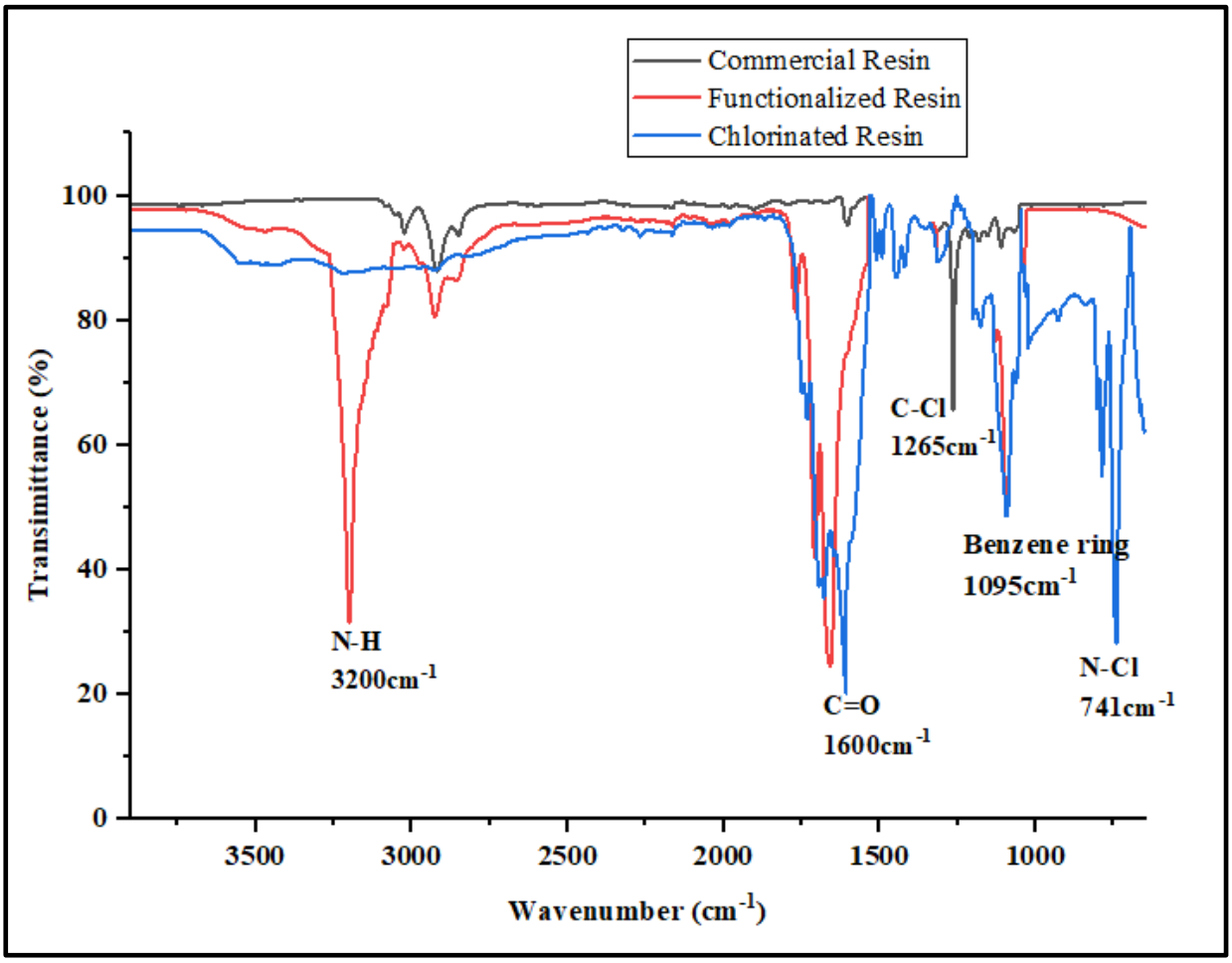

Figure 3-18: FTIR of the chlorinated resin

Figure 3-18 shows FTIR spectra of the commercial Merrifield resin, the resin containing the hydantoin compound and the chlorinated resin. The peak at 1265 cm^{-1} corresponding to the C–Cl bond in the starting commercial Merrifield resin disappeared, and it was replaced by a new peak corresponding to the C=O group at 1655 cm^{-1}. The new characteristic bands at 1655 cm^{-1} are assigned to the carbonyl group (C=O) (amide I), which indicates introducing an amide group of the hydantoin ring in the resin. A characteristic band at 1095 cm^{-1} indicated the aromatic ring belonging to the hydantoin group

grafted on the resin. The characteristic bands at 3200 cm^{-1} were attributed to the N-H (amide II) stretching vibrations of the hydantoin rings, indicating a successful covalent bonding of the amide functional group onto the resin. After chlorination, the N-H band at 3200 cm^{-1} had disappeared, and a new band at 741 cm^{-1}, assigned to the N-Cl groups, was detected. A shift in the C=O group from 1655 cm^{-1} to 1600 cm^{-1} was also observed. Observed changes indicate the successful chlorination of the hydantoin ring in the resin. Chlorination introduces electronegative chlorine atoms, which can influence electron density distribution around the carbonyl group. This change in electron density results in a shift in the C=O peak. A comparable finding was noted when Fe_3O_4 nanoparticles, having a polydopamine coating, underwent a simple two-step reaction to incorporate a barbituric acid structure. Subsequently, these barbituric acid components on the surface of the magnetic nanoparticles were utilized to create antibacterial N-halamine groups through exposure to NaOCl. After the chlorination procedure, the N-H bonds were converted into N-Cl bonds, as evidenced by the distinct broad peak at 748 cm^{-1} in the FTIR analysis (Akter et al., 2018).

3.4.3.2 Iodometric titration results

The iodometric titration calculation results are shown in appendix Table A 8. The yield percentages in comparison to the theoretical yield are shown in appendix Table A 9. Theoretically, a chlorine content of 6.75% (mass%) was expected from the resin, but 6.18% was obtained as the optimum value, representing a 91.5% yield (mass balance yield of 92.3%). The lowest yield obtained was 85.9%. The chlorination reaction parameters explain why the yield did not reach 100%. Section 3.4.3.3 discusses how the chlorination process parameters affected the yield.

3.4.3.3 Optimization of the chlorination process

A three-factor CCD was implemented to find the optimal values of the chlorination process of the modified resin. The experimental design layout and the results are presented in appendix A, Table A 6, with the chlorine content (% by mass) as the response variable.

3.4.3.3.1 Validation of the experimental runs

The experiment's validation was evaluated using five centre point repetitions during optimization. These repetitions were carried out under a constant temperature of 25°C, a reaction time of 45 minutes and a pH of 6. Figure 3-19 illustrates the chlorine content (%) analyzed for the five centre points.

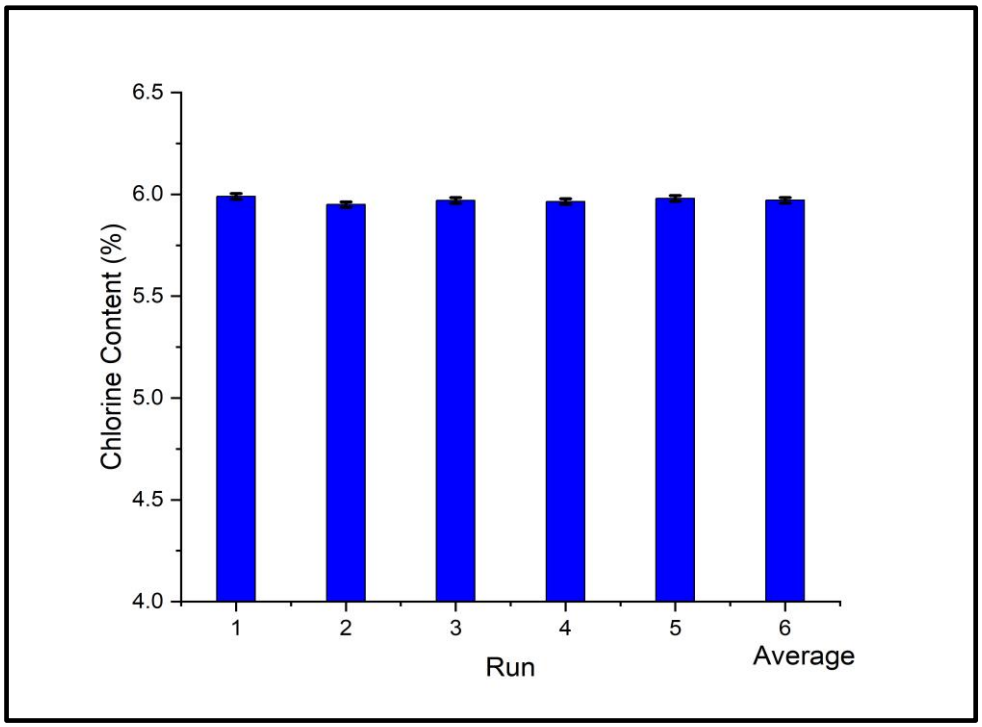

Figure 3-19: 5 Centre Point runs of the chlorination reaction

The figure above indicates that the average chlorine content across five repeated runs was 5.971%, with a narrow standard deviation of +/- 0.013565. These results show the validation of the experimental runs in the optimization process, as the small standard deviation indicates minimal variation among the repeated runs.

3.4.3.3.2 Optimization

A mathematical model was developed using the regression coefficients presented in the appendix, Table A 7. The mathematical model was used to describe the relationship between the optimization factors: the temperature(X_1), the reaction time (X_2) and the pH (X_3) to the response variable (percentage of chlorine in the resin signal (Y) of the chlorination reaction. X_1, X_2, and X_3 were the independent variables, and Y was the dependent variable. Equation 3-6 was obtained.

$$Y = 5.343 + 0.0676X_1 - 0.0015X_1^2 + 0.0083X_2 - 0.187X_3 + 0.0206X_3^2 + 0.0034X_1X_3 \quad \textbf{(Eq. 3-6)}$$

The ANOVA analysis indicated that temperature's linear and quadratic effects significantly impacted the response variable. They exhibited p-values of 0.000533 and 0.000778, respectively. Similarly, the reaction time had a significant linear effect on the chlorine content with a p-value of 0.000157. pH exhibited significant linear and quadratic effects on the response variable. A

significant interaction between the temperature and pH also affected the chlorine content. A summary of these findings is provided in Table 3-6. All the variables affecting the response variable were integrated into the model equation, as expressed in Equation 3-6.

Table 3-6 ANOVA values of the chlorination procedure performed at a 95% confidence level

Parameters	P-value	Test of significance (α=0.05)	Significance
Temperature (Linear)	0.000533	p< α	Significant
Temperature (Quadratic)	0.000778	p< α	Significant
Reaction Time (linear)	0.000157	p< α	Significant
Reaction Time (Quadratic)	0.534989	p> α	insignificant
pH (Linear)	0.000003	p< α	Significant
pH (Quadratic)	0.033080	p< α	Significant
1L*2L	0.261746	p> α	insignificant
1L*3L	0.033841	p< α	Significant
2L*3L	0.051328	p> α	insignificant

Figure 3-20 displays a strong linear relationship between the model's predictions and the observed experimental data and validates the accuracy of the model Equation 3-6.

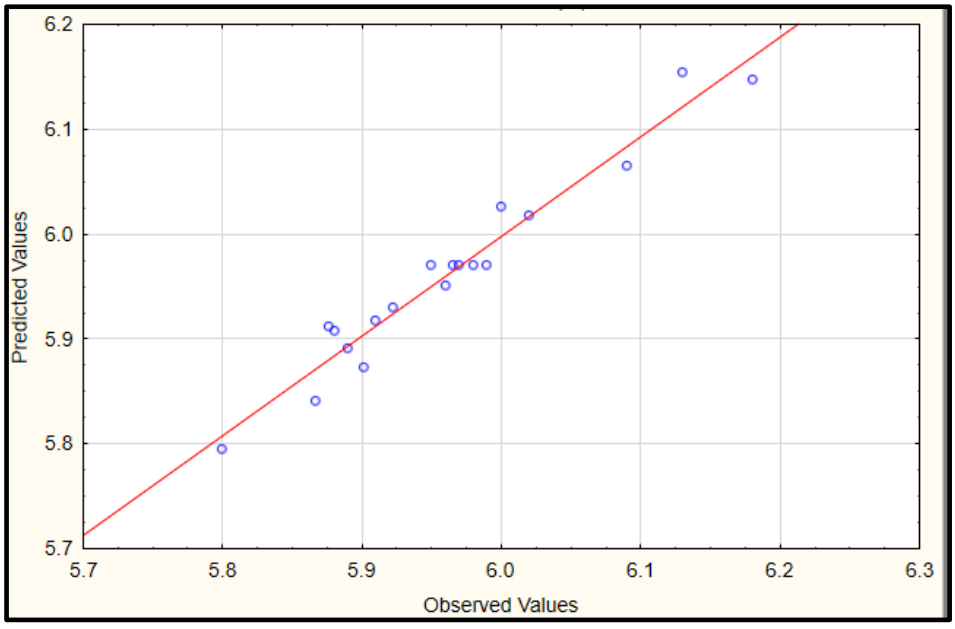

Figure 3-20 Profile of the predicted chlorine content (%) vs. the observed chlorine content (%)

The model's validity was further confirmed by the high R^2 value of 0.95. The model was used to identify the optimal parameters for chlorination of the resin. The model was solved using the experimental data from Table A 7, revealing that the optimal conditions were as follows: a temperature of 25 °C, a reaction time of 54 minutes, and a pH of 5.1 resulting in a predicted chlorine content of 6.18% by mass %. The desirability profile also confirmed these optimal conditions set, as Figure 3-21 depicts. Therefore, these conditions were the ideal parameters for chlorinating the resin.

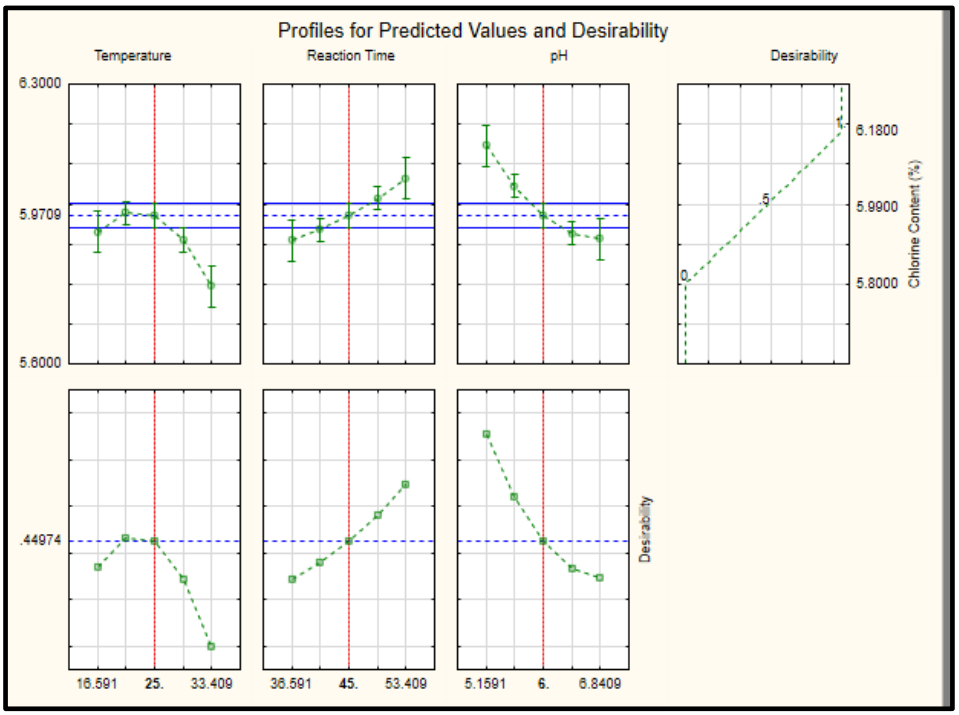

Figure 3-21: Profile of the predicted optimum values

3.4.3.4 Effects of the chlorination reaction factors on the response variable

The chlorination kinetics of the functionalized resin was studied at different pH values, temperature, and reaction time. From the ANOVA analysis, all the reaction factors influenced the chlorine content. An interaction between temperature and reaction time also affected the response variable (chlorine content % by mass%). This section discusses the effects of the chlorination reaction factors on the chlorine content (%).

I. Effect of the reaction time on the response variable

Figure 3-22 illustrates the effect of reaction time on the chlorine content at a temperature of 20°C and pH of 3.

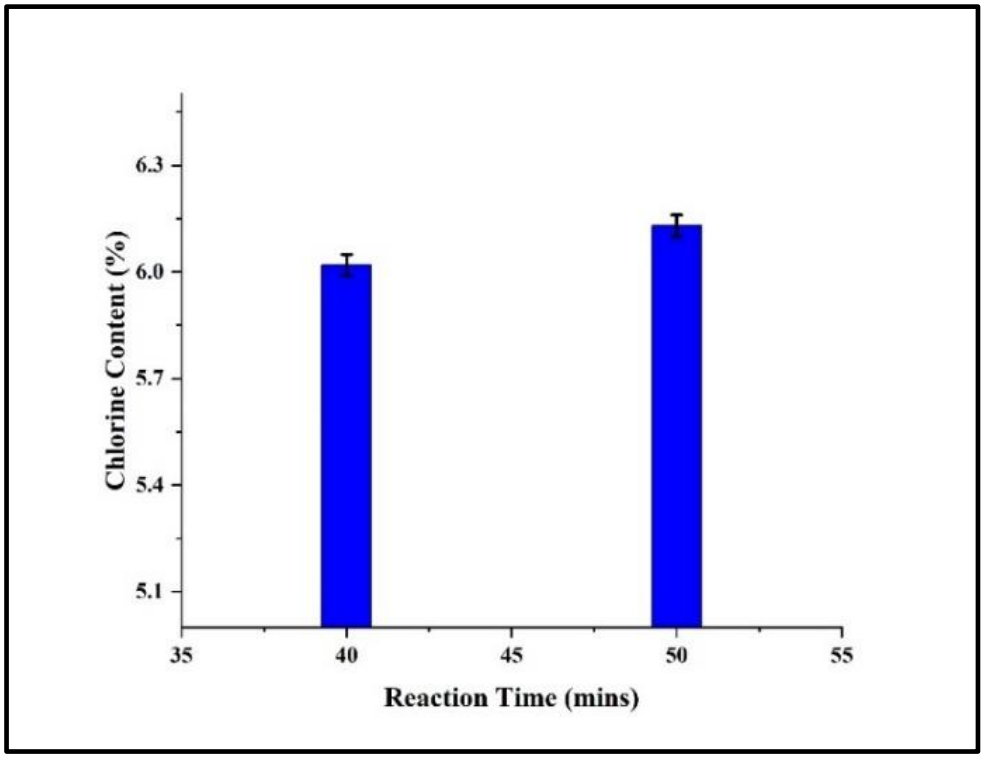

Figure 3-22: Effect of the reaction time on the chlorine content in resin (%)

From Figure 3-22, the chlorine content in the resin approached the predicted theoretical value of 6.75% with an increase in the reaction time. The chlorine content increased from 6.02% to 6.13% when the reaction time increased from 40 to 50 minutes. The increase in yield with an increase in reaction time is because of the inductive effect of chlorine. During electrophilic substitution reactions involving halogens, the electron density of the benzene ring (hydantoin functional group) is decreased by the electronegativity and inductive effect of halogens, making it less reactive. As a result, electrophilic substitution reactions involving halogenated compounds often require longer reactions to provide the resins benzene ring sufficient time to activate their electrophilicity to receive the electrophile chlorine (Zhang et al., 2023). This results in yield increasing as the reaction time increases.

II. Temperature and pH

Figure 3-23 shows how an interaction of the temperature and pH at constant reaction times of 40 minutes, 45 minutes, and 50 minutes affects the chlorine content.

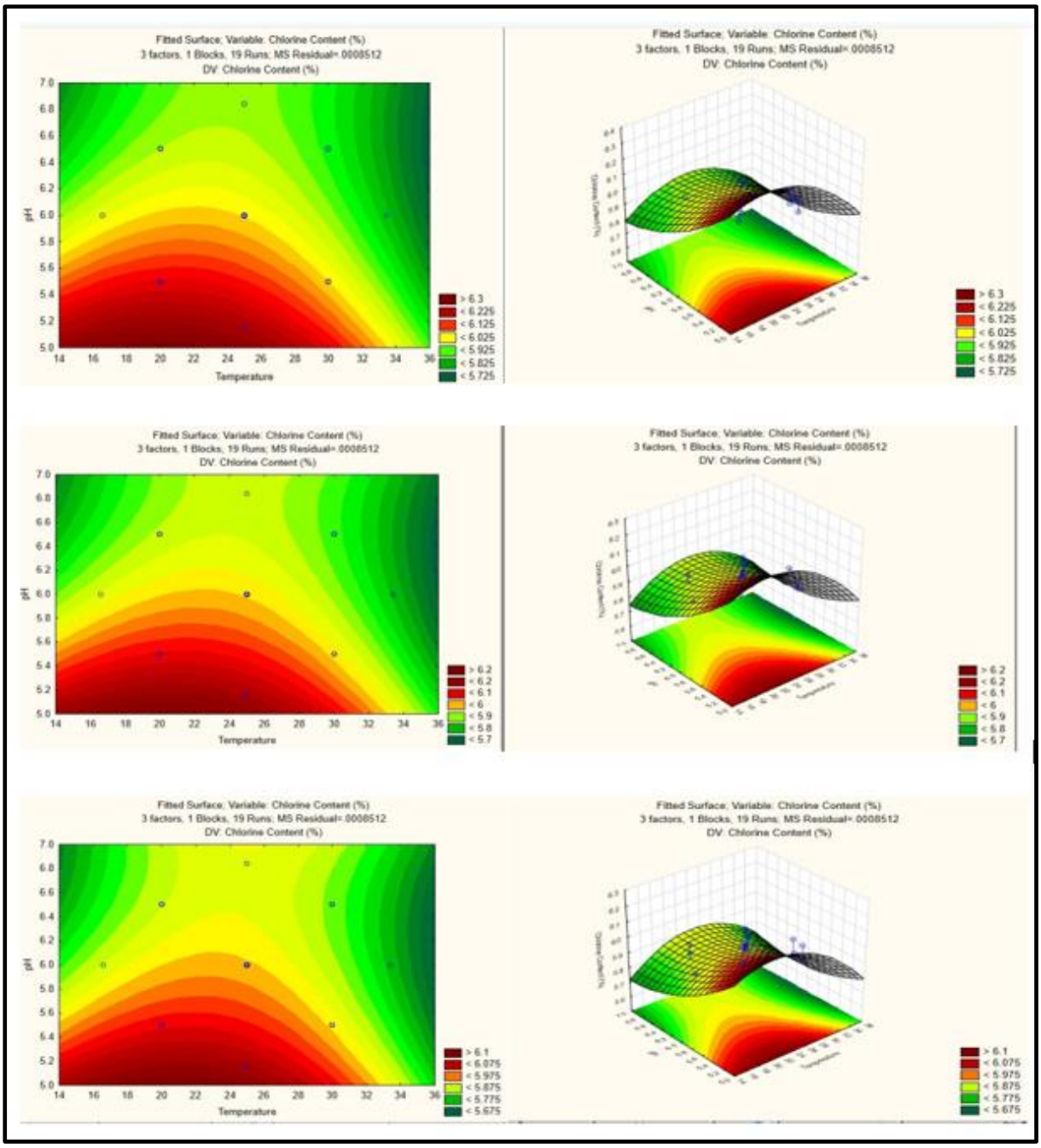

Figure 3-23: Interactive effect of the temperature and the pH on the chlorine content at reaction times of 40 mins, 45 mins and 50 mins

As shown in Figure 3-23, the oxidative chlorine content increased from 5.9% to 6.2% with the decrease in temperature from 36°C to 20°C. Furthermore, the chlorine content in the resin approached the predicted theoretical value of 6.75% with a decreased pH in an acidic environment. The chlorine content increased from 6.025 % to 6.22% when the pH decreased from 6 to 5.

The effect of temperature on the yield is attributed to the regioselectivity, where the hydrogen substitution position on the benzene ring with Cl^+ depends on temperature. The amide group (NH) is located at carbon 4 of the benzene ring in the resin, also known as the para position, as shown in

section 3.3.1. In electrophilic substitution reactions involving halogens, the electron density of the benzene ring is decreased by the electronegativity and inductive effect of halogens, making it less reactive and stable. At elevated temperatures, the chlorine ions predominantly target the more reactive methyl group, substituting the hydrogen at the methyl position instead of the hydrogen in the NH bond of the benzene ring (Pérez et al., 2004). This form of substitution is termed side-chain substitution and reduces the yield. The substitution of hydrogen on a para position (NH position) by chlorine is favourable in low temperatures.

In electrophilic substitution reactions, lower pH environments enhance the reaction rate, thus the electrophilicity of the benzene ring. H^+ ions protonate benzene rings in acidic conditions, making them more electron-deficient, reactive, and electrophilic. The increased electrophilicity of the benzene ring leads to a successful substitution reaction with the Cl^+ ion (Ge et al., 2006). As a result, yield increases in acidic conditions.

Shi et al. (2022) studied the effect of temperature and chlorination time on the oxidative chlorine content in high-efficacy antimicrobial acyclic N-halamine-grafted polyvinyl alcohol films. Their results indicated that the oxidative chlorine content increased with the decrease in reaction temperature. Furthermore, the oxidative chlorine content increased with the increase in reaction time.

The findings of the ANOVA also show that an interaction between pH and temperature influenced the yield. According to the plots, the resin had a low chlorine concentration (%) when the temperature was high and the pH was low. The percentage of chlorine reduced when the temperature was low and the pH was high. The chlorine loading (mass %) was highest at low pH and low temperature. At lower temperatures, free chlorine radicals exhibit elevated selectivity. Simultaneously, in acidic conditions (low pH), the electrophilicity of the benzene ring is increased. The pronounced regioselectivity observed indicates that the chlorine free radicals preferentially target the NH group position in the benzene ring. This preference is attributed to the high electrophilicity of the NH group, making it more prone to electrophilic substitution, consequently leading to increased chlorine loading. This brings the positive interaction between temperature and pH.

3.5 Summary

In this chapter, a Merrifield resin was functionalized with a chlorinated N-halamine. This was achieved by first preparing the N-halamine precursor, thus the functional group (amide in a hydantoin) to carry the chlorine ions. After that, the N-halamine precursor was grafted on the resin surface using the covalent grafting procedure. The results of the two procedures were characterised by NMR spectroscopy and FTIR, respectively. The resin with the grafted functional group was used in a

chlorination reaction with NaDCC as the chlorine source. The results of the chlorination reaction were analysed using an iodometric titration reaction.

The preparation of the N-halamine precursor involved a nucleophilic substitution reaction, with optimization conducted through a two-factor CCD. Variations in temperature and reaction time were incorporated into the experimental design. The optimization process predicted an integral of 1.02 in the N-H peak at an optimal temperature of 44°C and a reaction time of 29 minutes.

A covalent grafting reaction was employed for the grafting of the amide functional group onto the resin surface, with optimization conducted through a two-factor CCD. The experimental design involved varying temperatures and reaction times, with an optimum temperature of 83°C and a reaction time of 11 hours, resulting in a predicted transmittance (%) of 22 for the C=O bond.

The chlorination of the resin was carried out through an electrophilic substitution reaction, with optimization conducted using a three-factor CCD. A yield of 91.5% (with 6.18%) of chlorine in the resin was achieved at 25 °C, a reaction time of 54 minutes, and a pH of 5.

In conclusion, a Merrifield resin was successfully functionalized with chlorine from NaDCC.

4 Chapter 4: Performance evaluation of the developed resin

4.1 Introduction

Chapter 3 of the research concentrated on modifying a Merrifield resin to produce a chlorinated resin by employing NaDCC as the chlorination agent. The functionalized optimal resin exhibited a chlorine content of 6.18% (by mass %). This procedure's objective was to improve chlorine loading on the resin.

In this section, the developed resin underwent a performance evaluation using experimental procedures to study the chlorine release behaviour and the disinfection efficacy. The chapter includes the methodology used, the analysis of the results and a summary of the investigations.

4.2 Methodology

A series of experiments were conducted to evaluate the performance of the resin. The initial experiment focused on preparing bacteria for the complex experiments. The evaluation focused on the resin's chlorine release profile and disinfection efficacy.

4.2.1 Culturing of bacteria feed suspensions

The bacteria played a pivotal role in the experiments conducted for performance evaluation. The evaluation focused on assessing how the resin behaved when exposed to a water source containing bacteria. To ensure a comprehensive examination, certain physical characteristics such as pH, temperature, turbidity, and electric conductivity were carefully controlled to avoid interference with the disinfection process. Factors like salinity, alkalinity, hardness, and organic content were also maintained at appropriate levels to prevent any inadvertent impact on the disinfection process. This thorough approach was adopted to ensure that the assessment of the resin's performance under the influence of bacteria was accurate and reliable.

4.2.1.1 Choice of bacteria

Several methods can be used to evaluate the effectiveness of disinfection technologies. The two options were to artificially contaminate a water supply or experiment on actual contaminated water. Experiments with actual contaminated water can present several challenges due to the complex and unpredictable nature of real-world water sources. One of the challenges is that contaminant composition can change significantly over time and from one area to another. Because of this heterogeneity, it is challenging to regulate the conditions of experiments and produce reliable results.

One pure bacterial culture, E. coli DH5 alpha, was chosen as the feed contamination. E. coli DH5-alpha is a commonly used laboratory strain of Escherichia coli derived from the K-12 strain. E. coli DH5 alpha is safer and simpler to handle because it is a biosafety class 1 pathogen. Previous research studies by Primo et al., (2022) have used DH5 alpha to assess the disinfection efficacy of AgZnO core-shell nanoparticles. The choice was made to use distilled water as the bacteria medium.

4.2.1.2 Bacteria growth curve

Before performance evaluation experiments of the resin, it was essential to have a basic understanding of the growth pattern of E. coli DH5 alpha. To determine the concentrations of E. coli DH5 alpha, optical density (OD) and cfu/ml measurements were investigated.

To establish the overall growth trend of E. coli DH5 alpha, a comprehensive growth analysis was conducted spanning 24 hours. Three distinct bacterial cultures were cultivated from separate growth media: Nutrient Broth, Luria Bertani (LB), and Tryptic Soy Broth. The bacteria concentration was determined using a UV Spectrophotometer with a specific wavelength of 600 nm (OD600) for absorbance measurements. These absorbance readings were taken at two-hour intervals throughout the entire 24-hour duration. The growth curve is shown in Figure 4-1.

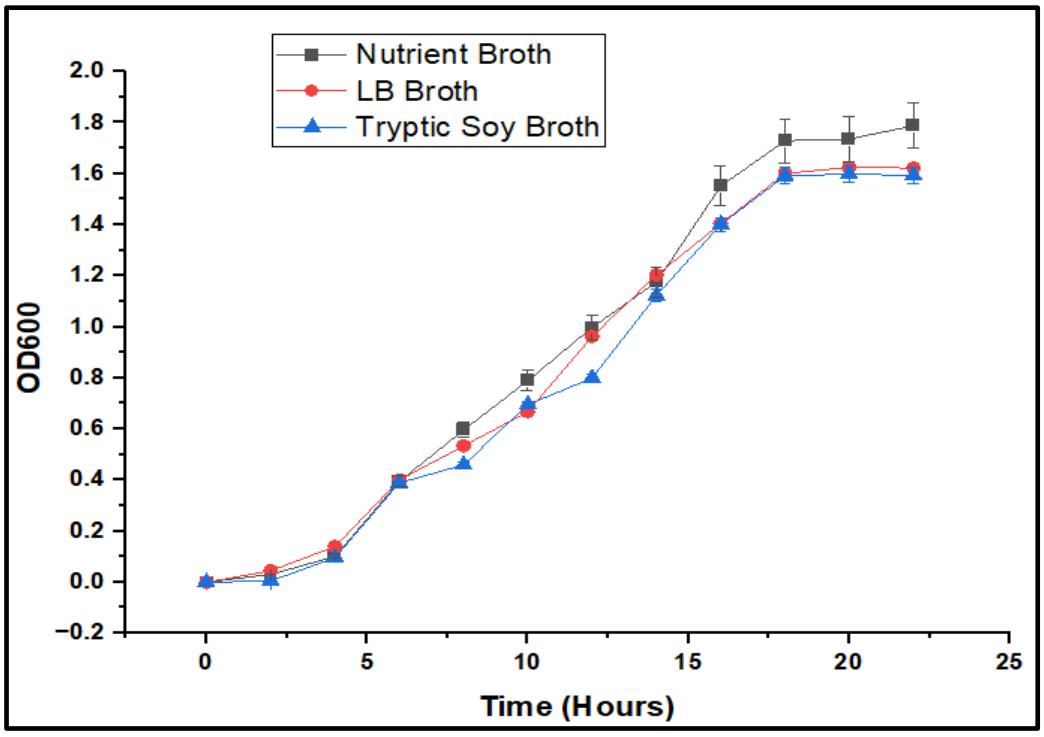

Figure 4-1: Bacteria growth curve of E. coli DH5 alpha using three different growth media

(Error bars indicate the standard deviation between triplicate experimental results)

All curves exhibited identical patterns, with only a minor discrepancy emerging after 22 hours. Bacteria grown in nutrient broth exhibited a faster growth rate; hence, this was the preferred growth media for the comprehensive experiments. Throughout the entire 24-hour timeframe, the OD600 value did not decline to a level below 1.4. Consequently, an OD600 measurement surpassing 1.4 could indicate that the bacteria had reached the stationary growth phase. The stationary phase was selected for experiments. The stationary growth phase selection for experiments was based on its ability to maintain consistent bacterial concentrations, ensuring repeatability. Additionally, using the stationary phase allows the feed to remain stable for a few hours, making it more manageable for experimental control.

Alternatively, to determine the actual cell concentration, three bacteria cultures were grown from different stock cultures, and full dilution plating was done every 2 hours to create the full 24-hour growth curve with standard deviations. Figure 4-2 shows the growth curve of bacteria (cfu/ml).

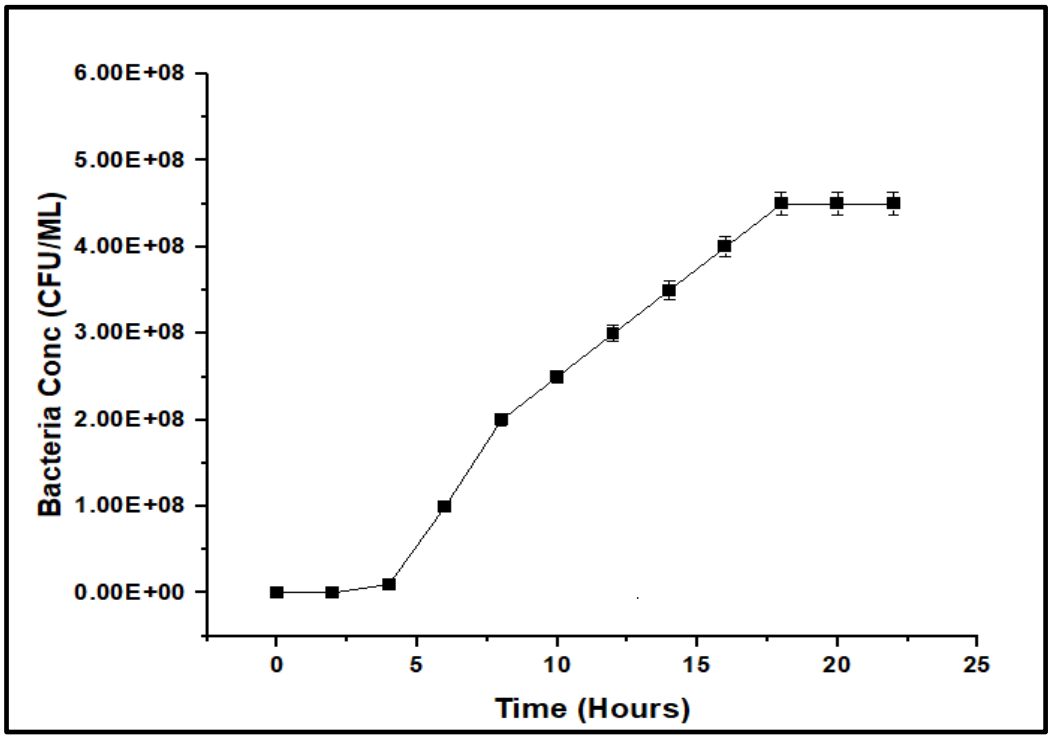

Figure 4-2: Bacteria concentration measured for over 24 hours

(Error bars indicate the standard deviation between triplicate experimental results)

The relationship between OD600 and cfu/mL is a useful approximation of bacterial concentration in liquid cultures. A calibration curve was generated to establish an accurate relationship between OD600 and cfu/ml. This involved measuring the OD600 of bacterial cultures with known cfu/mL concentrations. Figure 4-3 shows the calibration growth curve. The OD600 relationship is linear

compared to the bacterial concentration for 24 hours with an R-squared value of 0.98. The R^2 value supports the validity of the study.

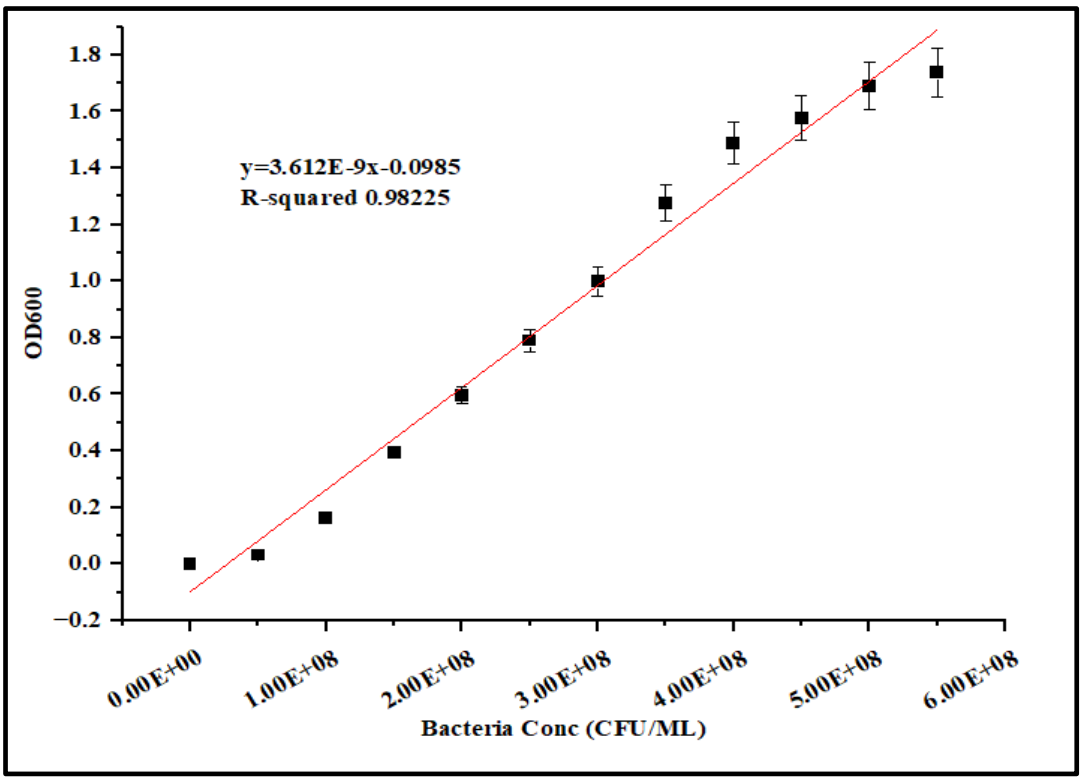

Figure 4-3: Bacteria concentration Vs. OD600

(Error bars indicate the standard deviation between triplicate experimental results)

4.2.1.3 Bacteria medium preparation

Plankenbrug river near Stellenbosch, known for having high bacterial concentrations ranging from 3.1 x 10^5 to 6.9 x 10^8 cfu/ml, was selected as a reference point (Alegbeleye et al., 2016). A feed concentration between 3.1 x 10^5 and 2.0 x 10^7 cfu/ml was chosen. The bacterial cultures cultivated in nutrient broth were diluted to achieve a bacteria concentration ranging from 3.1 x 10^5 to 2.0 x 10^7 cfu/ml.

4.2.2 Chlorine release experiments

The investigations into chlorine release aimed at understanding how the resin releases free chlorine upon exposure to water and the rate at which chlorine dissociates free chlorine. Measuring free chlorine in water is useful in conducting disinfection evaluations of the resin. Understanding the relationship between the chlorine release rate from the resin, the chlorine concentration within the resin, and the time is essential for designing a point-of-use (POU) system that uses the resin.

The kinetics of chlorine release were evaluated through two distinct experiments. The initial experiment involved introducing different resin amounts with varying chlorine quantities into the water with a constant concentration of bacteria to observe the gradual release of free chlorine over time. The second set of experiments monitored chlorine release at varying bacteria concentrations and a constant resin dosage.

It is important to highlight that, in this series of experiments, the quantity of water in contact with the resins is not regulated. The resin is submerged in a water bottle for over 12 hours. This accelerates chlorine depletion in the resin within a short timeframe. In practical applications, the resin's contact with water is typically controlled, i.e., for 5 minutes, thereby extending the lifespan of the resins. Despite the uncontrolled water volume in these experiments, they prove valuable for comprehending the release patterns of the resins under investigation before designing an actual point-of-use (POU) system that incorporates the resin.

4.2.2.1 Chlorine release kinetics: assessing the impact of varying resin mass on the release of chlorine

Four resin masses of 161.81 mg, 323.62 mg, 485.43 mg and 647.24 mg, each containing 6.18% chlorine by mass, were put in four bottles containing 1L of water with a bacteria concentration of 3.6 $x10^6$ cfu/ml. The temperature was maintained at a constant 25°C, and the pH was kept constant at 7. The bottles were put on a stirring apparatus with a constant speed of 200rpm and were stirred for 12 hours. The free chlorine in the bottles was measured using a colorimetry test kit at different time points. The release of chlorine was monitored for 11 hours. The entire experiment was replicated three times to ensure the consistency and reliability of the results.

4.2.2.2 Chlorine release kinetics: assessing the impact of varying bacteria concentration on chlorine release

Three bacteria concentrations, 3.1 $x10^5$ cfu/ml, 3.6$x10^6$cfu/ml, and 2.0 x 10^7 cfu/ml, were chosen for the experiment. A bottle containing zero bacteria was used as a control in this experiment. A resin mass of 323.62 mg containing 20 mg of chlorine was put in each of the four bottles. The experimental procedure was conducted as in section 4.2.2.1.

4.2.3 Disinfection efficacy test

A systematic experimental approach was used to understand the resin's efficacy as a disinfectant. The initial investigation focused on free chlorine, and the outcomes were used for more extensive experiments importantly, the relationship between the resin's concentration and contact time (CT).

The concentration of free chlorine and the contact time are the primary factors that impact the effectiveness of disinfection using chlorinated resin. Therefore, this section includes experiments that explore the relationship between free chlorine concentration and contact time to achieve optimal disinfection.

4.2.3.1 Experimental procedure

The resin's disinfectant capabilities in water were evaluated using the concentration-contact time (CT) test through a series of experiments. These tests aimed to determine the optimal resin concentrations and exposure durations for effective disinfection. This process introduced a bacterial concentration of 2.0 x 10^7 cfu/ml into four separate 1L treatment containers. Within these containers, five different quantities of resin were placed (323.62 mg, 485.43 mg, 647.24 mg, 809.0 mg and 1000 mg), each containing 6.18% of chlorine by mass. One container contained unchlorinated resin (1g) for comparison as a control. Water samples were collected from each container at three specific time points: 5 minutes, 15 minutes, and 25 minutes.

There are several methods of determining the efficacy of disinfectants. Some of these methods are more expensive, and others are more time-consuming. The most viable number was used to assess the counts of viable and living cells within the collected samples. The entire experiment was replicated three times to ensure the consistency and reliability of the results.

Most probable number method

After the experiments were conducted, samples were plated immediately without additional exposure to disinfectants, and after two days, the plates were investigated to determine treatment success. The following equations were used to calculate the reduction of bacteria in the samples:

$$\boldsymbol{log\ reduction = log\ 10\ (\frac{final\ cfu}{initial\ cfu})} \qquad \textbf{(Eq. 4-1)}$$

To translate calculated log reductions to a percentage value, Equation 4-2 was used:

$$\boldsymbol{\%\ reduction = 100 \times (\frac{initial\ cfu - final\ cfu}{initial\ cfu})} \qquad \textbf{(Eq. 4-2)}$$

4.3 Results and discussion

4.3.1 Chlorine release mass balance

The release of chlorine in the resin is governed by N-halamines undergoing electrophilic substitution reaction upon contact with water. In this process, N-halamines releases chlorine atom from the N-cl

bond in the N-halamine (resin), occupied by a hydrogen atom from a water molecule as shown in the equation below.

$$R'NCl \overset{H_2O}{\longleftrightarrow} R'NH + Cl^+ + OH^- \quad \textbf{(Eq. 4-3)}$$

To quantify the consumption of products in the reaction theoretically, extent of reaction mathematics was applied. This was to trace the amount of chlorine (mass balance) during the reaction.

For the electrophilic substitution reaction above the mass balance of chlorine and resin is of primary focus. The reaction occurs under constant temperature and pressure.

The extent of reaction (change in amount of reactants and products) was computed by;

$$\mathbf{0} = \sum_i \boldsymbol{u_i}\, \boldsymbol{s_i} \quad \textbf{(Eq. 4-4)}$$

Where:

- U denotes the specific species in the reaction (i.e. chlorine)
- S denotes the stoichiometric coefficient of specific species in the reaction

For the electrophilic substitution reaction above

- 1 mole of Cl corresponded to 1 mole delivered to water during disinfection.

$$-Cl\,(reactants) = +Cl(product) \quad \textbf{(Eq. 4-5)}$$

$$-\xi\,(reactant) = +\xi\,(product) \quad \textbf{(Eq. 4-6)}$$

- 1 mole of resin was consumed for every mole of water.

The experiments were done by varying the initial mass of resins, the Table 4-1 below shows the resin mass variations and expected theoretical mass balance.

Table 4-1: Estimation of consumption figures of the varying resin mass when put in 1 L of water

Resin mass (mg)	Chlorine mass in resin (mg)	Theoretical products mass (cl in water) (mg/L)	Experimental product mass Cl in water (mg/L)
161.18	10	10	7.41
323.62	20	20	16.92
485.43	30	30	27.31
647.24	40	40	37.02

4.3.2 Chlorine release kinetics of resin

The study examined the pattern of chlorine release from the resin. Free chlorine levels were monitored until they reached a state of equilibrium. Kinetic models were applied to the free chlorine data to study the chlorine release kinetics of the resin.

4.3.2.1 Kinetic models

Several mathematical kinetic models have been developed to describe resins' phenomena regarding adsorption reactions and diffusion processes. Adsorption kinetic models are valuable in various fields, including wastewater treatment, chromatography, and purification processes. Adsorption kinetic mathematical models help optimize adsorption systems and design efficient resin-based processes (Qiu et al., 2009). Nonetheless, the resin employed in this research was designed not for adsorption processes but for the gradual release of chlorine into water. Hence, applying adsorption kinetic models to investigate how the resin behaves regarding chlorine release was not feasible.

The free chlorine release data matched the first-order drug release model originally derived from drug release modelling. Gibaldi and Feldman (1967) were the first to suggest using this method in drug delivery research, and Wagner (1969) followed suit (Naiem et al., 2017). The first-order kinetic model effectively describes drug release from polymeric films, suggesting that the mechanism of drug release depends on its concentration. This model has previously been employed to explain the release of various therapeutic substances and control the administering of drug concentration in the bloodstream. The first-order drug release model has been used to optimize the design of new drug delivery systems with desired therapeutic efficacy and safety (Mohammed et al., 2010). Chlorine release from the resin polymer follows the first-order drug release kinetic model.

The first-order model was implemented to predict the rate of chlorine release from the resin and establish whether the mass of the resin and the concentration of bacteria in the water influenced the release rate. Additionally, by understanding the first-order kinetics, systems can be designed to regulate chlorine concentrations within a disinfection period, preventing over-chlorination in water system levels. It should be noted that this is the first study that has adopted the drug release model to predict the release of chlorine from the resin for water disinfection. The first-order drug release equation is presented using the Equation 4-7 (Trucillo, 2022):

$$Log\ Q_t = Log\ Q_0 - {Kt}/{2.303} \qquad \textbf{(Eq. 4-7)}$$

Where:

- Q_0 = initial amount of chlorine in resin
- Q_t = cumulative amount of chlorine in resin at a time “t”.
- K = first order release constant.
- t = time in minutes.

Using line fit, the slope is identified, and the K is calculated:

$$Slope = \frac{-k}{2.303} \quad \textbf{(Eq. 4-8)}$$

The data obtained are plotted as a log cumulative percentage of chlorine remaining in resin vs. time. The constant K is a key parameter in the model and describes the rate at which chlorine is released from a resin. It quantifies how fast the chlorine is released as the chlorine concentration in the resin changes over time.

4.3.2.2 Effect of the resin mass on the chlorine release

Concentrations of free residual chlorine in each water bottle were analysed for 11 hours with monitoring of free chlorine at different time points. Figure 4-4 shows the free chlorine results in the water with a constant feed concentration of $3.6x10^6$ cfu/ml and varying resin mass with varying chlorine amounts of 10 mg, 20 mg, 30 mg, and 40 mg for 30 mins. Figure 4-5 shows the free chlorine concentrations (mg/L) measured in 11 hours.

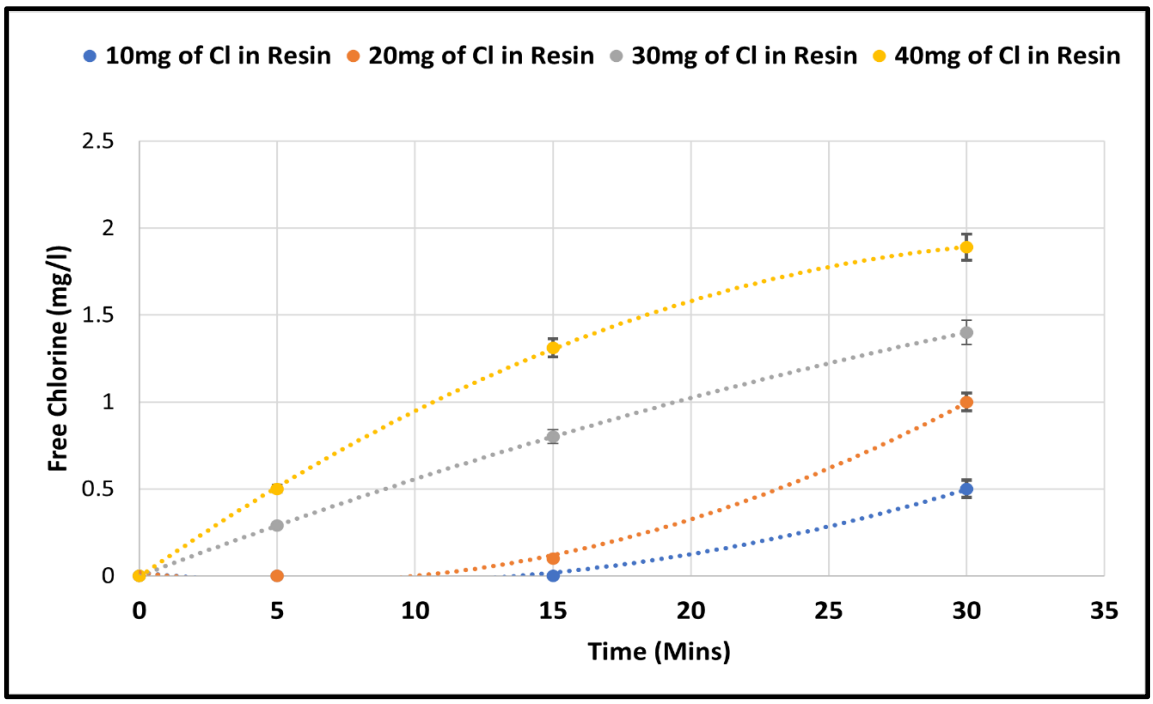

Figure 4-4: Free chlorine in water with a varying resin chlorine mass for 30 mins

(Error bars indicate the standard deviation between triplicate experimental results)

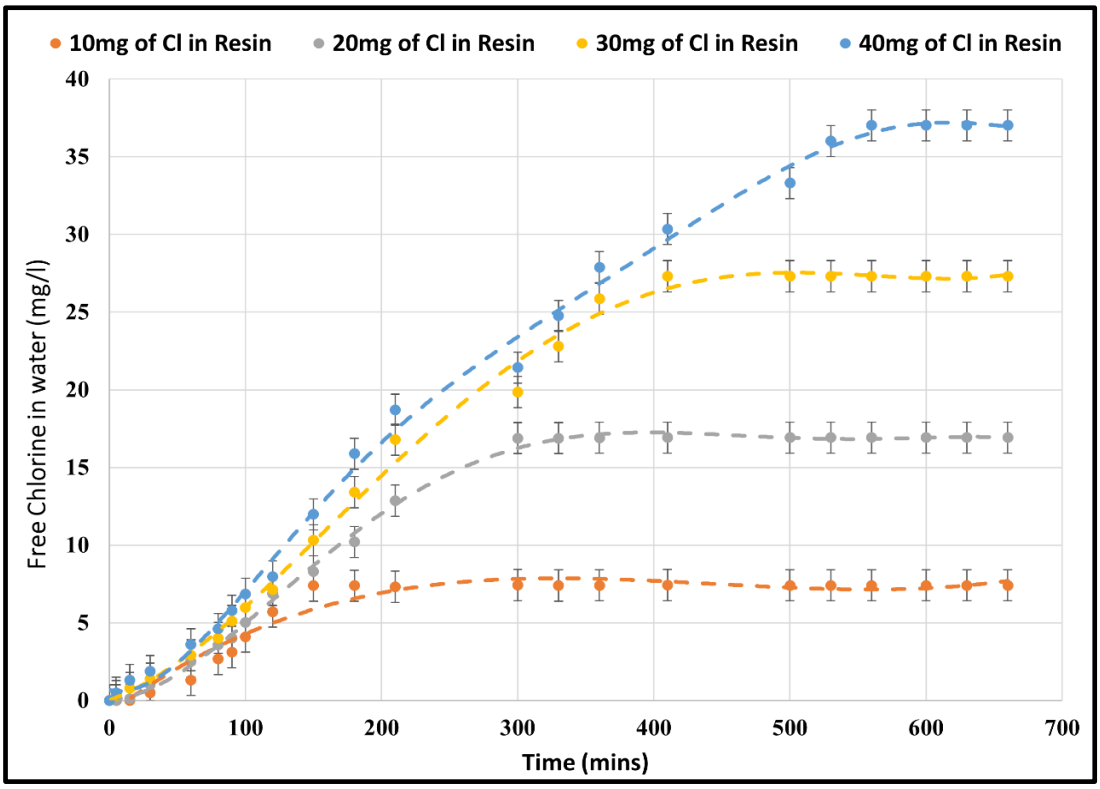

Figure 4-5: Free chlorine in water at a time (t) for varying resin mass for 11 hours

(Error bars indicate the standard deviation between triplicate experimental results)

From Figure 4-4, no free chlorine was observed in the first 5 minutes for the chlorine amounts of 10 mg and 20 mg. However, a free chlorine concentration of 0.5 mg/L was observed in the bottle containing the chlorine amount of 40 mg after 5 minutes, and a free chlorine concentration of 0.3 mg/L was observed in the bottle that had a resin dosage with chlorine concentration of 30mg after 5 minutes. For the chlorine amounts of 10 mg and 20 mg, free chlorine was detectable after 15 minutes. During the first moments, chlorine is consumed by the bacteria in the water; hence, no free chlorine is detected. However, free chlorine was detected within a brief five-minute period for the resin dosage containing the highest chlorine concentration, which implies that the resin dosage released enough chlorine species in water within five minutes that reacted with the bacteria and free chlorine residuals were detectable after five minutes. Based on these findings, it can be concluded that the interaction between chlorine and bacteria is rapid when chlorine levels are elevated, which results in the detection of free chlorine faster. A similar outcome was obtained by Helbling et al. (2007), where it was concluded that the inactivation time of E. coli by chlorine decreased with an increase in chlorine dosage.

Additionally, it can be deduced that free chlorine concentration is typically higher at a time t when the initial concentration of chlorine used in water treatment is high due to the principles of chemical equilibrium. The chemical reactions during chlorination influence the relationship between the initial

chlorine dose and the resulting free chlorine concentration in water. When added to water, chlorine undergoes a chemical reaction with water that forms hypochlorous acid (HOCl) and hypochlorite ion (ClO^-). The equilibrium between HOCl and ClO^- determines the free chlorine concentration in the water, directly related to the initial concentration of chlorine added. The higher the initial chlorine concentration, the more chlorine molecules can react with water and form both HOCl and ClO^-, leading to a higher free chlorine concentration (Solomon et al., 2009). An evaluation of the research conducted by Virto et al. (2004) supports this outcome. Their findings showed that three solutions with different beginning amounts of free chlorine exhibited different amounts of free concentration in the suspension containing a fixed concentration of Listeria monocytogenes. Their results suggested that systems that show higher free chlorine are those with higher beginning concentrations of chlorine.

A more interesting result is that the resin amounts reach saturation at different times (see Figure 4-5). The chlorine amount of 40 mg took longer to exhaust the free chlorine in water. The resin dosage with less chlorine amount exhausted the free chlorine faster and reached saturation faster. The resin with a higher initial chlorine amount (40 mg) had a larger chlorine reservoir available for release. According to Le Chatelier's principle, when a system experiences a change in concentration, the equilibrium shifts to counteract the imposed change partially (Liu et al., 1996). In this case, the concentration of the chlorine in the resin varied.

The free chlorine data was fitted in the first-order kinetic model presented by Equation 4-7 to describe the effect of resin dosage on the release rate of chlorine. The experimental data shown in Figure 4-5 was utilized to plot a straight line of log % cumulative chlorine remaining in resin as a function of time. The data was plotted as shown in Figure *4-6*. The first-order kinetics model parameters are shown in Table 4-2.

Table 4-2: First-order kinetic model parameters for varying resin masses

Resin mass (mg)	Cl amount in Resin (mg)	First Order Constant (K) K(min^{-1})	R^2-Value
161.81	10	0.153 mg	0.936
323.62	20	0.239 mg	0.997
485.43	30	0.351 mg	0.960
647.24	40	0.441 mg	0.945

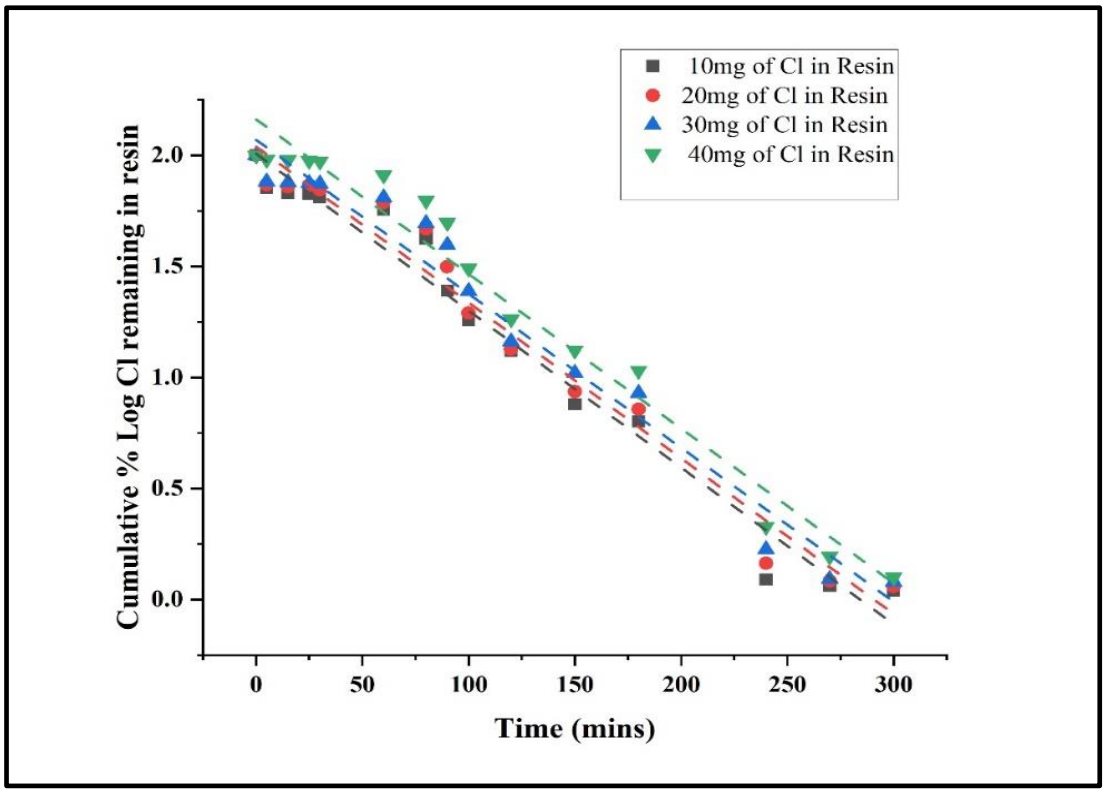

Figure 4-6: First-order mathematical model of chlorine release from resin at a constant bacteria concentration and a varying resin mass

The first-order drug release model accurately fits the experimental data with R^2 values, as shown in Table 4-2. This model can effectively be used to precisely predict the quantity of free chlorine that will be discharged by various resin doses, each having varying chlorine concentrations, at different time intervals. The rate constant (K) of the different resin amounts indicates the amount of chlorine released per minute. The rate constant results show that the release rate of the chlorine from the resin was different, with the higher chlorine dosage having the highest release rate. These results are attributed to the electrophilic substitution reaction between the Cl in the N-Cl bond of the resin and H from water molecules. When the N-halamine resin is exposed to water, it releases $Cl^{+,}$ which undergoes a substitution reaction with H from water. Concentration is one of the factors that affect the substitution reactions. Higher concentrations of electrophiles generally lead to faster reactions (Romeo et al., 1992). A greater chlorine dose leads to an elevated concentration of free chlorine species. With an increased concentration of free chlorine species in the water, the substitution reaction between the N-Cl bond of the resin and H molecules takes place more rapidly, resulting in a faster release of Cl^+. Additionally, in section 2.5.6.2, it was discussed that water is one of the factors that affects the stability of N-halamines. In the event that the volume of water was small, the release of free chlorine would have slowed down. Previous research by Abbasnezhad et al. (2021) investigated chlorine release from polyurethane films. Their results indicated that increasing the initial chlorine

loads enhanced chlorine liberation from the films. These results suggest that the chlorine release mechanism is concentration-dependent. The amount of chlorine released decreases with decreasing concentration gradient over time (Shafiei et al., 2021). In conclusion, the resin dosage affects the release rate of chlorine from the resin.

An incremental dosage/concentration of resin in the same volume of water leads to an increased release rate of chlorine. Using the first-order drug release model, the K parameters for each resin dosage can be used in designing a POU lab-scale device. Parameters such as the amount of resin (grams), flow rate, amount of water to be disinfected, and resin life span are highly dependent on the chlorine release behaviour studied in this section.

4.3.2.3 Effect of bacteria concentration on chlorine release rate

Free residual chlorine concentrations in water samples containing different bacteria concentrations were analysed for 10 hours at different intervals. Figure 4-7 shows the results of the free chlorine in the water with a varying feed concentration of 3.1 x10^5 cfu/ml, 3.6x10^6cfu/ml, and 2.0 x 10^7 cfu/ml and a resin amount containing 20mg of chlorine for 1 hour. Figure 4-8 shows the results of the free chlorine in the water with a varying bacteria concentration of 3.1 x10^5 cfu/ml, 3.6x10^6cfu/ml, and 2.0 x 10^7 cfu/ml and a resin amount containing 20mg of chlorine for 8.3 hours.

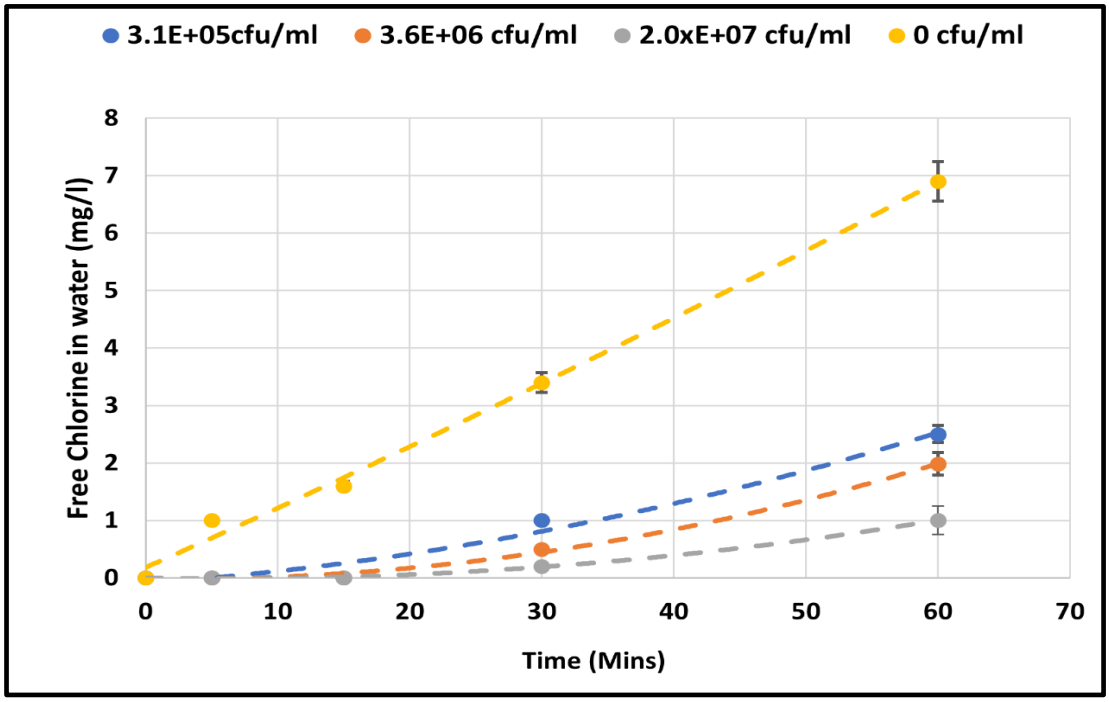

Figure 4-7: Free chlorine in water with a varying bacteria concentration of 3.1 x10^5 cfu/ml, 3.6x10^6cfu/ml, and 2.0 x 10^7 cfu/ml and a resin amount containing 20 mg of chlorine for 1 hour

(Error bars indicate the standard deviation between triplicate experimental results)

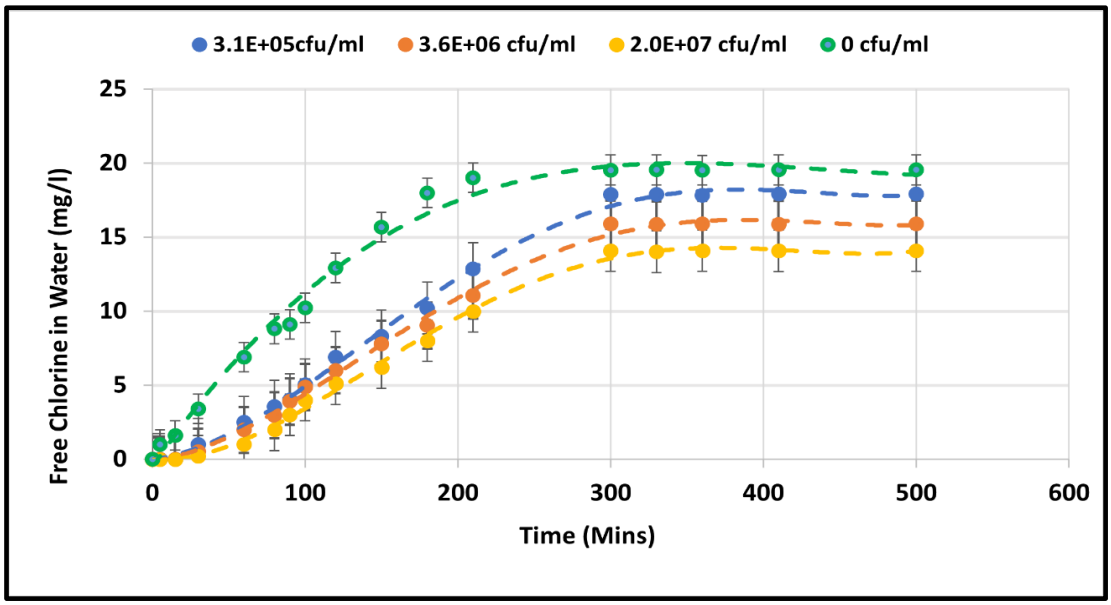

Figure 4-8: Free chlorine measured in water with a varying bacteria concentration and a constant resin mass

(Error bars indicate the standard deviation between triplicate experimental results)

From Figure 4-7, free chlorine was not detected in the samples with bacteria concentrations for at least 20 minutes. Free chlorine was detectable within five minutes in the sample with zero bacteria. After 20 minutes, free chlorine was detectable in the samples containing bacteria. A free chlorine concentration of 0.2 mg/L was detected in the sample containing the most bacteria (2.0×10^7 cfu/ml). After 20 mins, 0.5 mg/L was detected in the sample with the lower bacteria concentration (3.1×10^5 cfu/ml). Furthermore, after 300 minutes all resin dosages had reached saturation. Free chlorine concentration did not increase after this time, suggesting an exhaustion of chlorine from the resin. The behaviour can be explained in two folds. When the resin is exposed to water, it releases free chlorine. The chlorine immediately begins to oxidise the bacteria. This initial reaction wipes out a certain portion of chlorine, so nothing shows up on the release profile until after 15 minutes in the chlorine release profiles of water with different bacteria concentrations. The concentration of bacteria influences the residual chlorine level. Higher bacterial concentrations lead to more rapid depletion of free chlorine, as more bacteria concentration requires more chlorine for oxidation. This potentially results in lower residual chlorine concentrations in the water with more bacteria concentration at time t (Brooks et al., 2007). The conclusions from the Virto et al. (2005) study correspond with the results obtained in this study.

An interesting result was that the resin dosage in the 3 different bacteria concentrations reached saturation at the same time. This is because the amount of free chlorine available in water mainly depends on variations in the water volume and the chlorine concentration. The equilibrium time was unaffected since both volume and chlorine concentration were constant.

The free chlorine data was fitted in the first-order kinetic model presented by Equation 4-7 to describe the effect of bacteria concentration on the release rate of chlorine. The experimental data (see Figure 4-8) was utilized to plot a straight line of log % cumulative chlorine remaining in resin as a function of time. The data was plotted as shown in Figure 4-9. The first-order kinetics model parameters are shown in Table 4-3.

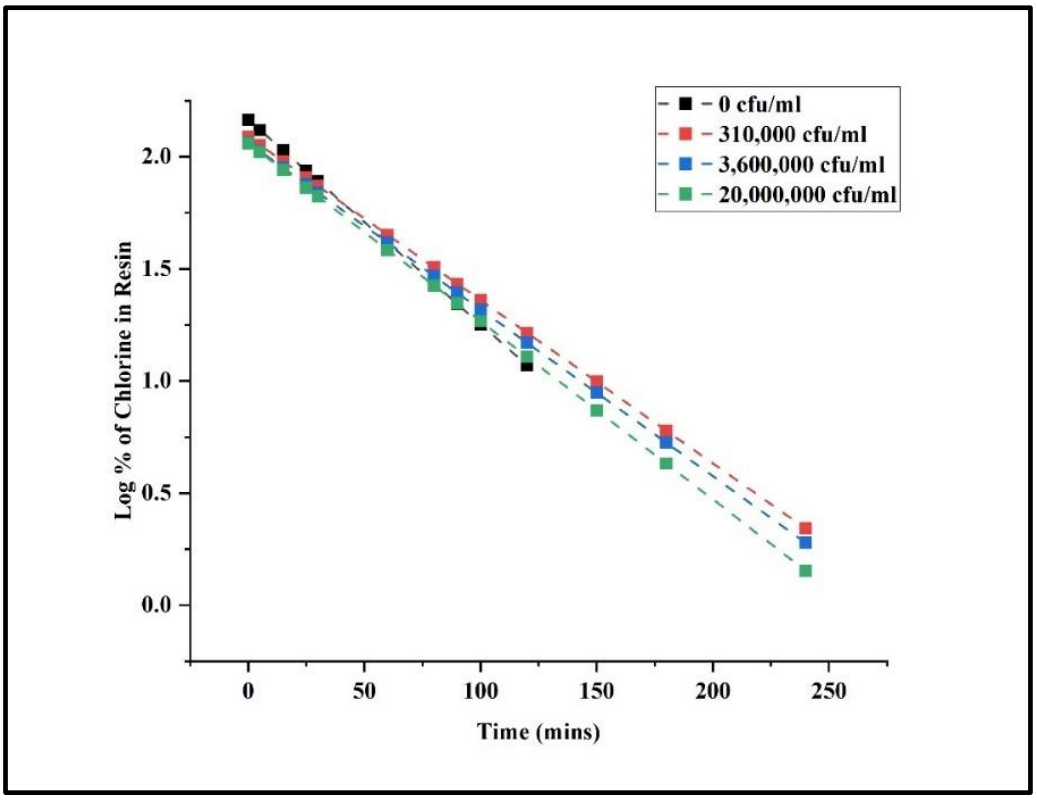

Figure 4-9: First-order mathematical model of chlorine release from resin at constant resin dosage and varying bacteria concentration

Table 4-3: First-order kinetic model parameters for varying bacteria concentration

Bacteria Concentration in the sample (cfu/ml)	First Order Constant (K) min^{-1}	R^2-Value
0	0.239	0.990
3.10E+05	0.238	0.997
3.60E+06	0.237	0.997
2.00E+07	0.238	0.997

The first-order drug release model accurately fits the experimental data with R^2 values, as shown in the table above. This model can effectively predict the amount of free chlorine released by the same resin amount when exposed to water with different bacteria concentrations. The rate constant (K) of the different resin amounts indicates the amount of chlorine released per minute. The rate constant

results show that the release rate of the chlorine from the resin was similar despite the difference in bacteria concentration. Bacteria concentration is not a direct factor affecting the release of chlorine, as evidenced by the constant value of K in the first-order models in Table 4-3. The release of chlorine from the resin depends on the chlorine concentration and the water's characteristics pH, temperature, and volume of water (How et al., 2017). The volume of water determines the amount of free hydrogen (H) atoms available for substitution reaction with chlorine (Cl) available in the resin. Bacteria concentration influences the fate of chlorine in water due to their metabolic activities. Bacteria concentration is a factor that must be considered when designing disinfection processes and maintaining appropriate chlorine residuals in water distribution systems (Qi et al., 2022).

4.3.3 Disinfection efficacy results

To develop an understanding of the chlorinated resin as a disinfectant, a sequential experimental process was followed. Five resin quantities (323.62 mg, 485.43 mg, 647.24 mg, 809.0 mg and 1000mg), each containing 6.18% chlorine, were investigated. The study was done in triplicate and aimed to explore the resin's concentration-contact time (CT) relationship, which was analysed with ANOVA analysis. Table 4-4 shows the results of the analysis.

Table 4-4: Significance test for the disinfection efficacy test parameters by use of p-values

Parameters	P-value	Test of significance (α=0.05)	Significance
(1) Contact Time (Linear)	0.031	p< α	Significant
Contact Time (Quadratic)	0.249	p> α	insignificant
(2) Chlorine amount in Resin (mg) (linear)	0.003	p< α	Significant
Chlorine amount in Resin (mg) (Quadratic)	0.037	p< α	Significant
1L*2L	0.018	p< α	Significant

Table 4-4 shows that the resin amount and contact time significantly influenced the disinfection efficacy. This is because their p-values were less than 0.05. The analysis also showed that the interaction of the contact time and chlorine amount in resin significantly affected the disinfection efficacy.

4.3.3.1 Effect of contact time and resin dosage on disinfection efficacy

Figure 4-10 illustrates the effect of the resin dosage (a representation of chlorine amount in resin) and the contact time on the disinfection efficacy of the resin in 1L of water containing a bacteria concentration of 2.0 x 10^7 cfu/ml.

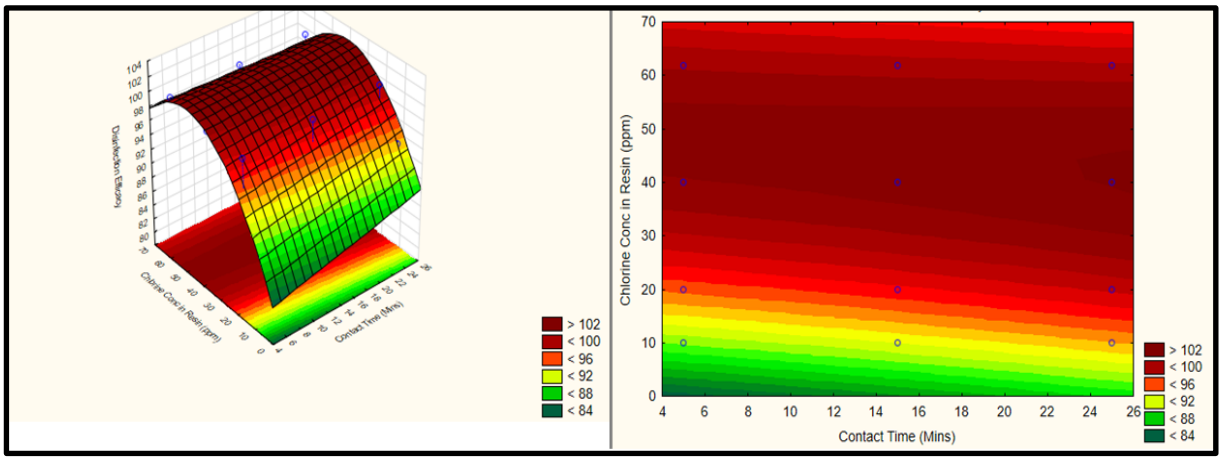

Figure 4-10: Effect of the resin mass and contact time on the disinfection efficacy of the resin

From Figure 4-10, It can be observed that the disinfection efficacy increased with an increase in contact time. A resin dosage containing 10mg chlorine increased its disinfection efficacy from 70% to 80% when the contact time increased from 4 to 26 minutes. However, it was noted that the resin dosage containing 10mg of chlorine failed to achieve a 90% bacterial kill in less than 30 minutes. A similar observation was made for a resin dosage containing 20mg of chlorine; the disinfection effectiveness increased from 96% to 99% with an increase in time. Furthermore, a resin dosage of 30mg of chlorine managed to attain a disinfection efficacy of 99% within a 5-minute contact time. An intriguing observation was that, from 30mg chlorine dosage above, a 99% disinfection efficacy was consistently achieved within just 5 minutes. From the kinetic models, 30 mg chlorine in resin releases 0.351mg per min, thus 1.75mg in 5 minutes. Three interesting conclusions can be drawn from the obtained results. An Increase in dosage influences the disinfection efficacy for resin dosages with less than 30mg of chlorine. A higher concentration provides more active chlorine molecules that can interact with hydrogen molecules and form more HOCL, which binds to acceptor regions on microorganisms and disrupts the microorganisms' cell membranes, proteins, or nucleic acids. An increase in the contact time influences the disinfection efficacy of the resin for resin mass with less than 30mg of chlorine. Longer contact times allow the resin to act on microorganisms (Voorn et al., 2023). The disinfection effectiveness is influenced by the combined impact of contact time and resin dosage for resin dosages with less than 30mg of chlorine, showing a synergistic effect. In summary, the developed resin can achieve 99.9% bacterial elimination within a 5-minute period for resin dosages containing 30mg or more of chlorine for a 1-litre water volume.

Based on the experiments involving free chlorine, it was deduced that the chlorine release depends on the resin mass, which directly impacts the disinfection effectiveness. This affects the residual chlorine after the disinfection phase. Observation of free residual chlorine levels was carried out for all resin dosages containing more than 30 mg of chlorine to assess the residual free chlorine after achieving 99% bacteria kill in 5 minutes for a 1L water volume. Figure 4-11 illustrates the residual chlorine after 5-minute disinfection time for resin dosages with more than 30 mg of chlorine.

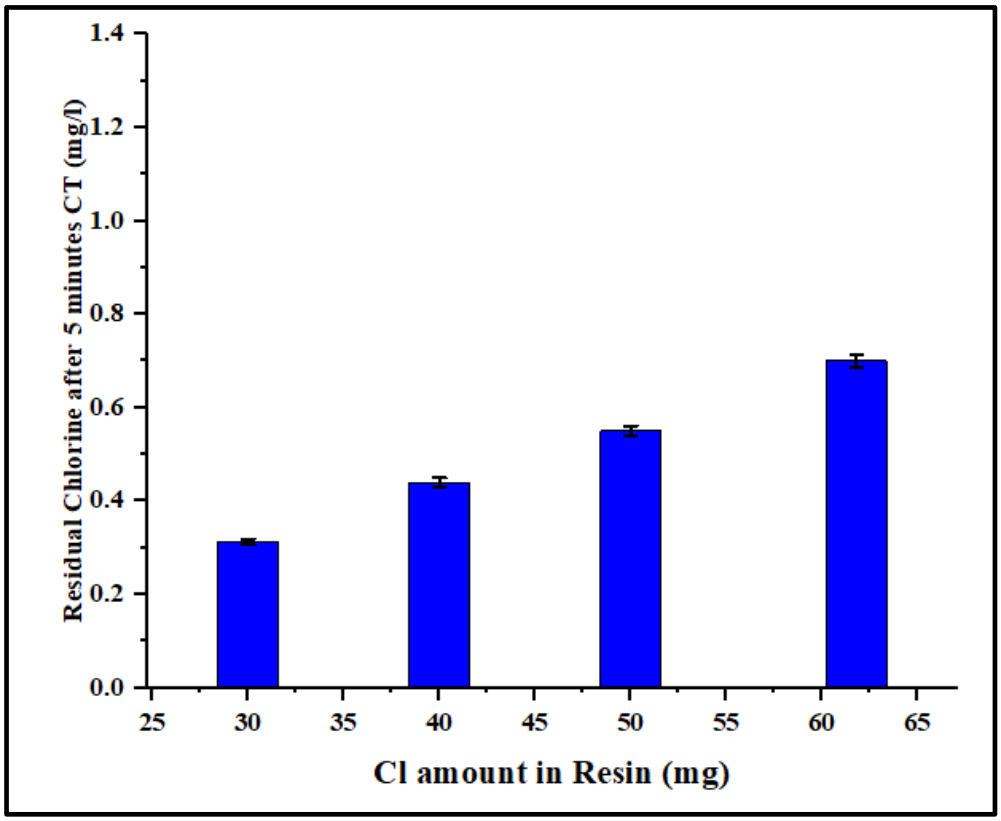

Figure 4-11: Free residual chlorine for resin dosages with more than 30mg of chlorine after treating 1L of water in 5 minutes

(Error bars indicate the standard deviation between triplicate experimental results)

As depicted in the figure above, the resin dosage with a chlorine amount of 30mg had a free residual of 0.3 mg/L, and the resin dosage of 61.8mg of chlorine had 0.7 mg/L of residual chlorine. It is important to highlight that while resin dosages containing more than 30mg of chlorine achieve optimal disinfection within 5 minutes, there is also a concurrent rise in residual chlorine levels after disinfection for a 1-litre water volume as the resin dosage increases. This suggests that an increase in the volume of the water to be disinfected is recommended as the resin mass increases to decrease the amount of residual free chlorine and simultaneously achieve maximum disinfection. This also implies that, in practical applications, when integrating the resin, it can be engineered to release a

specific quantity of chlorine while sustaining a minimum residual chlorine by regulating the flow rate within a system.

4.4 Summary

- At a constant water volume and bacterial concentration, the resin mass had an impact on the rate of chlorine release for a 1 L water volume. A resin mass of 647.2 mg (containing 40 mg of chlorine) released chlorine at a rate of 0.441 mg/min for 1 L of water and a resin mass of 485.43 mg (containing 30 mg of Cl) exhibited a chlorine release rate of 0.351 mg/minute for a 1 L volume of water.
- The release of chlorine from the resin was constant for varying bacteria concentration and constant resin mass for a constant water volume of 1 L.
- The minimum resin amount that can effectively achieve 99.99% bacteria kill in 5 minutes is 485.43 mg (containing 30 mg of Cl) for 1 litre of water.
- The residual chlorine concentration increased from 0.3 mg/L to 0.7 mg/L for a 1-litre volume of water when the resin mass increased from 30 mg to 61.8 mg, which implies that when more resin mass is used, the amount of water to be disinfected should also increase.
- It should be noted that the experiments in chapter 4 were conducted for a 1 L water volume.

5 Chapter 5: Performance evaluation experiments as a lab-scale continuous POU system

5.1 Introduction

In Chapter 4, the research focused on examining the resin's characteristics when exposed to a water source with bacteria concentration. The chlorine release behaviour of the resin was studied. A mathematical first-order kinetic model from drug release models was used to analyse the chlorine release behaviour of the resin. The first-order chlorine release parameters were used in this chapter to design a lab-scale continuous POU system. In continuous-release systems, the first-order parameters assist in designing systems that can maintain a constant chlorine release rate, providing a steady and sustained disinfection effect over an extended period. Knowledge of first-order parameters is essential for scaling up manufacturing processes.

In this chapter, a lab-scale Point of Use (POU) water treatment continuous system was designed. Performance evaluation experiments were conducted regarding the feasible flowrates of the continuous system and the stability of the continuous system.

5.2 Methodology

The assessment of the developed resin's performance in a lab-scale Point of Use (POU) system involved a series of experiments to determine its viability as a point-of-use water treatment method. The experimental procedures focused first on determining the flow rate of the system. This was followed by experimental runs on the resin's stability, examining factors such as chlorine loss, disinfection efficacy, and residual chlorine after 20 disinfection cycles.

5.2.1 Experimental setups

5.2.1.1 Resin column

A Perspex cast acrylic plastic material was used to design the resin column (3 cm diameter). To accommodate the resin, the column's design was specifically configured to prevent the resin from traversing the tubing. Both sides of the column were affixed with two circular plaques measuring 6 cm in diameter. Onto these plaques, fabric sheets measuring 6 cm in diameter were applied, and an additional set of plaques were securely attached above the fabric sheets using screws to secure and

hold the fabric sheets in position. To determine how much resin the column could hold, the following procedure was followed:

- To find the amount (mass) of resin that can be accommodated in the resin column, the volume of the resin column was calculated using Equation 5-1**.**

$$v = \pi r^2 L \qquad \textbf{(Eq. 5-1)}$$

V is the column's volume, r is the column's radius, and L is the column's length.

- The volume obtained was then used to determine the resin mass to be loaded in the column using Equation 5-2

$$\rho = \frac{m}{V} \qquad \textbf{(Eq. 5-2)}$$

Where;

- ρ is the density of the resin (provided by the manufacturer, (Density of resin 483.4g/l)
- V is the volume of the column
- m is the mass of the resin

Figure 5-1 shows the resin column with the resin in it:

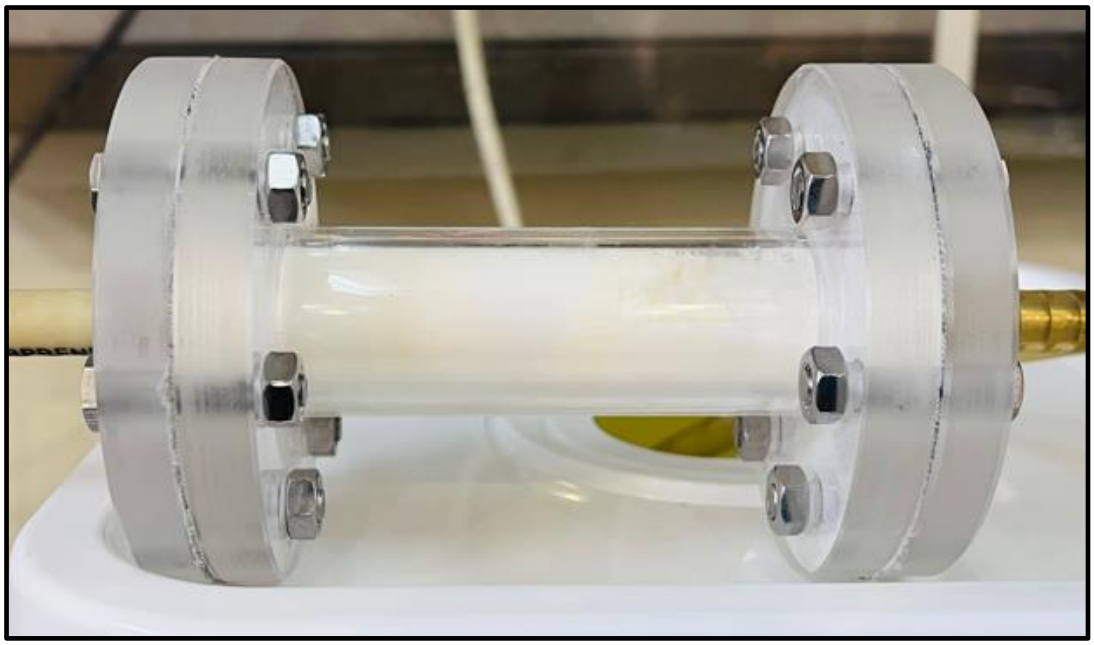

Figure 5-1: The resin column

5.2.1.2 Hydrodynamic conditions of the POU device

This section outlines the hydrodynamic characteristics of the point-of-use (POU) device experimental setup, specifically within the resin column. The section addresses pressures, temperatures, flow velocity, and mass flow rate in the horizontal flow system. Hydrodynamics employs mathematical equations such as the Bernoulli equation to describe and predict fluid behavior when designing a water treatment system (Qin & Duan, 2017). Figure 5-2 shows the schematic diagram of the resin column used in this study.

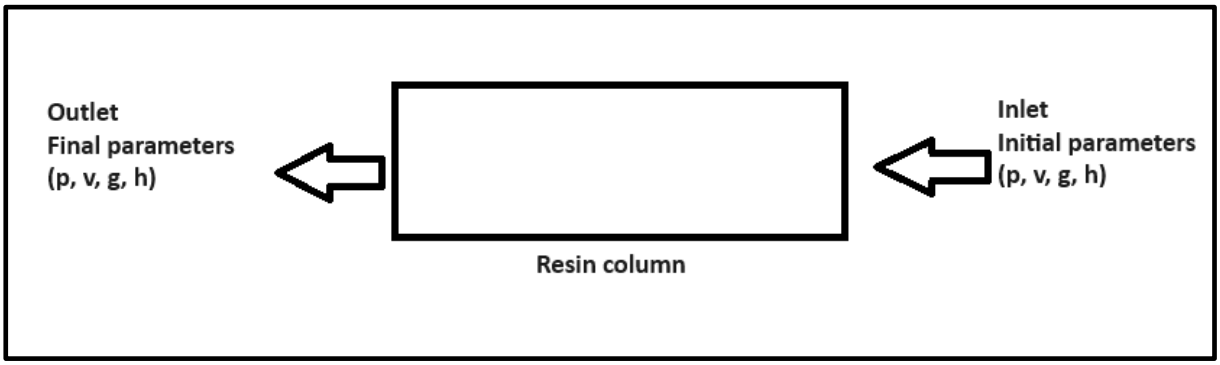

Figure 5-2: Schematic diagram of the resin column

The device was operated under room temperature and atmospheric pressure (these variables were kept constant) this implies that the total Gibbs energy of the substitution reaction for Cl and H is zero. The flow velocity and mass flow rate can be computed from the Bernoulli equation. In a column with negligible height and with flowing fluid, the Bernoulli equation is:

$$p_1 + \frac{1}{2}\rho g v_1^2 = p_2 + \frac{1}{2}\rho g v_2^2 \qquad \textbf{(Eq. 5-3)}$$

Where;

- *p* is the pressure in the column
- *g* is the acceleration due to gravity
- *v* is the velocity
- ρ is the density of water

The flow velocity (m/s) at the inlet was calculated as

$$v = \frac{Q}{A} \qquad \textbf{(Eq. 5-4)}$$

Where;

- v is the flow velocity
- Q is the flowrate

- A is the cross-sectional area ($A = \pi r^2$)

Finding the velocity difference at the outlet can be useful in calculating energy loss in the resin column during design; but for these experiments *p* and *g* were constant as the experimental setup was designed in a horizontal flow. The output velocity for the experimental procedure was calculated as Equation 5-5.

$$v_1^2 = v_2^2 \qquad \textbf{(Eq. 5-5)}$$

The initial velocity in the device accounts for both the initial and output flow velocity.

Mass flow rate affects mass transfer in the system hence, the mass flow rate of this system was calculated by:

$$m = \rho \times A \times v \qquad \textbf{(Eq. 5-6)}$$

From the above, it can be noted that all the water by mass was expected to exit to the collecting tank.

5.2.1.3 The resin column disinfecting unit

Figure 5-3 is a schematic diagram of the complete experimental setup. Figure 5-4 is a photo of the experimental setup.

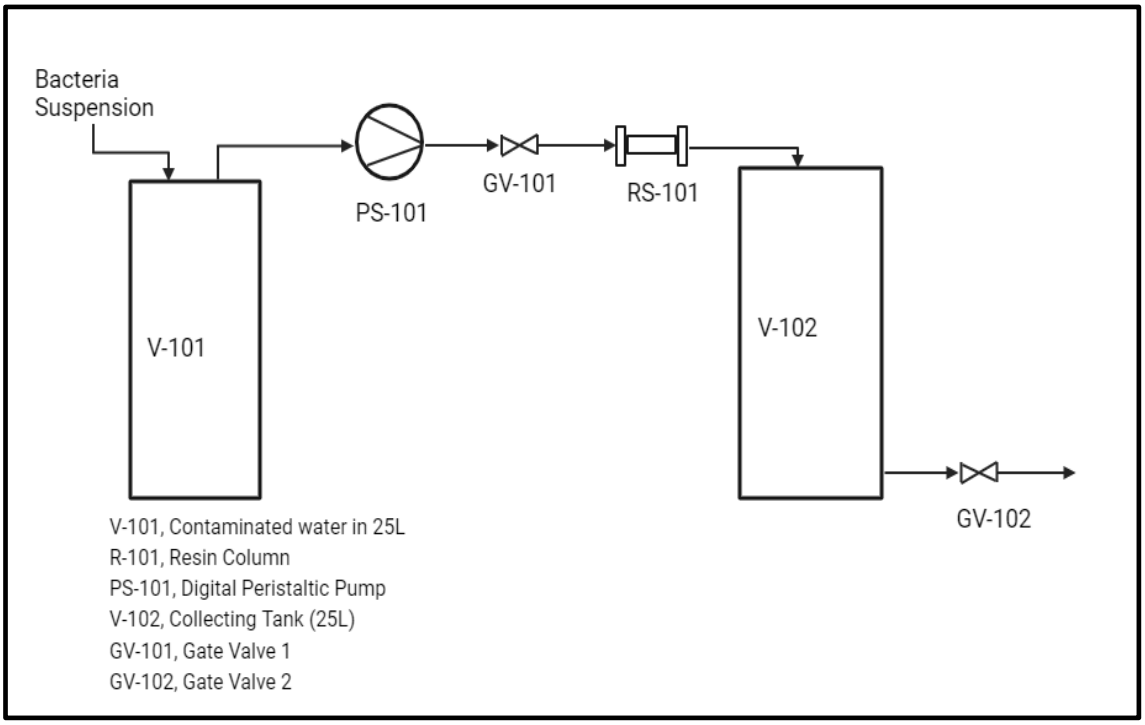

Figure 5-3: A schematic diagram of the lab-scale POU water disinfecting unit

Figure 5-4: Lab setup of resin disinfecting unit

The setup for performance evaluation consisted of a 25L tank for holding the contaminated water (2.0 x 10^7 cfu/ml of bacteria) and a peristaltic pump for pumping the water through the resin column to the receiving tank. Gate valve 1 was used to collect water samples and assess bacteria viability before entering the disinfection column. The pumping procedure, which sometimes induces cavitation in fluid systems like pumps, can potentially kill bacteria. Cavitation secondary effects, like shear forces and shock waves, disrupt and kill bacteria (Zupanc et al., 2019). A collecting tank of 25 L was used to collect the treated water. Gate valve 2 was used to collect the treated water and test the disinfection efficacy of the system and the residual chlorine in the treated water.

5.2.2 Experimental procedures

5.2.2.1 Flowrate experiments

Flow rate experiments were conducted to assess the required flow rate a resin amount of 27.31g with 1687mg of chlorine can be set to achieve maximum disinfection and minimum residual chlorine after 5 minutes. As stated in section 5.1, the first-order parameters obtained in section 4.3.2.2, were used to design the system. The following experimental procedure was followed:

The first-order equation given by Equation 4-7 was used to calculate the amount of chlorine the resin amount of 27.31 g (1687 mg of chlorine) can release at 5 minutes for 1 L of water with the different k values obtained in section 4.3.2.2.

From the findings in Chapter 4, it is essential to highlight that only two (k) values were utilized in this procedure. This decision was informed by the disinfection efficacy tests, which indicated that the

minimum chlorine amount required to effectively disinfect 1 litre of water with a bacterial concentration of 2.0 x 10^7 cfu/ml is 30 mg. The Q_t values obtained are the amount of chlorine remaining in the resin (27.31g with 1687mg of chlorine) at 5 minutes after being exposed to 1L of water. However, the amount of chlorine released is a lot which means the volume of water had to be increased. From section 4.3.2.2, it was concluded that at the chlorine release rate of 0.351 mg/min, the resin disinfects 1 litre of water in 5 mins. An equation of disinfection rate (DR) was formulated to relate the volume of water and chlorine amount. Table 5-1 shows the calculated flowrate required (27.31g with 1687mg of chlorine) to release the required chlorine for effective disinfection. It is important to highlight that the flow rate is a function of the volume of water that needs to be in contact with the 27.31g resin for the resin to achieve a 99.99% disinfection efficacy.

Table 5-1: Flowrate required for a resin amount of 27.31g packed in a resin column of 3 cm diameter

Chlorine amount(mg)	K-Value/min	Disinfection rate (DR)	cumulative amount of chlorine in resin at a time "t" (Qt)	Chlorine released at time t per L (Initial chlorine in resin-Qt)	Flowrate= Chlorine released at time t per L/ DR
30	0.351mg	1.755mg/5mins	1677.1mg	1687mg-1677.1mg =9.9mg	0.89L/min
40	0.441mg	2.205mg/5mins	1675.7mg	1687mg-1675.7mg =11.3mg	2.2L/min

The flow rate obtained in Table 5-1 was used in the continuous experimental setup. Due to resource limitations during the study, a pump capable of achieving a flow rate of 2.2 L/min was unavailable. As a result, a flow rate of 0.89 L/min was selected for the experimental procedures. Identifying an optimal pump speed for disinfecting 0.89 litres of water within one minute involved experimentation with different pump speeds. Pump speeds ranged from 100 to 300 revolutions per minute. This was conducted at intervals of 50 revs per min. The results are shown in appendix Table A 23.

Relating flowrate and flow velocity is essential for redesigning and scaling-up purposes. Equation 5-4 was used to calculate the flow velocity for a resin column of 3 cm diameter housing 27.31g of resin. Table 5-2 shows the specifications of the resin column used in this study.

Table 5-2: Design parameters of the resin column derived from this study

Parameter	Specification
Cross sectional area	0.0007 m^2
Flowrate	1.483 X 10^{-5} m^3/s
Resin capacity	27.31 g
V_s (Superficial velocity)	0.021 m/s
V_i (interstitial velocity)	0.0525 m/s
Mass flowrate	0.014 Kg/s

For up-scaling and redesign purposes, the parameters such as pressure differences, gravity, velocity, and resin column dimensions should be carefully considered and calculated using flow dynamic equations discussed in section 5.2.1.2. For example, a vertical experimental setup would require gravity and pressure drop parameters due to height. The parameters can be used to redesign a system that can use gravitational force instead of a water pump, adjustments to the resin column dimensions, specifically the diameter, can be made to attain the recommended flow rate that ensures optimal disinfection efficiency.

5.2.2.2 Evaluation of the stability of the resin

Understanding the volume of water that the resin can disinfect before chlorine depletion is crucial for estimating the theoretical lifespan of the developed resin. Ideally, a well-designed resin should have the capacity to disinfect a significant water volume before requiring replacement, offering economic and environmental advantages to the user. A stable resin should demonstrate the capability to consistently disinfect water, achieving a high percentage (up to 99%) even after prolonged usage through multiple cycles. Therefore, stability experiments are conducted to assess the resin's performance over an extended period of use. To calculate the water disinfection capacity of the resin, the following equations were used:

$$\boldsymbol{Water\ disinfection\ dapacity} = \frac{\boldsymbol{DR \times RCC}}{\boldsymbol{CR}} \quad \textbf{(Eq. 5-7)}$$

$$\boldsymbol{DR} = \frac{\boldsymbol{mg}}{\boldsymbol{min}} \quad \textbf{(Eq. 5-8)}$$

$$\boldsymbol{RCC} = \boldsymbol{mg/g} \quad \textbf{(Eq. 5-9)}$$

$$\boldsymbol{CR} = \frac{\boldsymbol{mg}}{\boldsymbol{min}}/\boldsymbol{l} \quad \textbf{(Eq. 5-10)}$$

Where:

- Water disinfection capacity is the amount of water the resin can disinfect before chlorine depletion.
- DR is the disinfection rate
- RCC is the resin chlorine capacity (amount of chlorine in resin)
- CR is the chlorine release rate

The resin unit in this study has a water treatment capacity of 4806 Litres to deplete the whole chlorine in the resin.

i. Oxidative chlorine loss

Resin initially containing 1687 mg chlorine loading was loaded in a column. In this experiment, the resin column was subjected to 20 disinfection cycles (thus 1L/cycle). The resin was periodically subjected to oxidative chlorine analysis using an iodometric/thiosulfate titration procedure to evaluate the amount of chlorine loss after every 4 cycles. The experiment was conducted in triplicate for error analysis and validation of the experimental runs. However, theoretical values of the predicted chlorine loss from the resin after undergoing 20 disinfection cycles (thus 1L/cycle) were calculated using the procedure below:

Initially, the resin has 1687 mg of chlorine, but it requires 1.755 mg/Litre of chlorine for effective disinfection. Theoretically, chlorine loss from resin is calculated using Equation 5-11 below:

$$\boldsymbol{chlorine\ loss = initial\ chlorine\ in\ resin - Chlorine\ released} \qquad \textbf{(Eq. 5-11)}$$

ii. Disinfection efficacy experiment

In this experiment, the resin disinfection unit was subjected to 20 disinfection cycles (1L/cycle). Water samples were collected at the end of every 4 cycles of disinfection to assess the viability of bacteria in the samples. The disinfection efficacy was determined using the most probable number method described in section 4.2.3. The experiment was done in triplicate for error analysis and validation.

iii. Free chlorine after 20 cycles

Resin initially containing 1687mg chlorine loading was loaded in a column. In this experiment, the resin column was subjected to 20 disinfection cycles. Water samples were collected at the end of every 4 cycles of disinfection to assess the residual chlorine after the disinfection. The experiment was repeated thrice for error analysis and validation.

5.3 Results and discussion

5.3.1 Flowrate results

Figure 5-5 shows the relationship between the obtained k-values and the calculated flowrates.

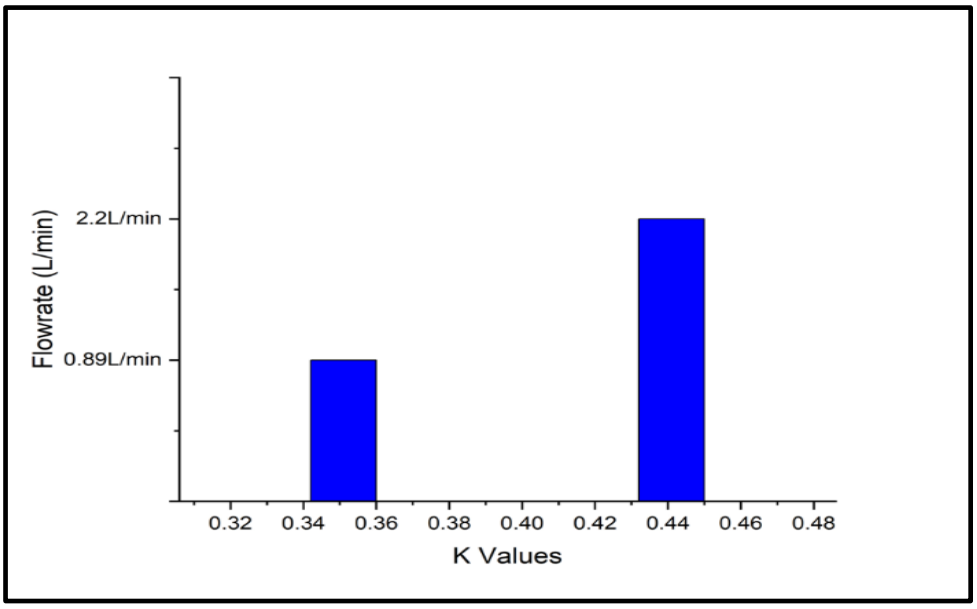

Figure 5-5: Relationship between flowrate and k values

From Figure 5-5 above, it can be noted that an increase in the K values increases the flow rate. The first-order kinetic model is used to describe the release of chlorine from a resin over time. Each K value corresponds to the rate of chlorine release. The relationship between the flow rate in the resin disinfection system and the K value is based on the fundamental principles governing the kinetics and design of a water disinfection unit. A higher K value requires a higher flow rate to ensure the chlorine concentration remains within the target range, preventing overchlorination and ensuring adequate disinfection. Developing this relationship assists in choosing the right kinetic model, which aids in designing a POU water disinfection system.

5.3.2 Stability results

The stability of the resin was evaluated by subjecting it to 20 disinfection cycles. The chlorine loss, disinfection efficacy and free residual chlorine were evaluated after 4 cycles. The results are discussed below.

5.3.2.1 Oxidative chlorine content loss

The theoretical amount of chlorine left in the resin was calculated using the equation described in section 5.2.2.2. A comparison was made between the calculated theoretical amount of chlorine expected in the resins after 20 disinfection cycles versus the experimental amount of chlorine in resin obtained after 20 disinfection cycles. The theoretical values and the experimental values were plotted in a ground truth correlation plot shown in Figure 5-6.

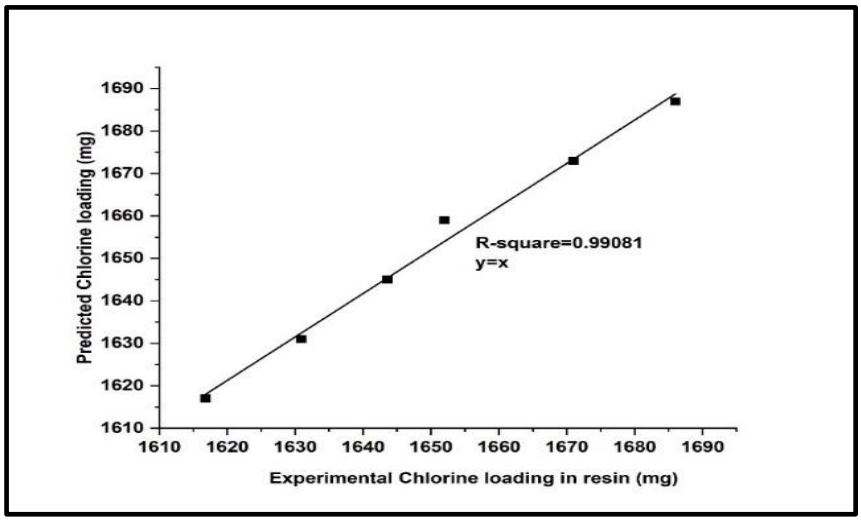

Figure 5-6: Ground truth correlation plot of the theoretical chlorine amount vs. the experimental chlorine loading in the resin.

From Figure 5-6, it can be observed that using a ground truth correlation plot at x=y, a coefficient of determination (COD) was observed to be around 99.95% at 5% confidence; this shows how practical the lab-scale POU can operate. The chlorine content in the resin is presented in the Figure 5-7 below:

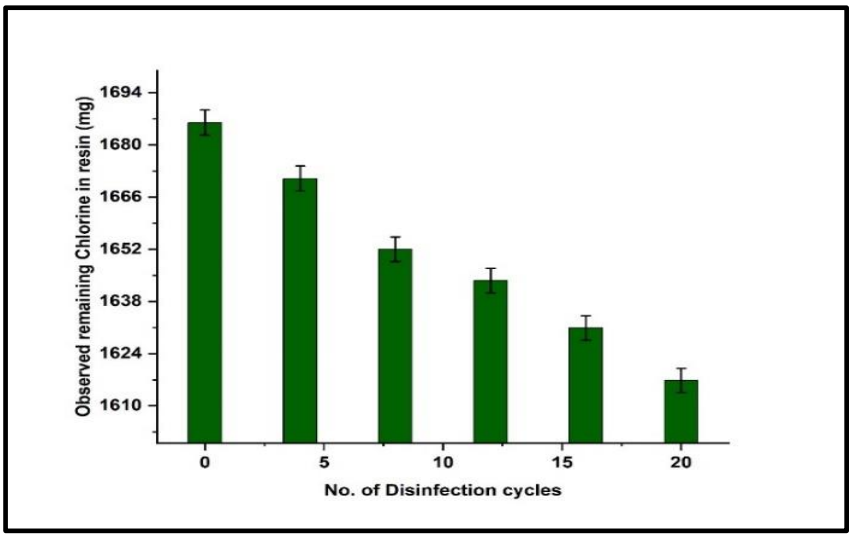

Figure 5-7: Chlorine loading amount in resin undergoing 20 disinfection cycles.

From Figure 5-7, the oxidative chlorine content in the resins decreased with increasing disinfection cycles, though a small margin. The oxidative chlorine content of the resin showed a reduction of 0.88% after four disinfection cycles. This decline increased to 2.016% and 2.69% after 8 and 12 cycles, respectively. The decline in the chlorine content of the developed resin is because of the behaviour of chlorine when it encounters water. Every time the chlorinated resin encounters water, it releases a Cl^+ ion from the N-Cl bond in the chlorinated resin. This position is then occupied by a hydrogen atom from a water molecule via the electrophilic substitution reaction, thus forming an N-H bond in the resin. This decrease in the resin chlorine content is considered normal for any N-halamine polymer. Similar findings were reported by Shi et al., (2022) concluded a 14.3% decrease in the oxidative chlorine content of PVA-MBA-Cl film after being stored for 9 weeks. Based on the findings, it can be concluded that the resin remained stable after multiple cycles, with only negligible chlorine loss. Additionally, the coefficient of determination (COD) was approximately 99.95% with a 5% confidence level, as evident from the correlation plot against the ground truth.

5.3.2.2 Disinfection efficacy

Figure 5-8 shows the disinfection efficacy of the resin after being subjected to 20 cycles of water disinfection. The disinfection efficacy was evaluated in terms of log reductions in percentage value.

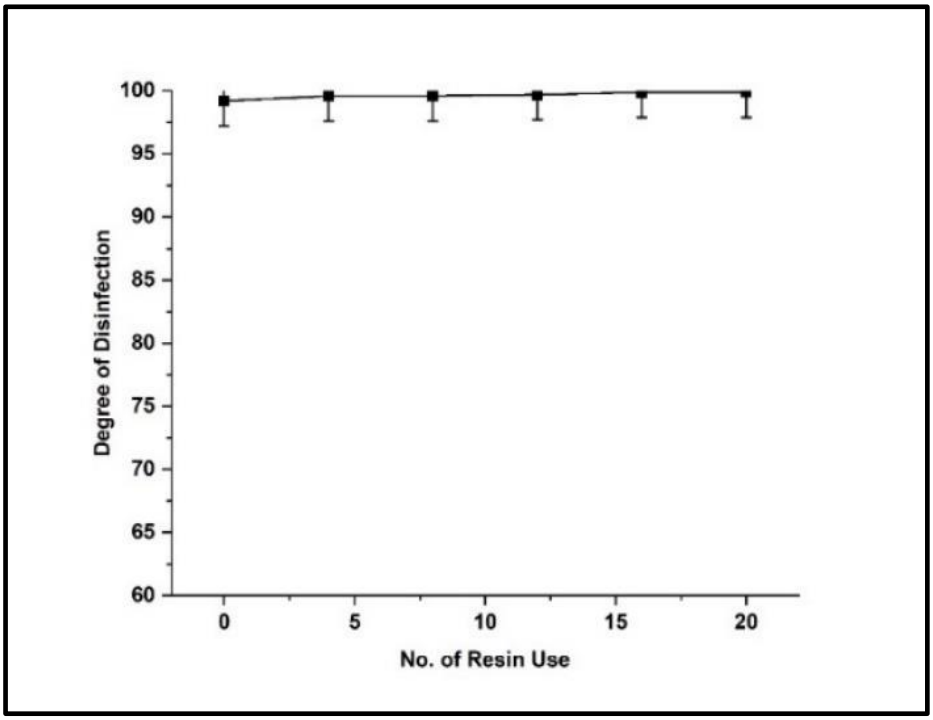

Figure 5-8: Disinfection efficacy of resin after 20 cycles

From the Figure 5-7, the disinfection efficacy was still at 99.9% after 20 disinfection cycles. The resin maintained its 100% effectiveness against bacteria because it continued to release the minimum chlorine concentration for disinfection. The main aim of assessing disinfection efficacy was determining the resin's capacity to disinfect water over multiple usage cycles. Theoretically, the resin can undergo 4806 disinfection cycles. It is expected to still maintain 99% disinfection efficacy after 20 cycles. If the disinfection efficacy declines, it would mean the resin exhausted all the chlorine before the intended life span. This would prove that the resin is unstable. This also means that the resin can disinfect a large volume of water before exhaustion whilst removing 99.9% of bacteria in drinking water. A similar stability study on chlorinated (polyurethane (PU) with 1,6-hexamethylene diisocyanate (HDI)) films conducted by Sun et al., (2012) showed that the antimicrobial efficacies of the polyurethane film samples against the bacterial and fungal species were unchanged after being used for 1 month. In conclusion, the resin's disinfection efficacy remained unchanged after multiple disinfection cycles.

5.3.2.3 Free chlorine after 20 cycles

Figure 5-9 shows the free residual chlorine in the water samples after 20 disinfection cycles.

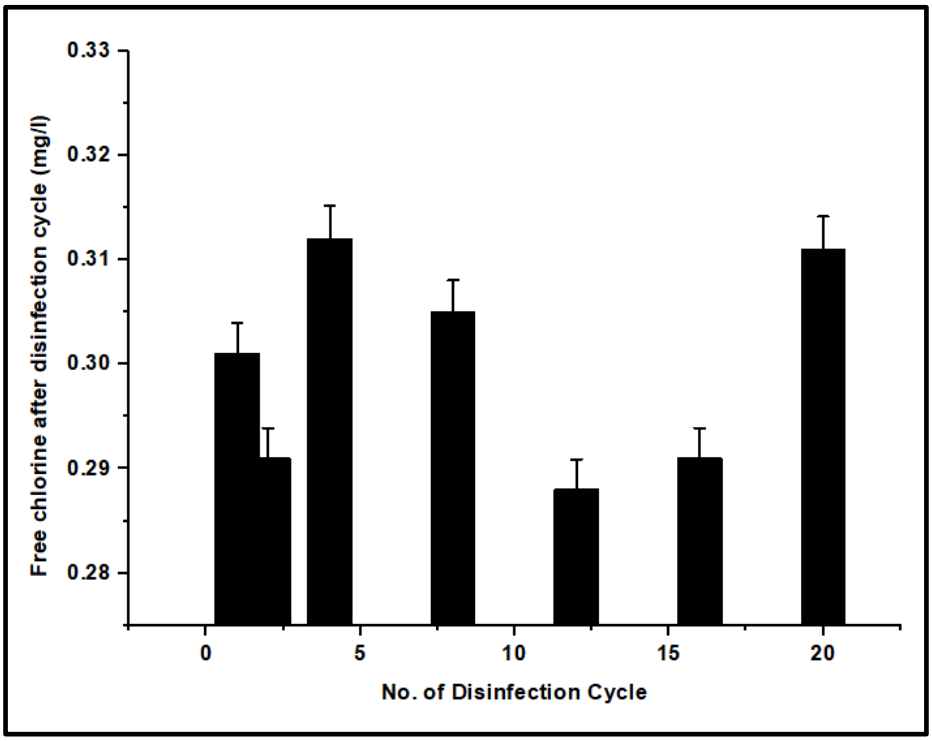

Figure 5-9: Free residual chlorine in water samples after every 4 cycles for 20 cycles of disinfection

Figure 5-9 above shows that the free chlorine measured after every 4 disinfection cycles ranged from 0.29 mg/L to 0.31 mg/L. From the mathematical modelling, the continuous disinfection system was

set to have a residual chlorine of 0.3 mg/L after every disinfection cycle. The 20 cycles maintained the free chlorine of 0.29 mg/L to 0.31 mg/L, with a deviation of +/-0.01 after 20 cycles. According to the literature, maintaining a consistent level of residual chlorine over an extended period is a measure of the stability of the resin (Coulliette et al., 2010). Furthermore, WHO recommends a residual chlorine level of between 0.2 and 0.5 mg/L for normal domestic use and a free residual chlorine concentration of at least 0.5 mg/Litre at the point of delivery to users for centralized systems (WHO, 2018). The resin disinfection unit follows the WHO recommendation about residual chlorine.

5.4 Limitations of the investigation

- The water under investigation had controlled/simulated contamination; more water samples from different water sources (dams, rivers, boreholes, etc.) should be used under study. There was only one species of bacteria during evaluation; various microorganisms must be investigated.
- The investigation was conducted over a short time.

5.5 General outcome of the investigation

- A resin column diameter of 3cm achieved a flowrate of 1.483 X 10^{-5} m^3/s, a superficial velocity of 0.021 m/s, an interstitial velocity of 0.0525 m/s and has the capacity to disinfect 4806 litres of water until the chlorine depletes from the resin.
- The resin disinfection unit can be redesigned using parameters calculated from this study i.e., the superficial velocity, interstitial velocity and the minimum flowrate can be used to design another setup with a bigger resin column diameter.
- Other hydrodynamic conditions such as pressure differences should be studied for a vertical flow column unit.
- The resin disinfection unit was stable, portrayed by the constant free residual chlorine measured after 20 disinfection cycles (1 L/cycle).
- The developed resin disinfection unit maintained a 99% efficacy after 20 disinfection cycles. Theoretically, the resin could undergo up to 4806 disinfection cycles while maintaining 99% efficacy.
- The resin column disinfection unit simplifies household water treatment since the user does not need to measure or mix disinfectant doses or adjust the dosage.

6 Chapter 6: Feasibility of the chlorinated resin as a POU disinfection system

6.1 Introduction

In Chapter 6, the practicality of using a chlorinated resin for disinfecting household water is evaluated by combining the knowledge gained from the literature review and the experimental results. Considering time and scope limitations, the feasibility assessment provides a thorough examination of the technology, covering a few factors. These include disinfection efficacy, ease of implementation, and environmental impact.

6.2 Feasibility study

It is essential to carry out a feasibility study to evaluate the viability and practicality of introducing a new technology. This section analyses the disinfection efficacy, ease of implementation and environmental impact of the resin disinfection technology in comparison to the standards made by the WHO and UNICEF.

6.2.1 Effectiveness of disinfection

Assessing alternative disinfectants involves ensuring they meet baseline pathogen elimination requirements and demonstrate improved efficacy. The effectiveness of chlorinated resin can only be concluded by comparing it to the WHO performance standard on water treatment technologies.

The developed resin in this study demonstrated a 99.99% bacterial elimination within 5 minutes for resin amounts containing 30mg or more of chlorine for a 1-litre water volume, corresponding to $4\log_{10}$ reduction against bacteria. The stability assessment in Chapter 5 demonstrated that the resin sustained a 99.99% disinfection rate even after undergoing multiple cycles if these cycles did not exceed its specified disinfection lifespan before the chlorine was depleted from the resin.

The World Health Organization (WHO) categorizes water disinfection techniques into three levels based on their performance. Products classified as 3-star demonstrate a 4 $\log_{10}$ reduction against bacteria and protozoa, and a minimum 5 $\log_{10}$ reduction against viruses. Those in the 2-star category exhibit at least a 2 $\log_{10}$ reduction against bacteria and protozoa, and a minimum 3 $\log_{10}$ reduction against viruses. Products falling under the 1-star category meet the performance targets of at least 2 stars for only two classes of pathogens. Both 3-star and 2-star products offer comprehensive protection against the three primary classes of pathogens causing diarrheal disease in humans. In

situations where the burden of diarrheal disease is high, the use of products in the 1-star category may be beneficial, particularly in targeted scenarios such as cholera outbreaks where chlorination plays a crucial role (WHO, 2018). The resin disinfection unit fully meets the performance targets for bacteria made by the WHO.

6.2.2 Ease of implementation

This section details the practical implementation of the resin column disinfection unit. The disinfection unit does not require any skill to operate. The WHO recommends consumers to monitor chlorine residual in the water regularly when using chlorine. One of the major challenges of chlorination using bleach at home is the need to measure the chlorine in the water. Diethyl paraphenylenediamine (dpd) kits are one recommended method for testing chlorine residual at home (Schwenke et al., 2019). The resin disinfection unit is preconfigured on how much chlorine is released and the amount of residual chlorine to be maintained. The end user is not responsible for adding chemicals to measure chlorine concentration. This design not only simplify the process for users but also provides financial advantages by eliminating the need for consumers to purchase dpd kits.

The resin disinfection unit has some scalability advantages. The resin disinfection unit can easily be implemented in different settings and scaled up or down based on the specific water treatment needs. The knowledge of first-order parameters studied in this investigation can be used for scaling up. In section 4.3.1.2, a resin amount of 485.43 mg and a chlorine amount of 30 mg was used to study the chlorine release behaviour of the resin. The first-order parameters obtained from the study were used to design a lab-scale POU disinfection unit that embodied a resin column with 27.31 g of the resin (1687mg of chlorine). This is an example that shows the scalability of resin disinfection.

According to UNICEF guidelines, household water treatment systems should have a minimum treatment capacity of 4,500 L to 5,000 L, which aligns with the basic survival needs (2.5 L to 3 L/day as per Sphere standards) for a family of five over one year (UNICEF, 2010). In the context of this study, the resin disinfection unit exhibits a treatment capacity of 4,806 litres before the chlorine becomes depleted from 27g of resin. Additionally, UNICEF recommends a flow rate of at least 1.7 L/h, with an optimal performance goal of 0.5 L/min (30 L/h). The designed resin column with a 3 cm diameter, achieved a flow rate of 0.89 L/min, demonstrating alignment with UNICEF's recommended flow rates. This meets and surpasses the minimum requirements, showcasing an implementation advantage as a possible POU water disinfection system for a family's basic needs.

6.2.3 Environmental impact and human health

The need for water treatment stems from both historical and ongoing mismanagement of water resources. Ironically, the processes employed for treatment can adversely affect the environment and human health. The adverse health impacts of chlorine treatment on humans and the environment are key to exploring alternative disinfectants. Theoretical comparisons in environmental impact between resin disinfection units and chlorine disinfection are discussed.

As stated in Chapter 1, section 1.1, The negative impacts of chlorination have increased because of challenges in controlling dosage at the household level. Obtaining the correct amount of chlorine for home use is difficult, often resulting in over-chlorination. Excessive halogen disinfectant typically increases the production of trihalomethanes (THMs) and haloacetic acids (HAAs). THMs or HAAs increase the risk of cancer (Mazhar et al., 2020).

The resin disinfection unit also poses potential implications for human health and the environment because the unit contains chlorine, which carries similar health risks. However, the resin disinfection unit ensures residual chlorine is present at lower concentrations. The mathematical model developed for this study showed that the resin disinfection unit can release 0.35mg/L of chlorine/minute and maintain a residual chlorine of 0.3mg/L after disinfection of 5 minutes. WHO recommends a residual chlorine level between 0.2 and 0.5 mg/L for domestic use (WHO, 2018).

6.3 Limitations of the study

While the feasibility assessment of the resin POU disinfection unit proved successful, a techno-economic analysis was not undertaken. An economic analysis holds significance in shaping decisions regarding adopting alternative water treatment technologies, as it explores manufacturing costs, maintenance, energy usage, and operational expenses. However, this comprehensive analysis was not conducted due to project constraints and scope limitations.

6.4 Summary of the study

To summarize, the resin column disinfection unit has several advantages. The resin column disinfection unit demonstrates potential as a POU water treatment unit. Table 6-1 summarizes the feasibility study of the resin disinfection unit.

Table 6-1: Summary of how the resin disinfection unit meets the WHO standards of a water treatment system

Parameter	Performance classification by the WHO[a] and UNICEF[b]	Resin disinfection technique
[a]Disinfection efficacy	3-star (★★★)-removes at least 4 log_{10} of bacteria, 5 log_{10} of viruses, 4 log_{10} of protozoa	✘
	2-star (★★)-removes at least, 2 log_{10} of bacteria, 3 log_{10} of viruses, 2 log_{10} of protozoa	✘
	1-star (★)-removes at least 4 log_{10} of bacteria	✓ achieved a 4log_{10} reduction against bacteria
[b]Ease of implementation	Operation skill- easy to use	✓ The system is pre-configured to determine the release of chlorine, with the end user not responsible for adding chemicals to measure chlorine concentrations
	Flowrate-achieves at least a 0.5 L/min flowrate	✓ A resin column with a 3 cm diameter achieved a minimum flow rate of 0.89 L/min.
	Treatment capacity-a minimum of 4,500 L for a family of 5 for 1 year	✓ 27.31g of resin has a treatment capacity of 4,806 L before the chlorine depletes
	Scalability	✓ can be scaled up/down
[a]Environmental impact and human health	A residual chlorine level between 0.2 and 0.5 mg/L for domestic use	✓ maintained a residual chlorine of 0.3mg/L after disinfection of 5 minutes

[a](WHO, 2018); [b](UNICEF, 2010)

7 Chapter 7: Conclusion and recommendations

7.1 Conclusion

This study was aimed at investigating the viability of employing a chlorinated resin as a potential point-of-use (POU) water treatment system. To conduct this study, objectives were formulated, and this section outlines the conclusions derived from the investigation, aligning with the objectives.

7.1.1 Functionalisation of a resin

A Merrifield resin was modified with a hydantoin and chlorinated using NaDCC in an electrophilic substitution reaction. A three-factor CCD was used for chlorination, optimising the temperature, reaction time, and pH. The chlorine content (by mass %) was quantified through iodometric titration. The outcomes of the experiments were analysed using Statistica software. An optimum chlorine content of 6.18% (by mass %) in the resin was achieved at a temperature of 25°C, 54 minutes, and pH 5, representing a 91.5% yield compared to the theoretical content (6.75%). The achieved chlorine content was lower compared to previously synthesized chlorine resins, which typically exhibited chlorine loadings exceeding 20% by mass. Conclusion drawn from this investigation was that using a different chlorine source (NaDCC) indeed reduces the chlorine loading on the resin.

7.1.2 Performance evaluation of the developed resin

The developed resin was evaluated to understand the chlorine release behaviour from the resin and assess the disinfection efficacy of the resin. A first-order kinetic model adapted from drug release models was effective for the chlorine release studies and a resin mass of 485.4 mg (30 mg of chlorine) released 0.351 mg of chlorine per minute in a water volume of 1 litre. Disinfection efficacy results showed that a resin mass containing 30 mg of chlorine is enough to eradicate 99.99% of bacteria from an initial bacteria concentration of 2.0 x 10^7 cfu/ml within 5 minutes for 1 litre of water.

7.1.3 Performance evaluation as a lab-scale POU device

The performance evaluation of a lab-scale resin disinfection system focused on determining viable flow rates and assessing stability. A resin column with a 3 cm diameter achieved a minimum flowrate of 0.89 L/min and maintained a 99.9% disinfection efficacy after 20 cycles, with a gradual reduction in oxidative chlorine content after every cycle. This reduction was attributed to controlled chlorine release, typical for N-halamine polymers. Free residual chlorine levels ranged from 0.29 mg/L to 0.31

mg/L after every four cycles, closely matching the targeted 0.3 mg/L over 20 cycles. The study concluded that a resin column with a cross sectional area of 0.0007 m^2 can achieve a flowrate of 1.483 X 10^{-5} m^3/s, a superficial velocity V_s of 0.021 m/s, an interstitial velocity (V_i) of 0.0525 m/s. These parameters are applicable for redesigning various setups, and a vertical flow experimental setup can help identify parameters essential for designing a resin disinfecting unit utilizing gravitational force. Hence, the unit shows promise as a point-of-use water treatment system in peri-urban areas, pending further investigation.

7.1.4 Feasibility study of the resin

The feasibility study demonstrated that the resin exhibited disinfection effectiveness meeting the standards set by the WHO for water treatment methods. The scalability advantage of the resin disinfection unit demonstrated the ease of implementing the technology. The safe residual chlorine level of 0.3 mg/L after a 5-minute disinfection interval indicated that the resin disinfection unit was safe, aligning with WHO recommendations for typical home use. However, a techno-economic analysis was not conducted hence it was not possible to conclude that the technology was economically viable.

7.2 Recommendations for future research

The chlorinated resin holds a promising prospect as a potential point of use water treatment device for peri-urban and rural areas. However, further investigations on the resin technology should be done. Future studies should focus on the following:

1. Conduct experimental studies on the hydrophobic characteristics of chlorinated resins.
2. Conduct experimental studies on the resin column in a vertical flow to investigate other hydrodynamic conditions.
3. Assess the resin column disinfection unit's long-term effectiveness on an actual water source with various bacteria and other water properties.
4. Conduct experimental comparative studies with other water disinfection methods (e.g., chlorine, UV, ozone, brominated resins) to assess the advantages and disadvantages of chlorinated resins in different scenarios.
5. A techno-economic analysis of the resin disinfection unit to determine if the technology is economically viable.

References

Abbasnezhad, N., Zirak, N., Shirinbayan, M., Kouidri, S., Salahinejad, E., Tcharkhtchi, A., & Bakir, F. (2021). Controlled release from polyurethane films: Drug release mechanisms. *Journal of Applied Polymer Science*, *138*(12). https://doi.org/10.1002/app.50083

Abdou, J., Lu, A., & Abney, M. (2021). *Identification of the Chlorine-and Bromine-Based Biocides-Task 1 of the NESC Assessment of Biocide Impacts on Life Support (LS) and Extravehicular Activity (EVA) Architectures* (Vol. 29).

Adefisoye, M. A., & Olaniran, A. O. (2022). Does Chlorination Promote Antimicrobial Resistance in Waterborne Pathogens? Mechanistic Insight into Co-Resistance and Its Implication for Public Health. In *Antibiotics* (Vol. 11, Issue 5). MDPI. https://doi.org/10.3390/antibiotics11050564

Ahmed, A. E. S. I., Hay, J. N., Bushell, M. E., Wardell, J. N., & Cavalli, G. (2008). Biocidal polymers (II): Determination of biological activity of novel N-halamine biocidal polymers and evaluation for use in water filters. *Reactive and Functional Polymers*, *68*(10), 1448–1458. https://doi.org/10.1016/j.reactfunctpolym.2008.06.021

Ahmed, A. E. S. I., Hay, J. N., Bushell, M. E., Wardell, J. N., & Cavalli, G. (2010). Macroscopic N-halamine biocidal polymeric beads. *Journal of Applied Polymer Science*, *116*(4), 2396–2408. https://doi.org/10.1002/app.31774

Akdag, A., Okur, S., McKee, M. L., & Worley, S. D. (2006). The stabilities of N-Cl bonds in biocidal materials. *Journal of Chemical Theory and Computation*, *2*(3), 879–884. https://doi.org/10.1021/ct060007s

Akter, N., Chowdhury, L., Uddin, J., Ullah, A. K. M. A., Shariare, M. H., & Azam, M. S. (2018). N-halamine functionalization of polydopamine coated Fe3O4 nanoparticles for recyclable and magnetically separable antimicrobial materials. *Materials Research Express*, *5*(11). https://doi.org/10.1088/2053-1591/aadc56

Alegbeleye, O. O., Opeolu, B. O., & Jackson, V. A. (2016). Investigation into the bacterial pollution levels at various sites along the Diep and Plankenburg river systems, 3 Western Cape, South Africa. *Water Science and Technology*, *73*(11), 2590–2599. https://doi.org/10.2166/wst.2016.054

Alsulaili, A., Al-Harbi, M., & Elsayed, K. (2020). The influence of household filter types on quality of drinking water. *Process Safety and Environmental Protection*, *143*, 204–211. https://doi.org/10.1016/j.psep.2020.06.051

Annan, E., Mustapha, K., Azeko, S. T., Odusanya, O. S., Malatesta, K., & Soboyejo, W. O. (2015). Flow Statistics and the Scaling of Ceramic Water Filters. *Advanced Materials Research*, *1132*, 267–283. https://doi.org/10.4028/www.scientific.net/amr.1132.267

Arnold F Benjamin, & Colford M Jr John. (2007). Treating water with chlorine at point-of-use to improve water quality and reduce child diarrhea in developing countries: a systematic review and meta-analysis. *The American Journal of Tropic Medicine and Hygiene*, *76*(2), 354–364.

Ashbolt, N. J. (2004). Microbial contamination of drinking water and disease outcomes in developing regions. *Toxicology*, *198*(1–3), 229–238. https://doi.org/10.1016/j.tox.2004.01.030

Ashok Paidalwar IshaP Khedikar Tech Student Assistant Professor, A. M. (2016). Overview of Water Disinfection by UV Technology-A Review. *IJSTE-International Journal of Science Technology & Engineering |*, *2*. https://doi.org/10.13140/RG.2.2.30976.25608

Bä, J. E., Baldwin, J. E., & Williams, R. M. (2009). *TETRAHEDRON ORGANIC CHEMISTRY SERIES Series Editors: High-Resolution NMR Techniques in Organic Chemistry Second Edition*. www.elsevierdirect.com

Baker, M. N. (1948). *The Quest for Pure Water: The History of Water Purification from the Earliest Record to the Twentieth Century*. American Water Works Association.

Balcı, Metin. (2005). *Basic ^{1}H- and ^{13}C-NMR spectroscopy* (1st ed.) [Book]. Elsevier.

Behnam, H., Saeedfar, S., & Mojaveryazdi, S. (2013). Biological Contamination of the Water and Its Effects. *Technology, Education, and Science International Conference (TESIC)*.

Bhandari, S., & Chandra, S. (1993). Chlorinated resins and polymers: a survey of the present state. *Progress in Organic Coatings*, *23*(2), 155–182. https://doi.org/10.1016/0033-0655(93)80009-Y

Bhattacharya, S. (2021). Central Composite Design for Response Surface Methodology and Its Application in Pharmacy. In *Response Surface Methodology in Engineering Science*. IntechOpen. https://doi.org/10.5772/intechopen.95835

Bitew, B. D., Gete, Y. K., Biks, G. A., & Adafrie, T. T. (2020). Barriers and enabling factors associated with the implementation of household solar water disinfection: A qualitative study in Northwest Ethiopia. *American Journal of Tropical Medicine and Hygiene*, *102*(2), 458–467. https://doi.org/10.4269/ajtmh.18-0412

Bloomfield, S. F., & Uso, E. E. (1985). The antibacterial properties of sodium hypochlorite and sodium dichloroisocyanurate as hospital disinfectants. In *Journal of Hospital Infection* (Vol. 6).

Bohinc, R., Žitnik, M., Bučar, K., & Kavčič, M. (2014). Dissociation dynamics of simple chlorine containing molecules upon resonant Cl K-σ* excitation. *Journal of Chemical Physics*, *140*(16). https://doi.org/10.1063/1.4871878

Borde, P., Elmusharaf, K., McGuigan, K. G., & Keogh, M. B. (2016). Community challenges when using large plastic bottles for Solar Energy Disinfection of Water (SODIS). *BMC Public Health*, *16*(1). https://doi.org/10.1186/s12889-016-3535-6

Bovey, F. A. (1969). *Nuclear magnetic resonance spectroscopy* [Book]. Academic Press.

Brandt, M. J., Johnson, K. M., Elphinston, A. J., & Ratnayaka, D. D. (2017). Water Filtration. In *Twort's Water Supply* (pp. 367–406). Elsevier. https://doi.org/10.1016/b978-0-08-100025-0.00009-0

Brooks, M. A., Godrej, A. N., Grizzard, T. J., & Angelotti, R. W. (1999). *BREAKPOINT CHLORINATION AS AN ALTERNATE MEANS OF AMMONIA-NITROGEN REMOVAL AT A WATER RECLAMATION PLANT*.

Brown, K. W., Gessesse, B., Butler, L. J., & MacIntosh, D. L. (2017). Potential Effectiveness of Point-of-Use Filtration to Address Risks to Drinking Water in the United States. *Environmental Health Insights*, *11*. https://doi.org/10.1177/1178630217746997

Cao, Z., & Sun, Y. (2009). Polymeric N-halamine latex emulsions for use in antimicrobial paints. *ACS Applied Materials and Interfaces*, *1*(2), 494–504. https://doi.org/10.1021/am800157a

Carlsson, F. H. H., & South Africa. Water Research Commission. (2003). *Elementary handbook of water disinfection*. [Water Research Commission].

Chen, Y., Worley, S. D., Kim, J., Wei, C. I., Chen, T. Y., Santiago, J. I., Williams, J. F., & Sun, G. (2003). *Biocidal Poly(styrenehydantoin) Beads for Disinfection of Water*. https://doi.org/10.1021/ie020266

Chen, Y., Worley, S. D., Kim, J., Wei, C. I., Chen, T. Y., Suess, J., Kawai, H., & Williams, J. F. (2003). Biocidal Polystyrenehydantoin Beads. 2. Control of Chlorine Loading. *Industrial and Engineering Chemistry Research*, *42*(23), 5715–5720. https://doi.org/10.1021/ie0303303

Chen, Z., & Sun, Y. (2006). N-halamine-based antimicrobial additives for polymers: Preparation, characterization, and antimicrobial activity. *Industrial and Engineering Chemistry Research*, *45*(8), 2634–2640. https://doi.org/10.1021/ie060088a

Cheng, Z., Zhu, X., Shi, Z. L., Neoh, K. G., & Kang, E. T. (2006). POLYMER MICROSPHERES WITH PERMANENT ANTIBACTERIAL SURFACE FROM SURFACE-INITIATED ATOM TRANSFER RADICAL POLYMERIZATION OF 4-VINYLPYRIDINE AND QUATERNIZATION. *Surface Review and Letters*, *13*(3), 313–318. www.worldscientific.com

Cheremisinoff P Nicholas. (2002). *Handbook of Water and Wastewater Treatment Technologies Chemical, Petrochemical & Process Pollution engineering* (illustrated). Elsevier Science.

Chien, H. W., & Chiu, T. H. (2020). Stable N-halamine on polydopamine coating for high antimicrobial efficiency. *European Polymer Journal*, *130*. https://doi.org/10.1016/j.eurpolymj.2020.109654

Chylińska, M., & Kaczmarek, H. (2014). Thermal degradation of biocidal organic N-halamines and N-halamine polymers. *Thermochimica Acta*, *583*, 32–42. https://doi.org/10.1016/j.tca.2014.03.009

Chylińska, M., Ziegler-Borowska, M., Kaczmarek, H., Burkowska, A., Walczak, M., & Kosobucki, P. (2014). Synthesis and biocidal activity of novel N-halamine hydantoin-containing polystyrenes. *E-Polymers*, *14*(1), 15–25. https://doi.org/10.1515/epoly-2013-0010

Clasen, T. (2015). Household Water Treatment and Safe Storage to Prevent Diarrheal Disease in Developing Countries. *Current Environmental Health Reports*, *2*(1), 69–74. https://doi.org/10.1007/s40572-014-0033-9

Clasen, T., & Edmondson, P. (2006). Sodium dichloroisocyanurate (NaDCC) tablets as an alternative to sodium hypochlorite for the routine treatment of drinking water at the household level. *International Journal of Hygiene and Environmental Health*, *209*(2), 173–181. https://doi.org/10.1016/J.IJHEH.2005.11.004

Committee, S. D. Water. (1980). *Drinking Water and Health.* National Academies Press.

Coulliette, A. D., Peterson, L. A., Mosberg, J. A. W., & Rose, J. B. (2010). Evaluation of a new disinfection approach: Efficacy of chlorine and bromine halogenated contact disinfection for reduction of viruses and microcystin toxin. *American Journal of Tropical Medicine and Hygiene*, *82*(2), 279–288. https://doi.org/10.4269/ajtmh.2010.09-0279

Demir, B., Broughton, R. M., Qiao, M., Huang, T. S., & Worley, S. D. (2017). N-halamine biocidal materials with superior antimicrobial efficacies for wound dressings. *Molecules*, *22*(10). https://doi.org/10.3390/molecules22101582

Demir, B., Taylor, A., Broughton, R. M., Huang, T. S., Bozack, M. J., & Worley, S. D. (2022). N-halamine surface coating for mitigation of biofilm and microbial contamination in water systems for space travel. *Biofilm*, *4*. https://doi.org/10.1016/j.bioflm.2022.100076

Dong, A., Wang, Y. J., Gao, Y., Gao, T., & Gao, G. (2017). Chemical Insights into Antibacterial N-Halamines. In *Chemical Reviews* (Vol. 117, Issue 6, pp. 4806–4862). American Chemical Society. https://doi.org/10.1021/acs.chemrev.6b00687

Dos Santos, S., Adams, E. A., Neville, G., Wada, Y., de Sherbinin, A., Mullin Bernhardt, E., & Adamo, S. B. (2017). Urban growth and water access in sub-Saharan Africa: Progress, challenges, and emerging research directions. In *Science of the Total Environment* (Vols. 607–608, pp. 497–508). Elsevier B.V. https://doi.org/10.1016/j.scitotenv.2017.06.157

Ehdaie, B., Rento, C. T., Son, V., Turner, S. S., Samie, A., Dillingham, R. A., & Smith, J. A. (2017). Evaluation of a silver-embedded ceramic tablet as a primary and secondary point-ofuse water purification technology in Limpopo Province, S. Africa. *PLoS ONE*, *12*(1). https://doi.org/10.1371/journal.pone.0169502

Eknoian, M. W., Worley, S. D., Bickert, J., & Williams, J. F. (1998). *Novel antimicrobial N-halamine polymer coatings generated by emulsion polymerization*.

Elimelech, M. (2006). The global challenge for adequate and safe water. *Journal of Water Supply: Research and Technology - AQUA*, *55*(1), 3–10. https://doi.org/10.2166/aqua.2005.064

Estopiñá-Durán, S., & Taylor, J. E. (2021). Brønsted Acid-Catalysed Dehydrative Substitution Reactions of Alcohols. In *Chemistry - A European Journal* (Vol. 27, Issue 1, pp. 106–120). Wiley-VCH Verlag. https://doi.org/10.1002/chem.202002106

Fawell, J., & Nieuwenhuijsen, M. J. (2003). Contaminants in drinking water. In *British Medical Bulletin* (Vol. 68, pp. 199–208). https://doi.org/10.1093/bmb/ldg027

Gallandat, K., Stack, D., String, G., & Lantagne, D. (2019). Residual maintenance using sodium hypochlorite, sodium dichloroisocyanurate, and chlorine dioxide in laboratory waters of varying turbidity. *Water (Switzerland)*, *11*(6). https://doi.org/10.3390/w11061309

Ge, F., Zhu, L., & Chen, H. (2006). Effects of pH on the chlorination process of phenols in drinking water. *Journal of Hazardous Materials*, *133*(1–3), 99–105. https://doi.org/10.1016/j.jhazmat.2005.09.062

Geremew, A., & Damtew, Y. T. (2020). Household water treatment using adequate methods in sub-saharan countries: Evidence from 2013–2016 demographic and health surveys. *Journal of Water Sanitation and Hygiene for Development*, *10*(1), 66–75. https://doi.org/10.2166/washdev.2019.107

Gilman, R. H., & Skillicorn, P. (1985). Boiling of drinking-water: can a fuel-scarce community afford it? In *Bulletin ofthe World Health Organization* (Vol. 63, Issue 1).

Gopal, K., Tripathy, S. S., Bersillon, J. L., & Dubey, S. P. (2007). Chlorination byproducts, their toxicodynamics and removal from drinking water. In *Journal of Hazardous Materials* (Vol. 140, Issues 1–2, pp. 1–6). https://doi.org/10.1016/j.jhazmat.2006.10.063

Hall, E. L., & Dietrich, A. M. (2000). A Brief History of Drinking Water. *Opflow*, *26*(6), 46–49. https://doi.org/10.1002/j.1551-8701.2000.tb02243.x

Helbling, D. E., & VanBriesen, J. M. (2007). Free chlorine demand and cell survival of microbial suspensions. *Water Research*, *41*(19), 4424–4434. https://doi.org/10.1016/j.watres.2007.06.006

Hijnen, W. (1992). *Practical Eperiences with UV-Disinfection in the Netherlands*. https://www.researchgate.net/publication/230718229

How, Z. T., Linge, K. L., Busetti, F., & Joll, C. A. (2017). Chlorination of Amino Acids: Reaction Pathways and Reaction Rates. *Environmental Science and Technology*, *51*(9), 4870–4876. https://doi.org/10.1021/acs.est.6b04440

Hu, J., Chu, W., Sui, M., Xu, B., Gao, N., & Ding, S. (2018). Comparison of drinking water treatment processes combinations for the minimization of subsequent disinfection by-products formation during chlorination and chloramination. *Chemical Engineering Journal*, *335*, 352–361. https://doi.org/10.1016/J.CEJ.2017.10.144

Hui, F., & Debiemme-Chouvy, C. (2013). Antimicrobial N-halamine polymers and coatings: A review of their synthesis, characterization, and applications. *Biomacromolecules*, *14*(3), 585–601. https://doi.org/10.1021/bm301980q

Hung, W. Y., Liu, B., Shou, W., Wen, T. Bin, Shi, C., Sung, H. H. Y., Williams, I. D., Lin, Z., & Jia, G. (2011). Electrophilic substitution reactions of metallabenzynes. *Journal of the American Chemical Society*, *133*(45), 18350–18360. https://doi.org/10.1021/ja207315h

Ibrahim, N., Edri, L., Bellizzi, A., Kozlovsky, C., Wiley, M., Jacobitz, F. G., Fuller, M. G., Macdonald, K., Bolender, J. P., Ndaruhutse, G. R., & Lester, Y. (2022). Plant-based point-of-use water filtration: A simple solution for potable water in developing countries. *Groundwater for Sustainable Development*, *18*, 100802. https://doi.org/10.1016/J.GSD.2022.100802

Jain, S., Sahanoon, O. K., Blanton, E., Schmitz, A., Wannemuehler, K. A., Hoekstra, R. M., & Quick, R. E. (2010). Sodium dichloroisocyanurate tablets for routine treatment of household drinking water in periurban Ghana: A randomized controlled trial. *American Journal of Tropical Medicine and Hygiene*, *82*(1), 16–22. https://doi.org/10.4269/ajtmh.2010.08-0584

Keeler, James. (2010). *Understanding NMR spectroscopy* (Second edition.) [Book]. John Wiley and Sons.

Kesharwani, N., & Haldar, C. (2022). Synthesis and characterization of Merrifield resin-supported vanadium complexes for the catalytic oxidation of straight-chain aliphatic alcohols. *Polyhedron*, *219*. https://doi.org/10.1016/j.poly.2022.115787

Kılıç, Z. (2020). The importance of water and conscious use of water. *International Journal of Hydrology*, *4*(5), 239–241. https://doi.org/10.15406/ijh.2020.04.00250

Kluczyk, A., Rudowska, M., Stefanowicz, P., & Szewczuk, Z. (2010). Microwave-assisted TFA cleavage of peptides from Merrifield resin. *Journal of Peptide Science*, *16*(1), 31–39. https://doi.org/10.1002/psc.1191

Kocer, H. B. (2009). *Synthesis, Structure-Bioactivity Relationship, and Application of Antimicrobial Materials*.

Kocer, H. B., Worley, S. D., Broughton, R. M., & Huang, T. S. (2011). A novel N-halamine acrylamide monomer and its copolymers for antimicrobial coatings. *Reactive and Functional Polymers*, *71*(5), 561–568. https://doi.org/10.1016/j.reactfunctpolym.2011.02.002

Komarov, I. V., Ishchenko, A. Y., Hovtvianitsa, A., Stepanenko, V., Kharchenko, S., Bond, A. D., & Kirby, A. J. (2019). Fast amide bond cleavage assisted by a secondary amino and a carboxyl group—a model for yet unknown peptidases? *Molecules*, *24*(3). https://doi.org/10.3390/molecules24030572

Kovacic, P., Lowery, M. K., & Field, K. W. (1970). CHEMISTRY OF N-BROMAMINES AND N-CHLORAMINES *. *Chemical Reviews*, *70*(6), 639–665. https://pubs.acs.org/sharingguidelines

Leela, C. V. M., & Rao, S. P. (1976). *MECHANISM OF DISINFECTION: EFFECT OF CHLORINE ON CELL MEMBRANE FUNCTIONS*.

Levisky, J. A., Thesis, M. S., Kovacic, P., Hopper, R. J., Gormish, J. F., & Knapczyk, W. (1965). Table II Amination Products from ¿-Butyl Halide and Trichloramine-Aluminum Chloride-Basic. In *J. Org. Chem* (Vol. 23, Issue 13).

Liang, J., Chen, Y., Barnes, K., Wu, R., Worley, S. D., & Huang, T.-S. (2006). N-halamine/quat siloxane copolymers for use in biocidal coatings [Article]. *Biomaterials*, *27*(11), 2495–2501. https://doi.org/10.1016/j.biomaterials.2005.11.020

Liang, J. K., Lu, Y., Song, Z. M., Ye, B., Wu, Q. Y., & Hu, H. Y. (2022). Effects of chlorine dose on the composition and characteristics of chlorinated disinfection byproducts in reclaimed water. *Science of the Total Environment*, *824*. https://doi.org/10.1016/j.scitotenv.2022.153739

Liu, S., Rong, C., & Lu, T. (2017). Electronic forces as descriptors of nucleophilic and electrophilic regioselectivity and stereoselectivity. *Physical Chemistry Chemical Physics*, *19*(2), 1496–1503. https://doi.org/10.1039/c6cp06376d

Liu, Z.-K., Agren, J., & Hillert, M. (1996). EQIINJBHIA Application of the Le Chatelier principle on gas reactions. In *Fluid Phase Equilibria* (Vol. 121).

Maity, N., & Dawn, A. (2020). Conducting Polymer Grafting: Recent and Key Developments. *Polymers*, *12*(709). https://doi.org/10.3390/polym12030709

Mąkosza, M. (2020). Electrophilic and Nucleophilic Aromatic Substitutions are Mechanistically Similar with Opposite Polarity. *Chemistry - A European Journal*, *26*(67), 15346–15353. https://doi.org/10.1002/chem.202003770

Makowski, M., & Bogunia, M. (2020). Influence of ionic strength on hydrophobic interactions in water: Dependence on solute size and shape. *Journal of Physical Chemistry B*, *124*(46), 10326–10336. https://doi.org/10.1021/acs.jpcb.0c06399

Mazhar, M. A., Khan, N. A., Ahmed, S., Khan, A. H., Hussain, A., Rahisuddin, Changani, F., Yousefi, M., Ahmadi, S., & Vambol, V. (2020). Chlorination disinfection by-products in municipal drinking water – A review. In *Journal of Cleaner Production* (Vol. 273). Elsevier Ltd. https://doi.org/10.1016/j.jclepro.2020.123159

Mazur, D. M., & Lebedev, A. T. (2022). Transformation of Organic Compounds during Water Chlorination/Bromination: Formation Pathways for Disinfection By-Products (A Review). *Journal of Analytical Chemistry*, *77*(14), 1705–1728. https://doi.org/10.1134/S1061934822140052

McGuigan, K. G., Conroy, R. M., Mosler, H. J., du Preez, M., Ubomba-Jaswa, E., & Fernandez-Ibañez, P. (2012). Solar water disinfection (SODIS): A review from bench-top to roof-top. *Journal of Hazardous Materials*, *235–236*, 29–46. https://doi.org/10.1016/J.JHAZMAT.2012.07.053

Mintz E, & Bartram J. (2001). *Not Just a Drop in the Bucket: Expanding Access to Point-of-Use Water Treatment Systems*.

Mohamed Abed El Aziz, M., Sadek Gomha Melad, A., & Said Ashour, A. (2019). *Grindstone neutralization reactions for the preparation of various salts of carboxylic acids*. https://doi.org/10.15406/mojboc.2019.03.00095

Mohammed, W. H., Ali, W. K., & Al-Awady, M. J. (2018). *Evaluation of in vitro drug release kinetics and antibacterial activity of vancomycin HCl-loaded nanogel for topical application*.

Monteiro, J. L., Pieber, B., Corrêa, A. G., & Kappe, C. O. (2016). Continuous Synthesis of Hydantoins: Intensifying the Bucherer-Bergs Reaction. *Synlett*, *27*(1), 83–87. https://doi.org/10.1055/s-0035-1560317

Muñoz-Bonilla, A., & Fernández-García, M. (2012). Polymeric materials with antimicrobial activity. *Polymer Science*, *37*(2), 281–339. https://doi.org/10.1016/J.PROGPOLYMSCI.2011.08.005

Murphy, H. M., McBean, E. A., & Farahbakhsh, K. (2010). A critical evaluation of two point-of-use water treatment technologies: Can they provide water that meets WHO drinking water guidelines? *Journal of Water and Health*, *8*(4), 611–630. https://doi.org/10.2166/wh.2010.156

Naiem, S., Bukhari, R., & Khan, N. A. (2017). *ROLE OF MATHEMATICAL MODELLING IN CONTROLLED RELEASE DRUG DELIVERY*. https://doi.org/10.5281/zenodo.582819

Natan, M., Gutman, O., Lavi, R., Margel, S., & Banin, E. (2015). Killing mechanism of stable N-halamine cross-linked polymethacrylamide nanoparticles that selectively target bacteria. *ACS Nano*, *9*(2), 1175–1188. https://doi.org/10.1021/nn507168x

Ndebele, N., Edokpayi, J. N., Odiyo, J. O., & Smith, J. A. (2021). Field investigation and economic benefit of a novel method of silver application to ceramic water filters for point-of-use water treatment in low-income settings. *Water (Switzerland)*, *13*(3). https://doi.org/10.3390/w13030285

Nielsen, A. M., Garcia, L. A. T., Silva, K. J. S., Sabogal-Paz, L. P., Hincapié, M. M., Montoya, L. J., Galeano, L., Galdos-Balzategui, A., Reygadas, F., Herrera, C., Golden, S., Byrne, J. A., & Fernández-Ibáñez, P. (2022). Chlorination for low-cost household water disinfection – A critical review and status in three Latin American countries. *International Journal of Hygiene and Environmental Health*, *244*, 114004. https://doi.org/10.1016/J.IJHEH.2022.114004

Öztürk, T., Göktaş, M., Savaş, B., Işiklar, M., Atalar, M. N., & Hazer, B. (2014). Synthesis and characterization of poly(vinyl chloride-graft-2- vinylpyridine) graft copolymers using a novel macroinitiator by reversible addition-fragmentation chain transfer polymerization. *E-Polymers*, *14*(1), 27–34. https://doi.org/10.1515/epoly-2013-0011

Pakharuddin, N. H., Fazly, M. N., Ahmad Sukari, S. H., Tho, K., & Zamri, W. F. H. (2021). Water treatment process using conventional and advanced methods: A comparative study of Malaysia and selected countries. *IOP Conference Series: Earth and Environmental Science*, *880*(1). https://doi.org/10.1088/1755-1315/880/1/012017

Papadopoulos, L., Kluge, M., Bikiaris, D. N., & Robert, T. (2020). Straightforward synthetic protocol to bio-based unsaturated poly(ester amide)s from itaconic acid with thixotropic behavior. *Polymers*, *12*(4). https://doi.org/10.3390/POLYM12040980

Parameswaranpillai, J., Thomas, S., & Grohens, Y. (2015). Polymer Blends: State of the Art, New Challenges, and Opportunities. In *Characterization of Polymer Blends: Miscibility, Morphology*

and Interfaces (Vol. 9783527331536, pp. 1–6). Wiley Blackwell. https://doi.org/10.1002/9783527645602.ch01

Paul, R. (2015). Grafting Polymerization. In *Functional Finishes for Textiles*.

Pérez, P., Parra-Mouchet, J., & Contreras, R. R. (2004). Quantitative representation of reactivity, selectivity and site activation concepts in organic chemistry. *Journal of the Chilean Chemical Society*, *49*(1), 51–63. https://doi.org/10.4067/s0717-97072004000100010

Phelps, E. B. (1914). The Chemical Disinfection of Water. In *Public Health Reports* (Vol. 29, Issue 41).

Porter, G. (1996). Chlorine-an introduction. In *Pure & Appl. Chem* (Vol. 68, Issue 9). IUPAC.

Primo, J. de O., Horsth, D. F., Correa, J. de S., Das, A., Bittencourt, C., Umek, P., Buzanich, A. G., Radtke, M., Yusenko, K. V., Zanette, C., & Anaissi, F. J. (2022). Synthesis and Characterization of Ag/ZnO Nanoparticles for Bacteria Disinfection in Water. *Nanomaterials*, *12*(10). https://doi.org/10.3390/nano12101764

Qi, Z., Li, G., Wang, M., Chen, C., Xu, Z., & An, T. (2022). Photoelectrocatalytic inactivation mechanism of E. coli DH5α (TET) and synergistic degradation of corresponding antibiotics in water. *Water Research*, *215*. https://doi.org/10.1016/j.watres.2022.118240

Qin, R., & Duan, C. (2017). The principle and applications of Bernoulli equation. *Journal of Physics: Conference Series*, *916*(1). https://doi.org/10.1088/1742-6596/916/1/012038

Qiu, H., Lv, L., Pan, B. C., Zhang, Q. J., Zhang, W. M., & Zhang, Q. X. (2009). Critical review in adsorption kinetic models. In *Journal of Zhejiang University: Science A* (Vol. 10, Issue 5, pp. 716–724). https://doi.org/10.1631/jzus.A0820524

Quattrini Sara, Pampaloni Barbara, & Luisa Brandi Maria. (2016). *Natural mineral waters: chemical characteristics and health effects*.

Rachwal, T., & Judd, S. (2006). A synopsis of membrane technologies in UK municipal potable water treatment: History, status and prospects. *Water and Environment Journal*, *20*(3), 110–113. https://doi.org/10.1111/j.1747-6593.2006.00038.x

Ratnayaka, D. D., Brandt, M. J., & Johnson, K. M. (2009). Water Filtration Granular Media Filtration. In *Water Supply* (pp. 315–350). Elsevier. https://doi.org/10.1016/b978-0-7506-6843-9.00016-0

Reis, B., Gerlach, N., Steinbach, C., Carrasco, K. H., Oelmann, M., Schwarz, S., Müller, M., & Schwarz, D. (2021). A complementary and revised view on the n-acylation of chitosan with hexanoyl chloride. *Marine Drugs*, *19*(7). https://doi.org/10.3390/md19070385

Roefs, I., Meulman, B., Vreeburg, J. H. G., & Spiller, M. (2017). Centralised, decentralised or hybrid sanitation systems? Economic evaluation under urban development uncertainty and phased expansion [Article]. *Water Research (Oxford)*, *109*, 274–286. https://doi.org/10.1016/j.watres.2016.11.051

Romeo, R., Grassi, A., & Scolaro7, L. M. (1992). Factors Affecting Reaction Pathways in Nucleophilic Substitution Reactions on Platinum(II) Complexes: A Comparative Kinetic and Theoretical Study. In *Inorg. Chem* (Vol. 31). https://pubs.acs.org/sharingguidelines

Rosa, G., Miller, L., & Clasen, T. (2010). Microbiological effectiveness of disinfecting water by boiling in rural Guatemala. *American Journal of Tropical Medicine and Hygiene*, *82*(3), 473–477. https://doi.org/10.4269/ajtmh.2010.09-0320

Roy, R. (2018). An Introduction to water quality analysis. *ESSENCE – International Journal for Environmental Rehabilitation and Conservation*, 94–100. https://doi.org/10.31786/09756272.18.9.2.214

Sandstrom, A., & Sun, G. (2006). Durability of Biocidal Nomex Fabrics for Multi-functional Firefighter Uniforms. *Research Journal of Textile and Apparel*, *10*(4), 13–18. https://doi.org/10.1108/rjta-10-04-2006-b002

Saqib Ishaq, M., Afsheen, Z., Khan, A., & Khan, A. (2019). Disinfection Methods. In *Photocatalysts - Applications and Attributes*. IntechOpen. https://doi.org/10.5772/intechopen.80999

Schwenke, K. U., Spiehl, D., Kraußе, M., Riedler, L., Ruppenthal, A., Villforth, K., Meckel, T., Biesalski, M., Rupprecht, D., & Schwall, G. (2019). Analysis of free chlorine in aqueous solution at very low concentration with lateral flow tests. *Scientific Reports*, *9*(1). https://doi.org/10.1038/s41598-019-53687-0

Shafiei, F., Ghavami-Lahiji, M., Sadat, T., Kashi, J., & Najafi, F. (2021). Drug release kinetics and biological properties of a novel local drug carrier system. In *Dental Research Journal* (Vol. 1). www.ncbi.nlm.nih.gov/pmc/journals/1480

Shah, A., Arjunan, A., Baroutaji, A., & Zakharova, J. (2023). A review of physicochemical and biological contaminants in drinking water and their impacts on human health. *Water Science and Engineering*. https://doi.org/10.1016/j.wse.2023.04.003

Sharma, S., & Bhattacharya, A. (2017). Drinking water contamination and treatment techniques. In *Applied Water Science* (Vol. 7, Issue 3, pp. 1043–1067). Springer Verlag. https://doi.org/10.1007/s13201-016-0455-7

Shi, Y., He, Y., Liu, J., Tang, X., Xu, H., & Liang, J. (2022). High-efficacy antimicrobial acyclic N-halamine-grafted polyvinyl alcohol film. *Polymer Bulletin*. https://doi.org/10.1007/s00289-022-04614-3

Sinikova, N. A., Shaydullina, G. M., & Lebedev, A. T. (2014). Comparison of chlorine and sodium hypochlorite activity in the chlorination of structural fragments of humic substances in water using GC-MS. *Journal of Analytical Chemistry*, *69*(14), 1300–1306. https://doi.org/10.1134/S106193481414010X

Sivey, J. D., McCullough, C. E., & Roberts, A. L. (2010). Chlorine monoxide (Cl2O) and molecular chlorine (Cl2) as active chlorinating agents in reaction of dimethenamid with aqueous free chlorine. *Environmental Science and Technology*, *44*(9), 3357–3362. https://doi.org/10.1021/es9038903

Smiley, S. L. (2017). Quality matters: incorporating water quality into water access monitoring in rural Malawi. *Water International*, *42*(5), 585–598. https://doi.org/10.1080/02508060.2017.1344818

Sobsey, M. D., Stauber, C. E., Casanova, L. M., Brown, J. M., & Elliott, M. A. (2008). Point of use household drinking water filtration: A practical, effective solution for providing sustained access to safe drinking water in the developing world. *Environmental Science and Technology*, *42*(12), 4261–4267. https://doi.org/10.1021/es702746n

Solomon, C., Casey, P., Mackne, C., & Lake, A. (1998). Chlorine Disinfection. In *ETI Environmental Technology Initiative Fact Sheet A Technical Overview*.

Stevens, D. P., Surapaneni, A., Thodupunuri, R., O'Connor, N. A., & Smith, D. (2017). Helminth log reduction values for recycling water from sewage for the protection of human and stock health [Article]. *Water Research (Oxford)*, *125*, 501–511. https://doi.org/10.1016/j.watres.2017.08.069

Sun, G., Allen, L. C., Luckie, E. P., Wheatley, W. B., & Davis Worley, S. (1995). Disinfection of Water by iV-Halamine Biocidal Polymers. In *Ind. Eng. Chem. Res* (Vol. 34). https://pubs.acs.org/sharingguidelines

Sun, G., Chen, T. Y., Habercom, M. S., Wheatley, W. B., & Worley, S. D. (1996). PERFORMANCE OF A NEW POLYMERIC WATER DISINFECTANT'. In *WATER RESOURCES BULLETIN* (Vol. 32, Issue 4).

Sun, X., Cao, Z., Porteous, N., & Sun, Y. (2010). Amine, melamine, and amide n -halamines as antimicrobial additives for polymers. *Industrial and Engineering Chemistry Research*, *49*(22), 11206–11213. https://doi.org/10.1021/ie101519u

Sun, X., Cao, Z., Porteous, N., & Sun, Y. (2012). An N-halamine-based rechargeable antimicrobial and biofilm controlling polyurethane. *Acta Biomaterialia*, *8*(4), 1498–1506. https://doi.org/10.1016/j.actbio.2011.12.027

Sun, Y. (2001). *Durable and Refreshable Polymeric N-Halamine Biocides Containing 3-(4-vinylbenzyl)-5,5-dimethylhydantoin*. https://doi.org/10.1002/pola.0000

Sun, Y., Chen, T.-Y., Worley, S. D., & Sun, G. (2001). Novel Refreshable N-Halamine Polymeric Biocides Containing Imidazolidin-4-one Derivatives. In *Polym Chem* (Vol. 39).

Thatai, S., Verma, R., Khurana, P., Goel, P., & Kumar, D. (2018). Water quality standards, its pollution and treatment methods. In *A New Generation Material Graphene: Applications in Water Technology* (pp. 21–42). Springer International Publishing. https://doi.org/10.1007/978-3-319-75484-0_2

Thomas, G. L., Böhner, C., Ladlow, M., & Spring, D. R. (2005). Synthesis and utilization of functionalized polystyrene resins. *Tetrahedron*, *61*(51), 12153–12159. https://doi.org/10.1016/j.tet.2005.07.118

Trucillo, P. (2022). Drug Carriers: A Review on the Most Used Mathematical Models for Drug Release. In *Processes* (Vol. 10, Issue 6). MDPI. https://doi.org/10.3390/pr10061094

Trussell, R. R. (2006). Water treatment: The past 30 years [Article]. *Journal - American Water Works Association*, *98*(3), 100–108. https://doi.org/10.1002/j.1551-8833.2006.tb07610.x

Tulchinsky, T. H. (2018). John Snow, Cholera, the Broad Street Pump; Waterborne Diseases Then and Now. In *Case Studies in Public Health* (pp. 77–99). Elsevier. https://doi.org/10.1016/b978-0-12-804571-8.00017-2

Verma, K., Gupta, K. D., & Gupta, A. B. (2015). A review on sewage disinfection and need of improvement. In *Desalination and Water Treatment* (Vol. 56, Issue 11, pp. 2867–2871). Bellwether Publishing, Ltd. https://doi.org/10.1080/19443994.2014.967307

Virto, R., Sanz, D., Álvarez, I., Condon, S., & Raso, J. (2004). Relationship between inactivation kinetics of a Listeria monocytogenes suspension by chlorine and its chlorine demand. *Journal of Applied Microbiology*, *97*(6), 1281–1288. https://doi.org/10.1111/j.1365-2672.2004.02414.x

Virto, R., Sanz, D., Álvarez, I., Condon, S., & Raso, J. (2005). MODELING THE EFFECT OF INITIAL CONCENTRATION OF ESCHERICHIA COLI SUSPENSIONS ON THEIR INACTIVATION BY CHLORINE. In *Journal of Food Safety* (Vol. 25).

Voorn, M. G., Kelley, A. M., Chaggar, G. K., Li, X., Teska, P. J., & Oliver, H. F. (2023). Contact time and disinfectant formulation significantly impact the efficacies of disinfectant towelettes against Candida auris on hard, non-porous surfaces. *Scientific Reports*, *13*(1). https://doi.org/10.1038/s41598-023-32876-y

Votruba, A. M., & Corman, J. R. (2020). Definitions of water quality: A survey of lake-users of water quality-compromised lakes. *Water (Switzerland)*, *12*(8). https://doi.org/10.3390/W12082114

Wahman, D. G. (2018). Chlorinated Cyanurates: Review of Water Chemistry and Associated Drinking Water Implications. In *Journal - American Water Works Association* (Vol. 110, Issue 9, pp. E1–E15). John Wiley and Sons Inc. https://doi.org/10.1002/awwa.1086

Wang, L. K., Hung, Y. T., Shammas, N. K., & Yuan, P. C. (2005). Halogenation and Disinfection. In *From: Handbook of Environmental Engineering* (Vol. 3, pp. 271–314). Physicochemical Treatment Processes.

West, A. M., Teska, P. J., Lineback, C. B., & Oliver, H. F. (2018). Strain, disinfectant, concentration, and contact time quantitatively impact disinfectant efficacy. *Antimicrobial Resistance and Infection Control*, *7*(1). https://doi.org/10.1186/s13756-018-0340-2

White, G. Clifford. (2010). *White's handbook of chlorination and alternative disinfectants* (G. Clifford. White, Ed.; 5th ed.) [Book]. Wiley.

WHO. (2015). *WHO International Scheme to Evaluate Household Water Treatment Technologies Summary results of Round I Background*. http://www.who.int/water_sanitation_health/publications/jmp-2015-update/en/

Wisniak Ben, J. (2002). The History of Chlorine-From Discovery to Commodity. In *Article in Indian Journal of Chemical Technology*. https://www.researchgate.net/publication/236233836

World Health Organization. (1971). *INTERNATIONAL STANDARDS FOR DRINKING-WATER*.

World Health Organization. (2008). *Guidelines for Drinking-water Quality THIRD EDITION INCORPORATING THE FIRST AND SECOND ADDENDA Volume 1 Recommendations Geneva 2008 WHO Library Cataloguing-in-Publication Data*.

World Health Organization. (2011). *Guidelines for drinking-water quality.* World Health Organization.

World Health Organization. (2017). *Guidelines for Drinking-water Quality FOURTH EDITION INCORPORATING THE FIRST ADDENDUM*.

World Health Organization. (2018). *WHO International Scheme to Evaluate Household Water Treatment Technologies Harmonized Testing Protocol: Technology Non-Specific Version 2.1*.

Worley, S. D., & Williams, D. E. (1988). Halamine water disinfectants. *Critical Reviews in Environmental Control*, *18*(2), 133–175. https://doi.org/10.1080/10643388809388345

Worley, S. D., Williams, D. E., & Barnela, S. B. (1987). THE STABILITIES OF NEW N-HALAMINE WATER DISINFECTANTS. In *Wac. Res* (Vol. 21, Issue 8).

Wu, J., Cao, M., Tong, D., Finkelstein, Z., & Hoek, E. M. V. (2021). A critical review of point-of-use drinking water treatment in the United States. In *npj Clean Water* (Vol. 4, Issue 1). Nature Research. https://doi.org/10.1038/s41545-021-00128-z

Zenkin, S., Kos, Š., & Musil, J. (2014). Hydrophobicity of Thin Films of Compounds of Low-Electronegativity Metals. *Journal of the American Ceramic Society*, *97*(9), 2713–2717. https://doi.org/10.1111/jace.13165

Zhang, C. B., Zhang, J., Hu, W. Q., Cui, Y. S., Liu, Y., Fu, J. Y., & Ding, T. (2016). Regioselective addition–elimination of Morita–Baylis–Hillman adducts with 2-naphthol or phenol catalyzed by functionalized ionic liquids: a direct strategy to construct functional alkenes [Article]. *Canadian Journal of Chemistry*, *94*(3), 211–214. https://doi.org/10.1139/cjc-2015-0358

Zhang, K., Qiu, C., Cai, A., Deng, J., & Li, X. (2020). Factors affecting the formation of DBPs by chlorine disinfection in water distribution system. *Desalination and Water Treatment*, *205*, 91–102. https://doi.org/10.5004/dwt.2020.26416

Zhang, T., & von Gunten, U. (2023). Chlorination of amides: Kinetics and mechanisms of formation of N-chloramides and their reactions with phenolic compounds. *Water Research*, *242*. https://doi.org/10.1016/j.watres.2023.120131

Zhang, Y., Zou, L., Li, P., Du, Z., Dou, M., Huang, Z., Liang, Z., & Qi, X. (2022). Differential characteristics and source contribution of water pollutants before and after the extreme rainfall event in the Huaihe River Basin. *Frontiers in Environmental Science*, *10*. https://doi.org/10.3389/fenvs.2022.1003421

Zupanc, M., Pandur, Ž., Stepišnik Perdih, T., Stopar, D., Petkovšek, M., & Dular, M. (2019). Effects of cavitation on different microorganisms: The current understanding of the mechanisms taking place behind the phenomenon. A review and proposals for further research. In *Ultrasonics Sonochemistry* (Vol. 57, pp. 147–165). Elsevier B.V. https://doi.org/10.1016/j.ultsonch.2019.05.009

Zyara, A. M., Torvinen, E., Veijalainen, A. M., & Heinonen-Tanski, H. (2016). The effect of chlorine and combined chlorine/UV treatment on coliphages in drinking water disinfection. *Journal of Water and Health*, *14*(4), 640–649. https://doi.org/10.2166/wh.2016.144

A. Appendix A: Unprocessed data

A.1 Preparation of 5,5-dimethylhydantoin (DMH)

Table A-1 : Experimental design layout and results for the optimization of the nucleophilic substitution reaction DMH and KOH using Central Composite Design (CCD)

Run	Type of point	Levels		Reaction variables		Integral NH peak (∫)
				Temp (◦C)	Reaction time (mins)	
1	Fact	-1	-1	45	30	1.02
2	Fact	-1	1	45	60	1.13
3	Fact	1	-1	60	30	1.15
4	Fact	1	1	60	60	1.19
5	Axial	α	0	41.8	45	1.059
6	Axial	-α	0	63.1	45	1.179
7	Axial	0	α	52.5	23.7	1.115
8	Axial	0	-α	52.5	66.2	1.22
9	Centre	0	0	52.5	45	1.171
10	Centre	0	0	52.5	45	1.175
11	Centre	0	0	52.5	45	1.18
12	Centre	0	0	52.5	45	1.181
13	Centre	0	0	52.5	45	1.176

Table A-2: Regression coefficients for the model used in predicting the NH integral for the nucleophilic substitution reaction

Factor	Regressn Coeff.	Std.Err.	t(7)	p	-95.% Cnf.Limt	+95.% Cnf.Limt
Mean/Interc.	-1.37060	0.258822	-5.29554	0.001129	-1.98262	-0.758585
(1)Temperature(L)	0.07644	0.008711	8.77459	0.000050	0.05584	0.097037
Temperature(Q)	-0.00060	0.000080	-7.58358	0.000128	-0.00079	-0.000416
(2)Reaction Time(L)	0.01455	0.003301	4.40705	0.003130	0.00674	0.022355
Reaction Time(Q)	-0.00004	0.000020	-2.17271	0.066351	-0.00009	0.000004
1L by 2L	-0.00016	0.000053	-2.96092	0.021077	-0.00028	-0.000031

A.2 Grafting reaction of amide functional group on resin

Table A-3: Experimental design matrix and experimental results for the optimization of the grafting reaction of amide group on resin using Central Composite Design (CCD)

Run	Type of point	Levels		Reaction variables		RSM Transmittance (%)
				Temp (◦C)	Reaction time (hours)	
1	Fact	-1	-1	85	12	22
2	Fact	-1	1	85	18	31
3	Fact	1	-1	95	12	26
4	Fact	1	1	95	18	34.3
5	Axial	α	0	82.9	15	24
6	Axial	-α	0	97.0	15	29
7	Axial	0	α	90	10.7	25
8	Axial	0	-α	90	19.2	36
9	Centre	0	0	90	15	28
10	Centre	0	0	90	15	28.9
11	Centre	0	0	90	15	29.1
12	Centre	0	0	90	15	30.1
13	Centre	0	0	90	15	29.9

Table A 4: ANOVA data for the grafting procedure

	ANOVA; Var.:Transimittance of C=O Group; R-sqr=.93778; Adj:.89333 2 factors, 1 Blocks, 13 Runs; MS Residual=1.380168 DV: Transimittance of C=O Group				
Factor	SS	df	MS	F	p
(1)Temperature(L)	28.3921	1	28.3921	20.57151	0.002682
Temperature(Q)	9.4011	1	9.4011	6.81155	0.034919
(2)Reaction Time(L)	107.4117	1	107.4117	77.82508	0.000049
Reaction Time(Q)	0.0533	1	0.0533	0.03859	0.849844
1L by 2L	0.0000	1	0.0000	0.00000	1.000000
Error	9.6612	7	1.3802		
Total SS	155.2708	12			

Table A 5: Regression coefficients for the model used in predicting the transmittance of the C=O peak of the grafting reaction

Factor	Regr. Coefficients; Var.:Transimittance of C=O Group; R-sqr=.93778; Adj:.8933 2 factors, 1 Blocks, 13 Runs; MS Residual=1.380168 DV: Transimittance of C=O Group					
	Regressn Coeff.	Std.Err.	t(7)	p	-95.% Cnf.Limt	+95.% Cnf.Limt
Mean/Interc.	-397.493	155.3363	-2.55892	0.037611	-764.805	-30.1815
(1)Temperature(L)	8.747	3.2614	2.68188	0.031453	1.035	16.4588
Temperature(Q)	-0.047	0.0178	-2.60990	0.034919	-0.089	-0.0044
(2)Reaction Time(L)	0.930	3.8269	0.24295	0.815011	-8.119	9.9789
Reaction Time(Q)	0.010	0.0495	0.19644	0.849844	-0.107	0.1268
1L by 2L	0.000	0.0392	0.00000	1.000000	-0.093	0.0926

A.3 Chlorination of the modified resin

Table A 6: Design matrix of chlorination reaction

Run	Type of point	Levels			Reaction variables			Cl % Content
					Temp (◦C)	Reaction time (mins)	pH	
1	Fact	-1	-1	-1	20	40	5.5	6.02
2	Fact	-1	-1	1	20	40	6.5	5.90
3	Fact	-1	1	-1	20	50	5.5	6.13
4	Fact	-1	1	1	20	50	6.5	5.96
5	Fact	1	-1	-1	30	40	5.5	5.91
6	Fact	1	-1	1	30	40	6.5	5.86
7	Fact	1	1	-1	30	50	5.5	6
8	Fact	1	1	1	30	50	6.5	5.89
9	Axial	-α	0	0	16	45	6	5.92
10	Axial	α	0	0	33	45	6	5.8
11	Axial	0	-α	0	25	36.59	6	5.88
12	Axial	0	α	0	25	53.40	6	6.09
13	Axial	0	0	-α	25	45	5.15	6.18
14	Axial	0	0	α	25	45	6.84	5.87
15	Centre	0	0	0	25	45	6	5.99
16	Centre	0	0	0	25	45	6	5.95
17	Centre	0	0	0	25	45	6	5.97
18	Centre	0	0	0	25	45	6	5.96
19	Centre	0	0	0	25	45	6	5.98

Table A 7: Regression coefficients for the model used to predict the resin's chlorine content (%)

Factor	Regressn Coeff.	Std.Err. Pure Err	t(4)	p	-95.% Cnf.Limt	+95.% Cnf.Limt
Regr. Coefficients; Var.:Chlorine Content (%); R-sqr=.95238; Adj:.90476 (2**(3) 3 factors, 1 Blocks, 19 Runs; MS Pure Error=.00023 DV: Chlorine Content (%)						
Mean/Interc.	5.343718	0.499065	10.70745	0.000431	3.958090	6.729345
(1)Temperature(L)	0.067657	0.013402	5.04813	0.007241	0.030446	0.104867
Temperature(Q)	-0.001534	0.000164	-9.34257	0.000731	-0.001990	-0.001078
(2)Reaction Time(L)	0.008334	0.016315	0.51082	0.636380	-0.036965	0.053633
Reaction Time(Q)	0.000220	0.000164	1.33770	0.251984	-0.000236	0.000676
(3)pH (L)	-0.187602	0.064364	-2.91471	0.043473	-0.366305	-0.008899
pH (Q)	0.020694	0.004105	5.04135	0.007275	0.009297	0.032091
1L by 2L	-0.000280	0.000214	-1.30551	0.261746	-0.000875	0.000315
1L by 3L	0.003400	0.001072	3.17052	0.033841	0.000423	0.006377
2L by 3L	-0.002950	0.001072	-2.75089	0.051328	-0.005927	0.000027

Table A 8: Iodometric titration results of the experimental runs

Run	Mass of Sample (g)	Burette Readings (i) (ml)	Burette Readings (f) (ml)	The volume of $Na_2S_2O_3$ used (f-i) (ml)	Cl (%)
1	0.5	0	16.9	16.9	6.02
2	0.5	16.9	33,5	16,6	5.901
3	0.5	33,5	50,8	17,263	6.13
4	0.5	50,8	67,6	16,7	5.96
5	0.5	67,6	84,2	16,64	5.91
6	0.5	0	16,5	16,52	5.86
7	0.5	16,5	33,4	16,90	6
8	0.5	33,4	49.9	16,5	5.89
9	0.5	49.9	66.5	16,68	5.922
10	0.5	66.5	82,8	16,3	5.8
11	0.5	0	16,56	16,56	5.88
12	0.5	16,56	33,71	17,15	6.09
13	0.5	33,71	61.14	17,43	6.18
14	0.5	61.10	77.65	16,55	5.87
15	0.5	77.65	94.52	16,87	5.99
16	0.5	0	16,76	16,76	5.95
17	0.5	16,76	33.57	16,81	5.97
18	0.5	33.57	50.37	16,8	5.96
19	0.5	50.37	67.21	16,84	5.98

Table A 9: Chlorine (%, mass%) in resins from 19 experimental runs and the yield (%)

Run	Cl % Content (by mass %)	Theoretical amount	Yield (%)
1	6.02	6.75	89.18
2	5.901	6.75	87.42
3	6.13	6.75	90,81
4	5.96	6.75	88,29
5	5.91	6.75	87,55
6	5.867	6.75	86,91
7	6	6.75	88,88
8	5.89	6.75	87,25
9	5.922	6.75	87,73
10	5.8	6.75	85,92
11	5.88	6.75	87,11
12	6.09	6.75	90,22
13	6.18	6.75	91,55
14	5.876	6.75	87,05
15	5.99	6.75	88,74
16	5.95	6.75	88,14
17	5.97	6.75	88,44
18	5.965	6.75	88,37
19	5.98	6.75	88,59

A.4 Bacteria growth

Table A 10: Results of bacteria growth curve in three different growth media absorbance in OD600 (nm)

Nutrient Broth	LB Broth	Tryptic Soy Broth	Time (Hours)
0	0	0	0
0.031	0.045	0.005	2
0.101	0.14	0.097	4
0.395	0.401	0.389	6
0.596	0.534	0.46	8
0.79	0.668	0.696	10
0.998	0.962	0.8	12
1.176	1.203	1.123	14
1.552	1.404	1.401	16

Table A 11: Results of bacteria growth curve in one growth media (nm)

Time	Bacteria Concentration OD600			
Hours	Trial 1	Trial 2	Trial 3	Average
0	0.069	0.699	0.071	0.071
2	0.100	0.102	0.101	0.101
4	0.395	0.397	0.396	0.395
6	0.597	0.596	0.596	0.596
8	0.810	0.799	0.799	0.79
10	0.999	0.998	0.997	0.998
12	1.277	1.276	1.278	1.276
14	1.488	1.488	1.489	1.488
16	1.587	1.578	1.577	1.577
18	1.691	1.699	1.694	1.691
20	1.736	1.738	1.737	1.736
22	1.788	1.789	1.783	1.788

A.5 Chlorine release data

Table A 12: Preliminary studies on chlorine release from resin in ppm (mg/L)

A(X)	B(Y)	C(Y)	D(Y)	E(Y)	F(Y)	G(Y)	H(Y)	I(Y)
Time	5	10	15	20	30	40	50	61.8
mins	ppm	ppm	ppm	ppm	ppm	ppm	ppm	ppm
0	0	0	0	0	0	0	0	0
5	0.1	0.5	0.8	1	1.5	2	3	5
30	1	2	4	5	8	12.1	16.3	22
60	2	6	8.9	11.2	15.18	21.8	29.1	38.4
90	3	8	11.2	14.234	19.6	29.7	39.8	47.08
120	4.2	9.266	12.9	16.3	22.6	33.86	42.91	52.46
180	4.5	9.1666	14.2	18.3	27.4	38.66	47.9	56.96
210	4.8	9.2	14.8	19.21	28.6	38.9	48.67	58.5
240	4.7	8.866	14.8	19.33	28.9	39.66	48.9	58.66

Table A 13: Free chlorine concentration (mg/L) measured in water containing varying resin mass and constant bacteria concentration

Time (mins)	Free chlorine concentration measured in water (mg/L)			
	10mg of Cl in Resin	20mg of Cl in Resin	30mg of Cl in Resin	40mg of Cl in Resin
0	0	0	0	0
5	0	0	0	0.5
15	0	0	0.8	1.31
30	0.5	1	1.4	1.89
60	1.32	2.5	2.91	3.61
80	2.67	3.57	4.02	4.61
90	3.11	4.01	5.12	5.78
100	4.11	5.03	5.98	6.86
120	5.72	6.89	7.12	7.987
150	7.4	8.31	10.31	11.98
180	7.39	10.2	13.41	15.89
210	7.32	12.86	16.79	18.71
300	7.43	16.88	19.85	21.43
330	7.4	16.89	22.8	24.76
360	7.41	16.91	25.85	27.89
410	7.43	16.92	27.31	30.35
500	7.41	16.92	27.31	33.31
530	7.41	16.92	27.31	36.01
560	7.41	16.92	27.31	37.02
600	7.41	16.92	27.31	37.02
630	7.41	16.92	27.31	37.02
660	7.41	16.92	27.31	37.02

Table A 14: Cumulative log % of chlorine in resin

A(X)	B(Y)	C(Y)	D(Y)	E(Y)
Time	10	20	30	40
mins	mg of Cl in Resin	mg of Cl in Resin	mg of Cl in Resin	mg of Cl in Resin
0	2	2	2	2
5	1.85227	1.86719	1.88081	1.98181
15	1.83009	1.85795	1.87795	1.97895
25	1.8269	1.86523	1.87506	1.97606
30	1.81092	1.84526	1.87216	1.97316
60	1.75602	1.7867	1.80956	1.91056
80	1.62592	1.66829	1.69461	1.79561
90	1.39043	1.49865	1.5966	1.6976
100	1.25689	1.29078	1.38917	1.49017
120	1.11909	1.12678	1.16137	1.26237
150	0.87964	0.93681	1.02119	1.12219
180	0.80129	0.85643	0.92942	1.03042
240	0.09126	0.1641	0.227	0.328
270	0.06162	0.08269	0.09283	0.19383
300	0.04116	0.05829	0.07918	0.10121

Table A 15: Free chlorine release data in varying bacteria concentration (mg/L)

Free chlorine concentration measured in water (mg/L)				
Time (mins)	**$3.1x10^5$ cfu/ml**	**$3.6x10^6$ cfu/ml**	**$2.0x10^7$ cfu/ml**	**0 cfu/ml**
0	0	0	0	0
5	0	0	0	1
15	0	0	0	1.6
30	1	0.5	0.2	3.4
60	2.5	1.98	1	6.9
80	3.57	2.967	2	8.8
90	4.01	3.91	3	9.1
100	5.03	4.89	4	10.234
120	6.89	6.01	5.1	12.91
150	8.31	7.806	6.2	15.67
180	10.2	9.032	8	17.98
210	12.86	11.05	10	19.001
300	17.88	15.91	14.1	19.53
330	17.89	15.86	14.01	19.54
360	17.81	15.89	14.09	19.52
410	17.92	15.88	14.08	19.541
500	17.91	15.9	14.1	19.54

Table A 16: Log cumulative (%), kinetic modelling data

Time (mins)	3.10E+05 (cfu/ml)	3.60E+06 (cfu/ml)	2.00E+07 (cfu/ml)	Zero Bacteria
	2	2	2	2
0	1.880	1.863	1.845	1.977
5	1.877	1.841	1.83	1.929
15	1.875	1.832	1.822	1.903
25	1.872	1.812	1.781	1.893
30	1.809	1.778	1.774	1.845
60	1.694	1.677	1.602	1.832
80	1.596	1.574	1.568	1.752
90	1.389	1.301	1.290	1.653
100	1.161	1.146	1.136	0.716
120	1.021	1	0.845	0.725
150	0.929	0.812	0.301	0.719
180	0	0.041	0.079	0.711

Table A 17: Preliminary data on chlorine release

Resin amount	Relative chlorine amount	Saturation point, the chlorine concentration measured in water (mg/L)			
g	mg/L	Trial 1	Trial 2	Trial 3	Average
0.08	5	3.1	2.9	3	3
0.16	10	8.5	8.4	8.5	8.46
0.24	15	12.5	12	12.6	12.36
0.3	20	18.5	20	19	19.16
0.48	30	26	25.6	26	25.86
0.6	40	38	37	38	37.66
0.8	50	47	46	47	46.66
1	61.8	55	54	55	54.66
1.29	80	74	75	75	74.66
1.45	90	85	80	85	83.33
1.61	100	95	96	96	95.66
1.61	100	95	96	96	95.66

A.6 Disinfection efficacy

Table A 18: Preliminary trial on disinfection efficacy stationary phase bacteria, preliminary data to evaluate if the resin can kill bacteria in all its growth stages

Observed OD600 (absorbance of light) was measured for every sample after 24 hours of incubation.

Sample Name	Trial 1	Trial 2	Trial 3	Average	Std Deviation
Untreated Sample	1.427	1.459	1.434	1.44	0.013
Resin-1	0.287	0.288	0.2875	0.2875	0.000
NaDCC	0.387	0.439	0.469	0.431	0.033
Unchlorinated Resin	1.447	1.348	1.496	1.430	0.061
Resin-3	0.34	0.389	0.336	0.355	0.024
Resin-2	0.433	0.471	0.341	0.415	0.054
Conjugated Resin	1.471	1.254	1.354	1.359	0.085
DMH-K	0.406	0.469	0.457	0.444	0.027
DMH	1.127	1.069	1.169	1.121	0.049
Resin 4	0.681	0.629	0.636	0.648	0.021

Table A 19: Disinfection test using broth dilution method log phase bacteria

Measuring observed OD600 (absorbance of light) and relating to calibration curve of bacteria growth

Sample Name	Trial 1	Trial 1	Average	Std Deviation
Sample Name	1.273	1.354	1.313	0.040
Untreated Sample	0.197	0.201	0.199	0.002
Resin-1	0.236	0.24	0.238	0.002
NaDCC	0.638	0.683	0.660	0.021
Unchlorinated Resin	0.188	0.182	0.185	0.003
Resin-3	0.221	0.222	0.221	0.001
Resin-2	1.507	1.514	1.508	0.001
Conjugated Resin	1.634	1.695	1.662	0.028
DMH-K	0.406	0.469	0.437	0.031
DMH	1.127	1.069	1.098	0.029

Table A 20: Disinfection efficacy using predeath-phase bacteria, preliminary data to evaluate if the resin can kill bacteria in all its growth stages

Sample Name	Trial 1	Trial 1	Average	Std Deviation
Untreated Sample	1.438	1.43	1.434	0.004
Resin-1	0.287	0.288	0.287	0.000
NaDCC	0.081	0.082	0.081	0.005
Unchlorinated Resin	1.111	1.107	1.109	0.002
Resin-3	0.438	0.435	0.436	0.001
Resin-2	0.337	0.338	0.337	0.005
Conjugated Resin	1.249	1.25	1.249	0.005
DMH-K	0.406	0.469	0.437	0.031
DMH	1.227	1.269	1.248	0.021
Resin-4	0.53	0.526	0.528	0.002

Table A 21: Bacteria log reduction references adapted from (Stevens et al., 2017)

0 log reduction	0%	1×10^6
1 log reduction	90%	1×10^5
2 log reduction	99%	1×10^4
3 log reduction	99.9%	1×10^3
4 log reduction	99.99%	1×10^2
5 log reduction	99.999%	10

Table A 22: Disinfection efficacy data

Contact Time	Bacteria Conc	Concentration mg/L			
mins	**Cfu/ml**	**10 mg**	**20 mg**	**40 mg**	**61.8 mg**
5	initial	3.1×10^5	3.1×10^5	3.1×10^5	3.1×10^5
	Final cfu/ml	1×10^5	4×10^4	2×10^5	1×10^1
	Log reduction	0.4914	0.8893	2.1903	4.491
	Percentage reduction	67.742	87.097	99.355	99.997
15	initial	3.1×10^5	3.1×10^5	3.1×10^5	3.1×10^5
	Final cfu/ml	3×10^4	1×10^4	1×10^3	1×10^2
	Log reduction	1.0142	1.4914	2.4914	3.491
	Percentage reduction	90.323	96.774	99.677	99.96
25	initial	3.1×10^5	3.1×10^5	3.1×10^5	3.1×10^5
	Final cfu/ml	2×10^4	1×10^3	1×10^2	1X10
	Log reduction	1.1903	2.4914	3.4914	5
	Percentage reduction	93.548	99.677	99.968	99.999

Table A 23: ANOVA table for disinfection efficacy

Factor	ANOVA; Var.:Disinfection Efficacy; R-sqr=.8941; Adj:.80 2 factors, 1 Blocks, 12 Runs; MS Residual=17.51102 DV: Disinfection Efficacy SS	df	MS	F	p
(1)Contact Time (Mins)(L)	136.2789	1	136.2789	7.78247	0.031590
Contact Time (Mins)(Q)	28.5209	1	28.5209	1.62874	0.249050
(2)Chlorine Conc in Resin (ppm)(L)	381.3592	1	381.3592	21.77824	0.003443
Chlorine Conc in Resin (ppm)(Q)	123.1956	1	123.1956	7.03531	0.037906
1L by 2L	178.7804	1	178.7804	10.20959	0.018712
Error	105.0661	6	17.5110		
Total SS	992.0854	11			

A.7 Performance evaluation of lab scale POU water disinfection unit

Table A 24: Pump setting experiments

Pump settings (rev/min)	Volume(L)	Time (s)		
		Run 1	Run 2	Run 3
100	0.89	129	130	130
200	0.89	64	60	62
300	0.89	55	56	55

Table A 25: Disinfection efficacy of resin after 20 cycles

Trial	Bacteria Conc	Disinfection Cycle				
1	**Cfu/ml**	**4**	**8**	**12**	**16**	**20**
	initial	2.0×10^7	2.0×10^7	2.0×10^7	2.0×10^7	2.0×10^7
	Final cfu/ml	$1x10^1$	$1x10^1$	$1x10^1$	$1x10^1$	$1x10^1$
	Log reduction	4.491	4.491	4.491	4.491	4.491
	Percentage reduction	99.89	99.677	99.968	99.999	99.89
2	initial	2.0×10^7	2.0×10^7	2.0×10^7	2.0×10^7	2.0×10^7
	Final cfu/ml	$1x10^1$	$1x10^1$	$1x10^1$	$1x10^1$	$1x10^1$
	Log reduction	4.491	4.491	4.491	4.548	4.491
	Percentage reduction	99.89	99.677	99.968	99.999	99.89
3	initial	2.0×10^7	2.0×10^7	2.0×10^7	2.0×10^7	2.0×10^7
	Final cfu/ml	$1x10^1$	$1x10^1$	$1x10^1$	$1x10^1$	$1x10^1$
	Log reduction	4.491	4.491	4.491	4.491	4.491
	Percentage reduction	99.89	99.677	99.968	99.999	99.999

Table A 26: Predicted chlorine loading before stability test

Cycle	Predicted Chlorine loading (mg)	Observed chlorine amount in resin (mg)
0	1687	1686
4	1679	1675.7
8	1671	1669.8
12	1663	1661.1
16	1655	1653.9
20	1647	1643.8

Table A 27: Free residual chlorine (mg/L) after 20 cycles

Cycle	Free Residual Chlorine		
	Trial 1	Trial 2	Trial 3
1	0.3	0.31	0.30
2	0.29	0.289	0.29
4	0.312	0.311	0.310
8	0.321	0.320	0.321
12	0.28	0.281	0.289
16	0.291	0.290	0.291
20	0.322	0.321	0.322

A.8 Mass balance data for developing the resin

The evaluation of errors associated with weighing of the reactants was conducted using statistica and a standard deviation of +/-0.006 was reported. The weighing balance was calibrated before use.

Table A 28: Mass balance table for the nucleophilic substitution reaction

Run	Mass of reactants (theoretical)				The experimental mass of reactants weighed	Mass of products (DMH-K)	Yield (%)	Integral NH Peak
	DMH	KOH	DMH	KOH	Theoretical	Experimental		
1	3.20g	1.68g	3.199g	1.67g	4.869g	4.68g	95.9	1.02
2	3.20g	1.68g	3.21g	1.66g	4.87g	4.26g	87.3	1.13
3	3.20g	1.68g	3.19g	1.671g	4.861g	4.24g	87	1.15
4	3.20g	1.68g	3.20g	1.681g	4.881g	4.21g	86.4	1.19
5	3.20g	1.68g	3.211g	1.672g	4.87g	4.31g	88.11	1.059
6	3.20g	1.68g	3.201g	1.681g	4.881g	4.11g	84.3	1.179
7	3.20g	1.68g	3.199g	1.679g	4.878g	4.15g	85.12	1.115
8	3.20g	1.68g	3.211g	1.68g	4.891g	4.02g	82.3	1.22
9	3.20g	1.68g	3.20g	1.681g	4.881g	4.06g	83.31	1.171
10	3.20g	1.68g	3.19g	1.68g	4.87g	4.08g	83.6	1.175
11	3.20g	1.68g	3.198g	1.679g	4.877g	4.12g	84.42	1.18
12	3.20g	1.68g	3.21g	1.68g	4.89g	4.11g	84.2	1.181
13	3.20g	1.68g	3.20g	1.679g	4.879g	4.10g	84	1.176

Table A 29: Mass balance table for the grafting reaction

The evaluation of errors associated with weighing of the reactants was conducted using statistica and a standard deviation of +/-0.0043 was reported. The weighing balance was calibrated before use.

Run	Mass of reactants (g)	The experimental mass of reactants weighed (g)			Mass of products (modified Resin) g		Yield (%)	Transmittance (%)
	DMH-K	Resin	DMH-K	Resin	Theoretical	Experimental		
1	2g	2.66g	2.1g	2.65g	4.65g	4.3571g	93.5%	22
2	2g	2.66g	2g	2.66g	4.66g	4.14g	89%	31
3	2g	2.66g	2g	2.655g	4.67g	4.203g	90%	26
4	2g	2.66g	1.99g	2.66g	4.65g	4.073g	87.6%	34.3
5	2g	2.66g	2.01g	2.6g	4.61g	4.208g	91.3%	24
6	2g	2.66g	2.001g	2.656g	4.657g	4.16g	89.4%	29
7	2g	2.66g	1.991g	2.659g	4.65g	4.18g	89.9%	25
8	2g	2.66g	2g	2.64g	4.64g	4.004g	86.3%	36
9	2g	2.66g	1.99g	2.66g	4.65g	4.16g	89.5%	28
10	2g	2.66g	1.98g	2.66g	4.64g	4.11g	88.6%	28.9
11	2g	2.66g	2.01g	2.65g	4.66g	4.17g	89.5%	29.1
12	2g	2.66g	2g	2.66g	4.66g	4.10g	88%	30.1
13	2g	2.66g	1.99g	2.67g	4.66g	4.14g	88.9%	29.9

Table A 30: Mass balance table for chlorinating the resin

The evaluation of errors associated with weighing of the reactants was conducted using statistica and a standard deviation of +/-0.0013 was reported. The weighing balance was calibrated before use.

Run	Mass of reactants (theoretical) (g)		The experimental mass of reactants weighed (g)		Mass of products (chlorinated resin) (g)		Yield (%)	Cl % Content
	Resin	NaDCC	Resin	NaDCC	Theoretical	Experimental		
1	4.6g	1g	4.59g	1g	5.59g	5.01g	89.7%	6.02
2	4.6g	1g	4.58g	0.99g	5.57g	4.57g	82.18%	5.90
3	4.6g	1g	4.6g	1g	5.6g	5.07g	90.7%	6.13
4	4.6g	1g	4.59g	1.01g	5.6g	4.64g	82.93%	5.96
5	4.6g	1g	4.58g	1g	5.58g	4.63g	83.02%	5.91
6	4.6g	1g	4.6g	1.01g	5.61g	4.6g	82.03%	5.86
7	4.6g	1g	4.61g	1g	5.61g	4.99g	89%	6
8	4.6g	1g	4.59g	0.98g	5.57g	4.58g	82.3%	5.89
9	4.6g	1g	4.6g	0.99g	5.59g	4.65g	83.31%	5.92
10	4.6g	1g	4.59g	1g	5.59g	4.61g	82.6%	5.8
11	4.6g	1g	4.6g	1g	5.6g	4.54g	81.12%	5.88
12	4.6g	1g	4.59g	0.99g	5.58g	4.97g	89.2%	6.09
13	4.6g	1g	4.6g	0.99g	5.59g	5.16g	92.3%	6.18
14	4.6g	1g	4.59	1.02g	5.61g	4.54g	81%	5.87
15	4.6g	1g	4.6g	0.98g	5.58g	4.57g	83.13%	5.99
16	4.6g	1g	4.6g	1g	5.6g	4.64g	82.99%	5.95
17	4.6g	1g	4.58g	0.99g	5.57g	4.62g	83%	5.97
18	4.6g	1g	4.6g	1g	5.6g	4.642g	82.91%	5.96
19	4.6g	1g	4.59g	1g	5.59g	4.69g	84%	5.98

B Appendix B: Sample calculations

This section presents sample calculations for various calculations done throughout the different sections in this study.

B.1 Chlorine content in the resin

In this study, the resin was chlorinated with chlorine from NaDCC. The chlorine content in the resin was calculated as the mass % in the resin and was calculated as follows:

$$\boldsymbol{Cl\%} = \frac{\mathbf{35.45}}{\mathbf{2}} \times \frac{(\boldsymbol{V_i} - \boldsymbol{V_f}) \times \mathbf{10^{-3}} \times \boldsymbol{N}}{\boldsymbol{W_{cl}}} \times \mathbf{100}$$

$$\boldsymbol{Cl\%} = \frac{\mathbf{35.45\ g/mol}}{\mathbf{2}} \times \frac{\mathbf{17.43\ ml} \times \mathbf{10^{-3}} \times \mathbf{0.1\ mol/l}}{\mathbf{0.5\ g}} \times \mathbf{100}$$

$$\boldsymbol{Cl\%} = \mathbf{6.18\%}$$

Thus, 1 g of resin contains 61.8 mg of chlorine.

Where:

- (V_i -V_f) is the volume of thiosulfate Solution (in ml)
- N is the normality of thiosulfate solution (mol/l)
- W_{cl} is the weight of the sample (in grams)

B.2 Yield %

The obtained yield of the chlorine content in the resin was calculated as follows:

$$\boldsymbol{Yield}\ (\%) = \frac{\boldsymbol{Experimental\ chlorine\ loading}\ (\boldsymbol{g})}{\boldsymbol{Theoretical\ chlorine\ loading}\ (\boldsymbol{g})} \times \mathbf{100}$$

$$\boldsymbol{Yield}\ (\%) = \frac{\mathbf{6.18\ g}}{\mathbf{6.75\ g}} \times \mathbf{100}$$

$$\boldsymbol{Yield}\ (\%) = \mathbf{91.5\%}$$

B.3 Bacteria colony forming units/ml (cfu/ml)

$$\frac{\boldsymbol{cfu}}{\boldsymbol{ml}} = \frac{\boldsymbol{number\ of\ colonies} \times \boldsymbol{dilution\ factor}}{\boldsymbol{volume\ of\ culture\ plated}}$$

$$\frac{cfu}{ml} = \frac{31 \times 10^4}{1\ ml}$$

3.1 x 10^5 cfu/ml

B.4 Bacteria log reductions

The log reduction formula was used to calculate the efficacy of the chlorinated resin, and the efficacy was calculated as follows:

$$log\ reduction = log\ 10\ (\frac{final\ cfu}{initial\ cfu})$$

$$log\ reduction = log\ 10\ (\frac{1 \times 10^3}{2 \times 10^7})$$

$$log\ reduction = 4.301, \textit{4-log reduction}$$

The %reduction was calculated as follows:

$$\%\ reduction = 100 \times (\frac{initial\ cfu - final\ cfu}{initial\ cfu})$$

$$\%\ reduction = 100 \times (\frac{2 \times 10^7 - 1 \times 10^3}{2 \times 10^7})$$

% reduction=99.995

B.5 First order kinetic model

The first order kinetic model was used to estimate the amount of chlorine remaining in the resin at a time t (12 minutes)

$$Log\ Q_t = Log\ Q_0 - {Kt}/{2.303}$$

$$Log\ Q_t = Log\ (30) - {0.351t}/{2.303}$$

$$Log\ Q_t = 1.421$$

$$Q_t = 26.3mg$$

Where:

- Q_0 = initial amount of chlorine in resin, Q_t = cumulative amount of chlorine in resin at a time "t", K = first order release constant, t = time in minutes

B.6 Volume of the resin column

$$v = \pi r^2 L$$

$$v = \pi\ \times (1.5cm)^2 \times 8cm = 56.5cm^3$$

B.7 Flowrate of the column unit

Flowrate was obtained using the first order kinetic model parameters to find the amount of water to be disinfected for the resin amount of 27.31g (1687mg of Cl). Flowrate for the resin containing 1687mg of chlorine was calculated as follows:

$$\boldsymbol{Flowrate\ (Q) = \frac{chlorine\ released\ at\ time\ t}{DR}}$$

$$\boldsymbol{chlorine\ released\ at\ time\ t = initial\ cl\ amount\ in\ resin - Q_t}$$

The cumulative amount of chlorine remaining in resin time t (Q_t) was calculated from the first order kinetic model, using the K constant of 0.351mg/min and the time (t) was 5 mins, thus Q_t was 1677.1 mg.

Solving for chlorine released at time t (5 mins) for 1L of water: $\boldsymbol{1687\ mg - 1677.1\ mg = 9.9 mg/l}$

Solving for flowrate (a flowrate that would achieve a disinfection efficacy of 99.9% in the resin column)

$\boldsymbol{Flowrate\ (Q) = \frac{9.9\ mg/l}{1.755 mg/5 mins}}$ **= 0.89l/min or 1.483 X 10^{-5} (m^3/s)**

B.8 Flow velocity (m/s)

The flow velocity was calculated based on the flow rate of the column unit and the cross-sectional area of the column unit with a diameter of 3 cm. The cross-sectional area was calculated as the equation below:$\boldsymbol{A = \pi r^2}$

$$\boldsymbol{A = \pi \times 1.5\ cm\ \times 1.5\ cm}$$

$$\boldsymbol{A}$$ **=7.07 cm^2 or 0.0007 m^2**

Superficial flow velocity (m/s) was calculated as follows:

$$\boldsymbol{v = \frac{Q}{A}}$$

$$\boldsymbol{v_s = \frac{1.483 \times 10^{-5} m^3/s}{0.0007\ m^2}}$$

$$\boldsymbol{v_s = 0.021\ m/s}$$

The interstitial velocity was calculated as

$\boldsymbol{v_{i=} \frac{V_s}{A.voidage}}$ **= 0.0525 m/s**

Where A.voidage for uniform spheres is assumed as ~ 0.4

C. Appendix C: Chemicals used

C.1 Merrifield resin brochure

SIGMA-ALDRICH®

sigma-aldrich.com

3050 Spruce Street, Saint Louis, MO 63103, USA
Website: www.sigmaaldrich.com
Email USA: techserv@sial.com
Outside USA: eurtechserv@sial.com

Product Specification

Product Name:
Merrifield's peptide resin – 200–400 mesh, extent of labeling: 3.5–4.5 mmol/g Cl^- loading, 1 % cross-linked

Product Number:	**474517**
CAS Number:	55844-94-5
Formula:	C25H25Cl
Formula Weight:	360.9 g/mol
Storage Temperature:	2 - 8 °C

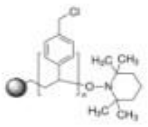

TEST	Specification
Appearance (Color)	White to Beige
Appearance (Form)	Powder or Crystals
Infrared spectrum	Conforms to Structure
Titration by AgNO3	12.4 - 15.9 %
% Cl	
Miscellaneous Assay	3.5 - 4.5
Titration by AgNO3 (mmol Cl/g)	
Substitution	3.5 - 4.5 mmol/g
Miscellaneous Assay	Conforms
Cross-Linking (1% DVB)	
Size	Conforms
Bead Size (200-400 Mesh)	
Loss on Drying	≤ 2.0 %
Miscellaneous Supplier Data	4.5 - 8.0
Swelling in DCM (ml/g)	
Miscellaneous Supplier Data	4.0 - 6.0
Swelling in DMF (ml/g)	

Specification: PRD.0.ZQ5.10000040247

Figure C 1: Supplier brochure for the Merrifield resin used in this study

C.2 Chemicals used in this study

Table C 1: Chemicals used in the study and the supplier

Chemical	Supplier
Sodium dichloroisocyanurate	Sigma-Aldrich
Merrifield peptide resin	Sigma-Aldrich
5,5-Dimethylhydantoin	Sigma-Aldrich
Potassium hydroxide	Sigma-Aldrich
Sodium hydroxide	Sigma-Aldrich
Ethanol	Sigma-Aldrich
Methanol	Sigma-Aldrich
Acetone	Sigma-Aldrich
Hexane	Sigma-Aldrich
Dimethyl sulfoxide	Sigma-Aldrich
Agar (05040-100G)	Sigma-Aldrich
LB broth (L3522-250G)	Sigma-Aldrich
Tryptic soya broth	Sigma-Aldrich
Nutrient broth	Sigma-Aldrich
Sodium thiophosphate	Sigma-Aldrich
Sulphuric acid	Sigma-Aldrich
Starch	Sigma-Aldrich
Potassium iodide	Sigma-Aldrich
Potassium bromide	Sigma-Aldrich
HCL	Sigma-Aldrich
Dimethylformamide	Sigma-Aldrich
Sodium hypochlorite	Sigma-Aldrich

D. Appendix D: Additional information

D.1 NMR spectra reference

Table 3.2

^{1}H-NMR chemical shifts of some characteristic functional groups

Functional group		Chemical shift, δ
Cyclopropane		0.2
Primary hydrocarbons	$R-CH_3$	0.9
Secondary hydrocarbons	R_2CH_2	1.3
Tertiary hydrocarbons	R_3CH	1.5–1.6
Allylic	$-C=C-CH_3$	1.7
Amine	$R-NH_2$	1.0–5.0
Alcohol	R–OH	1.0–5.5
Carbonyl	–CO–CH–	2.0–2.7
Acetylene	–C≡CH–	2.0–3.0
Benzylic	Ar–CH–	2.2–3.0
I	$-CH_2-I$	2.0–4.0
Br	$-CH_2-Br$	2.5–4.0
Cl	$-CH_2-Cl$	3.0–4.0
F	$-CH_2-F$	4.0–4.5
Alcohol	–CH–OH	3.4–4.0
Ether	RO–CH–	3.3–4.0
Ester	RCOOCH–	3.7–4.1
Olefine	–C=CH–	4.5–6.5
Aromatic	Ar–H	6.0–8.5
Aldehyde	R–CHO	9.0–10.0
Acid	R–COOH	10.0–14.0

Figure D 1: NMR spectra of some functional groups adapted from (Bovey, 1969)

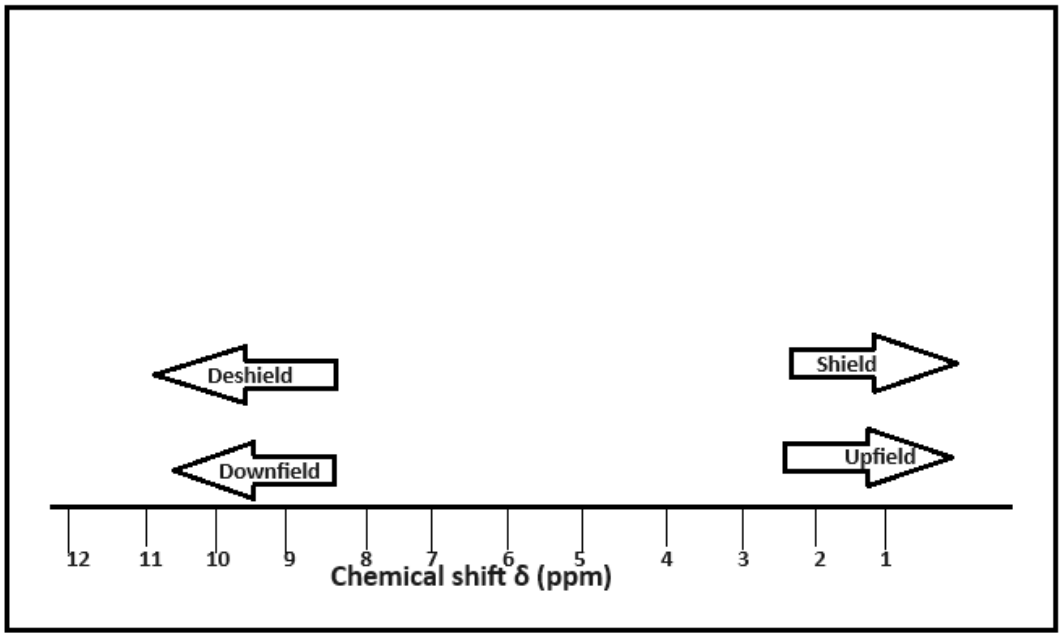

Figure D 2: Upfield and downshield in NMR spectroscopy redrawn from (Balcı, 2005)

D.2 FTIR spectra reference

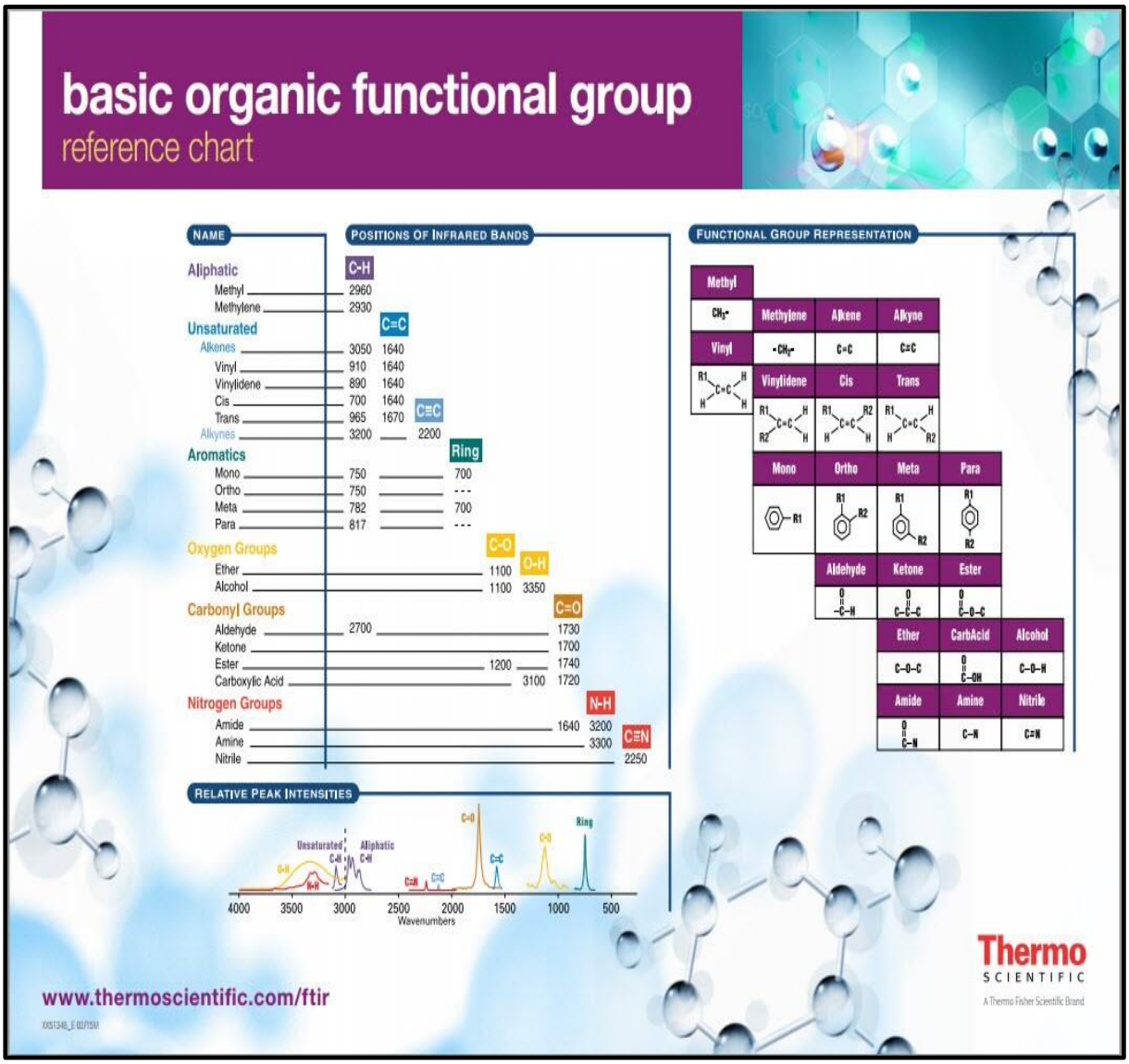

Figure D 3: FTIR reference of functional groups (provided by the manufacturer of the FTIR machine, which was used during analysis, Thermo Fischer Scientific)

D.3 Microbial procedure

To observe and calculate CFU, the following steps were followed:

1. A small amount of the bacteria sample was diluted several times in a sterile diluent (e.g., water) to reduce the number of cells in the sample and ensure that the countable range of colonies was obtained.
2. A known volume of the diluted sample was spread onto a solid agar medium, such as Petri dishes containing nutrient agar. The agar plates were then incubated under controlled conditions, such as temperature (37°C) and humidity, that favour the growth of the target microorganism.
3. After incubation, the number of colonies grown on the agar plate was counted. It is important to count only the colonies that are large enough to be visible to the naked eye, which typically corresponds to 30-300 CFUs per plate.
4. The CFU count was calculated by multiplying the number of colonies by the dilution factor used in the sample preparation.

Table D 1: Major microorganisms found in water samples adapted from (Ashbolt, 2004)

Group of microorganisms Examples	Major diseases	Primary Source
Bacteria	Typhoid fever	Human faeces
Salmonella typhi	Paratyphoid fever	Human faeces
Salmonella paratyphi	Salmonellosis	Human and animal faeces
Other Salmonella	Bacillary dysentery	Bacteria Human faeces
Shigella spp.	Cholera	Human faeces and freshwater
Vibrio cholera	Gastroenteritis	zooplankton
Enteropathogenic E. coli	Gastroenteritis	Human faeces
Yersinia enterocolitica	Gastroenteritis	Human and animal faeces
Campylobacter jejuni	Acute respiratory	Human and animal faeces
Legionella pneumophila	illness (legionellosis)	Thermally enriched water
Leptospira spp.	Leptospirosis	Animal and human urine
Various mycobacteria	Pulmonary illness	Soil and water
Opportunistic bacteria	Variable	Natural waters
Enteric viruses	Poliomyelitis	Human faeces
Enteroviruses Polio viruses	Aseptic meningitis	Human faeces
Coxsackie viruses A	Encephalitis	Human faeces
Coxsackie viruses B	Gastroenteritis	Human faeces
Echo viruses	Upper respiratory and	Human faeces
Other enteroviruses	gastrointestinal illness	Human faeces
Rotaviruses	Infectious hepatitis;	Human faeces
Adenoviruses	miscarriage and death	Human faeces
Hepatitis A virus	Gastroenteritis	Human faeces
Hepatitis E virus		Fomites and water
Norovirus		
Protozoa	Amoebic	Human faeces
Acanthamoeba castellani	meningoencephalitis	Human and animal faeces
Balantidium coli	Balantidosis	Water, human, and other
Cryptosporidium homonis, C.	(dysentery)	mammal faeces
parvum	Cryptosporidiosis	Human and animal faeces
Entamoeba histolytica	(gastroenteritis)	Water and animal faeces
Giardia lamblia	Amoebic dysentery	Warm water
Naegleria fowleri	Giardiasis	
	(gastroenteritis)	
	Primary amoebic	
	meningoencephalitis	
Helminths	ascariosis	Animal and human faeces
Ascaris lumbricoides		

D.4 Stirring machine

The experimental equipment used in the development of the resin was the Wiggens WH220 magnetic stirrer with hot plate. The picture is shown below in figure D 4 below. A 250ml round bottom flask was used during experimentation.

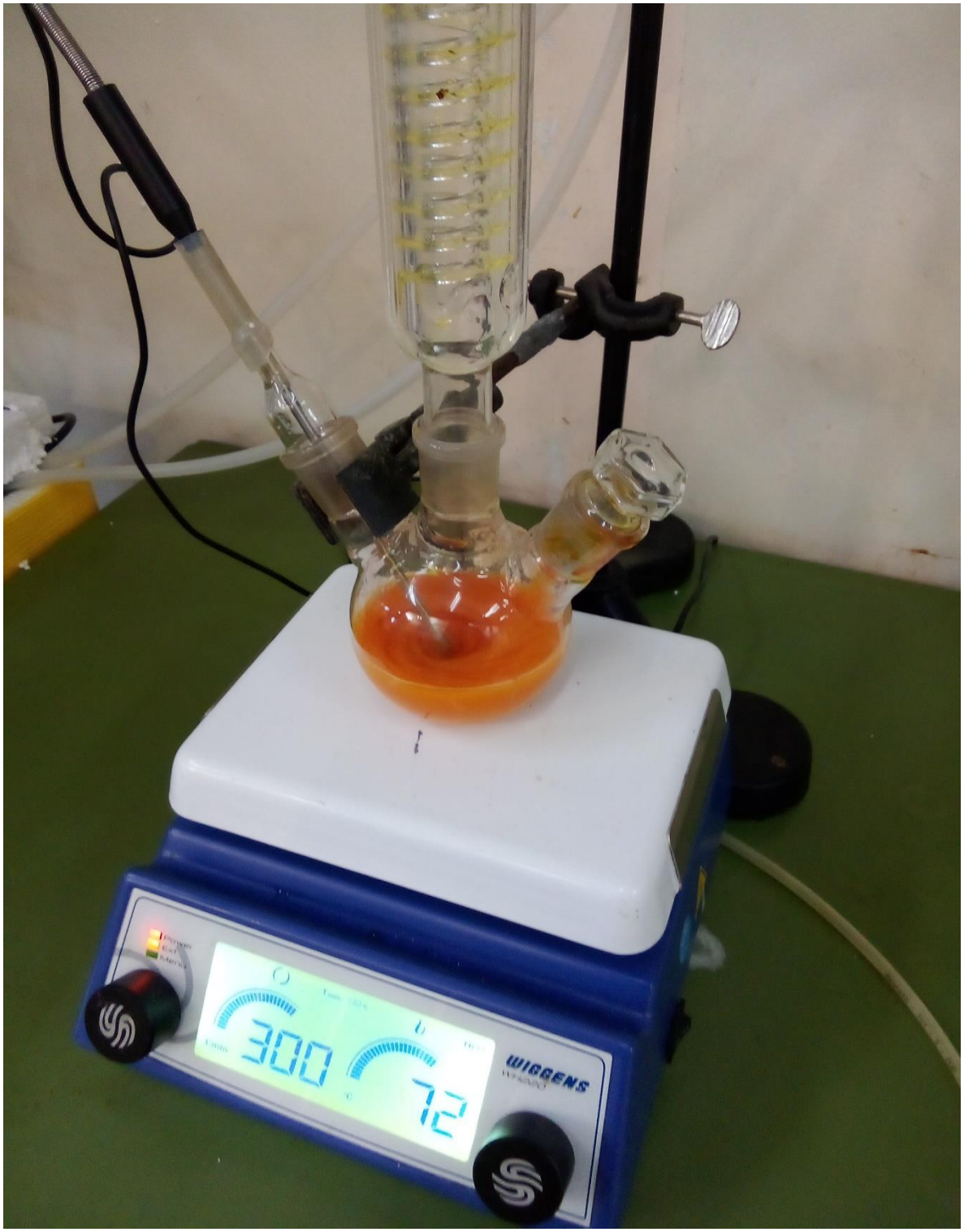

Figure D 4: Hotplate used in the experiments of developing the chlorinated resin

D.5 Procedure for the calibration of the pH meter

The calibration procedure involved the utilization of specified buffer solutions, as recommended in the pH meter's instruction manual from the supplier. The buffers used included HI 7004 M/L pH 4.00 buffer solution, HI 7007 M/L pH 7.00 buffer solution and HI 10007 M/L pH 10.00 buffer solution. To initiate the pH meter calibration, it was initially set to measurement mode, and the pH probe was submerged in the pH 7.00 buffer solution. Once the pH reading stabilized, adjustments were made to the offset trimmer until the display showed pH 7.00. Following this, the pH probe underwent rinsing with distilled water and was immersed in pH 4.00 buffer solution. The SLOPE trimmer was then adjusted until the screen displayed pH 4.00. The procedure was repeated for pH of 10.00.

Regarding the cleaning and storage of pH probes, the cleaning process involved soaking the pH probe in HI 7061M/L solution for 30 minutes, followed by rinsing with distilled water. During periods of non-use, the pH probes were stored in HI 70300 M/L solution.

The pH meter had an accuracy of around ±0.01 to ±0.02 pH units during experimentation. Table below shows the recorded pH values during calibration.

Table D 2: Calibration of the pH meter

pH reading				
pH	**Trial 1**	**Trial 2**	**Trial 3**	**Standard deviation**
4.00	4.01	4.00	4.01	0.005
7.00	7.00	7.02	7.01	0.008
10.00	10.00	10.01	10.01	0.005

D.6 Mass balance for the resin disinfection system in chapter 5

This design can be categorized as a continuous-flow reactor. A general mass balance of the form where the input flux (amount of moles of water passing the system / mass flowrate) is computed in conjunction with the production flux (amount of chlorine released to the system).

$$F_{in} + F_{prod} = F_{out} + \frac{dN}{dt}$$

Where;

- F is the Molar flux (mass flowrate)
- N is the amount (molar volume) of water in the system.

This can be simplified to

$$Q_{in}c_{in} + rV = Q_{out} + \frac{d(cV)}{dt}$$

Where;

- **Q** is the flowrate of water
- **c** is the concentration of chlorine on the resin
- **r** reaction rate (chlorine release rate for a 1 L water volume, see chapter 4)
- **V** is volume of the resin column

For this design the inlet flow rate was approximately equal to the outlet so $Q_{in} = Q_{out.}$ The temperature and pressure were kept constant so the total change in free energy (G) is 0. At steady state (optimal operation) the total volume is the resin column is constant here to compute the total mass and energy balance the equation is reduced to:

$$Q_{in}c_{in} + rV = Qc$$

The resin column flowrate and the chlorine release rate are the two vital parameters used to determine the mass and energy balance.